



universität
wien

MASTERARBEIT

Titel der Masterarbeit

„Molecular cross-talk of the Src-family tyrosine kinase
YES-1 with the Hippo pathway contributes to survival
and proliferation of hepatocellular carcinoma cells“

verfasst von

Katharina Ehrenhöfer Bakk. techn.

angestrebter akademischer Grad

Master of Science (MSc)

Wien, 2015

Studienkennzahl lt. Studienblatt: A 066 834

Studienrichtung lt. Studienblatt: Masterstudium Molekulare Biologie

Betreut von: Doz. Dr. Mag. Wolfgang Sommergruber

Danksagung

In erster Linie möchte ich mich bei meinem Betreuer Wolfgang Sommergruber bedanken, der durch wöchentliche Meetings den Fortschritt meines Projektes stets verfolgte, mir immer wieder wissenschaftliche Aspekte zu Gemüte führte und mich vor allem umfassend beim Verfassen meiner Masterarbeit unterstützte.

Außerdem gilt ein großes Dankeschön Nathalie Harrer, die mir sämtliche Methoden im Labor beibrachte und bei direkter Zusammenarbeit zum Voranschreiten des Projektes beitrug.

Bei Herwig Machat und allen weiteren Kollegen bedanke ich mich recht herzlich für die umfangreiche Unterstützung im Labor und für sämtliche Ratschläge, Protokolle und die Durchführung von Bestellungen, die im Zuge meines Projektes gemacht werden mussten. Außerdem bedanke ich mich für die gute Zusammenarbeit und die tolle Laune am Arbeitsplatz, sodass ich immer Spaß an meinem Projekt hatte. Natürlich möchte ich mich auch bei den Praktikanten Johannes und Farweh bedanken, die an den Versuchen mitarbeiteten.

Weiteres bedanke ich mich bei der Firma Boehringer Ingelheim für die Finanzierung des Projektes und die Verfügungsstellung zahlreicher Ressourcen, insbesondere der Generierung der AAV Partikel durch das Team von Dr. D. Mennerich und Dr. Lamla (BI/Biberach).

Bedanken möchte ich mich auch bei meinen Freunden, Bekannten und Verwandten, auf die ich mich stets verlassen konnte. Auch meinem Freund, der während meines Studiums immer an meiner Seite stand möchte ich hiermit Danke sagen.

Last but not least, gebührt ein großes Dankeschön meiner Familie, aber vor allem meinen Eltern, die mir meine Ausbildung ermöglicht und mich auf meinem Weg unterstützt haben.

Declaration

To the best of my knowledge and belief, I hereby declare that I have authored this thesis independently and that I have not used other than the cited sources.

Vienna, March 2015

Katharina Ehrenhöfer

Table of Contents

1	Introduction	1
1.1	The Hallmarks of Cancer	1
1.1.1	Self-Sufficiency	1
1.1.2	Insensitivity to Anti-growth Signals.....	3
1.1.3	Evading Apoptosis	4
1.1.4	Limitless Replicative Potential.....	5
1.1.5	Sustained Angiogenesis	6
1.1.6	Tissue Invasion and Metastasis	6
1.2	The Hippo Pathway	8
1.2.1	Discovery	8
1.2.2	Mechanism in Mammals	10
1.2.3	Regulation of the Hippo Pathway.....	12
1.2.4	Biological Functions of the Hippo Pathway	20
1.3	Hepatocellular Carcinoma	24
1.3.1	Liver Progenitor Cells and Tumorigenesis	24
1.3.2	Deregulation of the Hippo Pathway.....	25
1.4	Link between the Hippo Pathway and YES-1	28
1.4.1	Family of SRC Kinases	28
1.4.2	YES-1 kinase	28
1.4.3	Structures and Upstream Activators	30
1.4.4	Contribution of YES-1 to YAP/TEAD-dependent Transcription.....	31
1.5	Hippo Pathway and the Therapeutic Concept	32
1.6	Aim of the Project	33

2	Material and Methods	40
2.1	Cell Lines and Culture Conditions	40
2.1.1	Medium and Additives.....	41
2.1.2	Instrumentation	42
2.1.3	Equipment.....	43
2.2	Kits, Reagents and Buffers.....	44
	AMAXA™ Cell Line Nucleofector™ Kit V (Lonza)	44
	NE-PER® Nuclear and Cytoplasmic Extraction Reagents	44
	(Thermo Scientific)	44
2.2.1	Protein MW Markers	47
2.2.2	Antibodies	48
2.2.3	sHRNAs (Sigma-Aldrich).....	50
2.2.4	Plasmids	51
2.2.5	Antibiotics.....	52
2.2.6	Compounds.....	52
2.2.7	AAV-Particles.....	53
2.2.8	Seeding of Cells.....	53
2.2.9	siRNA Transfection with RNAiMAX or Dharmafect (Alamar Blue)	53
2.2.10	Lentivirus Transduction.....	54
2.2.11	Bacterial Transformation.....	56
2.2.12	Midi-Prep	57
2.2.13	DNA Purification (steril)	57
2.2.14	AMAXA Plasmid Transfection.....	58
2.2.15	Rescue Experiment	58
2.2.16	Alamar Blue Proliferation Assay	59
2.2.17	Reporter Gene Assay	59
2.2.18	Cytoplasmic and Nuclear Extracts	60
2.2.19	Immunoprecipitation	61

2.2.20	Western Blot	62
2.2.21	Compound Treatment.....	64
2.2.22	AAV-particle Experiment.....	64
3	Results	65
3.1	Protein Levels of Hippo-relevant Genes in a Panel of Human HCC Cell Lines	65
3.2	Expression Levels of Hippo Proteins in Cytoplasmic and Nuclear Extracts of HCC Cell Lines	69
3.3	siRNA-mediated Knockdown of TAZ, YAP, TEADs and YES-1 in HCC Cell Lines	72
3.4	Lentivirus- based shRNA-mediated Knockdown of TAZ, YAP, TEADs and YES-1 in HCC Cell Lines	77
3.4.1	Puromycin Killing Curves	77
3.4.2	Validation of shRNAs in Cell Line JHH-7	78
3.4.3	Lentiviral Transduction.....	83
3.5	Rescue Experiment for YES-1.....	106
3.6	Compound Treatment.....	108
3.6.1	Determination of IC ₅₀ Values	108
3.6.2	The anti-proliferative effect of Dasatinib treatment can be reversed by ectopic expression of the Dasatinib-resistant YES-1 mutant (T348I)	110
3.7	Reporter Gene Assay	111
3.7.1	Transfection Efficiency.....	111
3.7.2	Construction of TEAD-driven Reporter Gene Plasmids	111
3.7.3	Characterization of TEAD-driven Reporter Gene Constructs.....	114
3.7.4	Influence of Knocking down Proteins of the Hippo Pathway and YES-1 on the TEAD-driven Reporter Gene Activity	115
3.7.5	Influence of YES-1 on Reporter Gene Activity	116
3.7.6	Utilization of the <i>CTGF</i> -promoter driven Reporter Gene Assay for Compound Profiling.....	117

3.7.7	AAV particle-mediated expression of a Peptide derived from the YAP/TEAD interphase inhibits the <i>CTGF</i> -driven reporter gene assay.....	119
3.8	Co- Immunoprecipitation Studies to analyze the putative Interaction of YAP, TAZ, TEAD and YES-1	121
4	Discussion	122
5	Abstract.....	131
6	Zusammenfassung.....	132
7	References	133
8	Attachments.....	142
8.1	List of Tables	142
8.2	List of Figures.....	143
8.3	Mutation Analysis	146

1 INTRODUCTION

1.1 The Hallmarks of Cancer

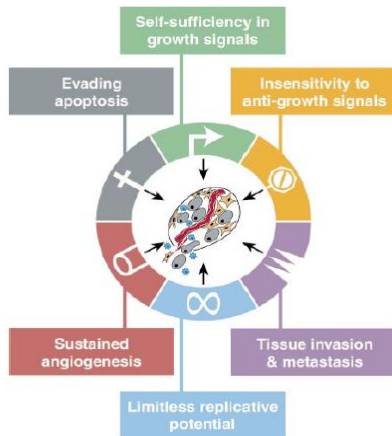


Figure 1: The Hallmarks of Cancer by Hanahan and Weinberg [1]:

Self-sufficiency in growth signals, insensitivity to anti-growth signals, avoiding of apoptosis, limitless replicative potential, sustained angiogenesis, and metastasis and tissue invasion.

Cancer as a disease relies on dynamic changes to the genome. The discovery of mutations that result in oncogenes with gain of function and tumor suppressor genes with recessive loss of function served as the basis for the description of the hallmarks of cancer by Hanahan and Weinberg (2000) [1]. They discussed the rules that describe the transformation of normal human cells into malignant ones and manifested six essential alterations in cell physiology that collectively rule malignant growth (Fig. 1). These alterations include **self-sufficiency in growth signals, insensitivity to anti-growth signals, avoiding of apoptosis, limitless replicative potential, sustained angiogenesis, metastasis and tissue invasion.** Furthermore, these six capabilities are proposed to be shared in common by many, perhaps all types of human tumors [1].

1.1.1 SELF-SUFFICIENCY

In contrast to tumor cells, normal cells are dependent on mitogenic **growth signals** (GS), which are transmitted into the cell by transmembrane receptors to move from quiescence to proliferation. These receptors can be activated by distinct factors including **diffusible growth factors (GFs), extracellular matrix components and cell-to-cell adhesion/interaction** molecules. Tumor cells develop a greatly reduced dependence on such exogenous growth stimulation because they are able to generate many of their own growth signals which lead to an autocrine stimulation (positive feedback signaling loop) [1].

Furthermore, **cell surface receptors** that transduce growth stimulatory signals into the cell are also targets for deregulated events during tumorigenesis. For example, GF receptors which exhibit tyrosine kinase activities in their cytoplasmic domains, are commonly over-expressed or constitutively activated by mutation in many cancers. Over-expression of these receptors may enable cancer cells to become hyper-responsive to low levels of GFs and therefore trigger proliferation [1]. Examples include the **EGF-R/erbB** (epidermal GF) receptor, which is up-regulated in the stomach, brain, and breast tumors and **HER2/neu** (human epidermal growth factor receptor) which is over-expressed in stomach and mammary carcinoma [2]. The effect of ligand-independent signaling by over-expression of GF receptors is mediated through structural alteration of receptors. The same holds true for the constitutive activation of single point mutated kinase domains or the truncated versions of the EGF receptor that lack a high portion of the cytoplasmic domain [3,4].

An event, which is also observable in cancer cells, is the **switch of integrins**. Located in the extracellular matrix, those types of integrins responsible for transmitting pro-growth signals are favored [5,6]. Both, **ligand-activated GF receptors** and **pro-proliferative integrins** associated with extracellular matrix components are able to activate the **SOS-RAS-RAF-MAP** kinase pathway. In 25% of human tumors, Ras proteins are present in structurally altered forms which are therefore able to release mitogenic signals into cells independently of stimulation of their normal upstream regulators. Interestingly, about half of the best studied tumors exhibit mutant *RAS* oncogenes [1,6,7].

Beside the central SOS-RAS-RAF-MAP kinase mitogenic cascade, novel downstream effector pathways have been discovered. Through cross-talk signaling with numerous pathways, extracellular communication allows for multiple biological effects. For example, interaction of RAS protein with the survival-promoting PI3 kinase enables growth signals to evoke survival signals within the cell [1].

Growth deregulation during tumorigenesis can be explained by understanding the contribution of bystanders such as **fibroblasts and endothelial cells**, which are proposed to play an essential role in driving tumor cell proliferation [1].

1.1.2 INSENSITIVITY TO ANTI-GROWTH SIGNALS

Growth-inhibitory signals received from transmembrane cell surface receptors and **immobilized inhibitors**, which are embedded in the extracellular matrix and on the surface of surrounding cells contribute to maintenance of cellular quiescence and tissue homeostasis in normal tissue. Most of these anti-growth signals are linked to the control of the cell cycle. Based on the input of signals, cells are able to decide whether to proliferate, to be quiescent or to enter into post-mitotic state [1].

The majority of anti-proliferative signals are funneled through **pRB**, the retinoblastoma protein and its two relatives: p107 and p130. In contrast, in its hypo-phosphorylated state, pRB is able to sequester and alter the function of E2F transcription factors and blocks proliferation. In turn, disruption of the pRb pathway sets E2F free, which is subsequently able to control the expression of genes essential for progression from G1 into S-phase. Furthermore, it provides the cell with insensitivity to anti-growth factors which usually influence the pathway by blocking advance through the G1 phase of the cell cycle [8].

TGF- β is able to prevent phosphorylation of pRb in a number of ways, including the inhibition of the cyclin::CDK complex formation, thereby blocking its progression through G1. Some cells lose TGF- β responsiveness through down-regulation of their TGF- β receptor while others display mutant, dysfunctional receptors [8].

Alternatively **DNA virus-induced tumors**, notably cervical carcinomas, are able to eliminate pRb function by viral oncoproteins such as the E7 of human papillomavirus [9].

Additionally, cancer cells are able to **turn off expression of integrins** and **other cell adhesion molecules** in order to prevent anti-growth signal propagation. Another strategy to avoid differentiation directly involves the **C-MYC oncogene**, which encodes a transcription factor and its over-expression has been described in many tumors [1].

1.1.3 EVADING APOPTOSIS

Programmed **cell death** and **apoptosis** are major events which control cell number and eliminate abnormal cells following the detecting DNA damage, signaling imbalance provoked by oncogene action, survival factor insufficiency or hypoxia. Once initiated it is an orchestrated series of steps including cellular membrane disruption, breaking down of cytoplasmic and nuclear skeletons, degradation of chromosomes and nucleus fragmentation [1]. The apoptotic machinery is composed of **sensors and effectors**. The sensors, like **cell surface receptors** bind factors for **survival or death** which are responsible for monitoring the extracellular and intracellular environment. Survival signals include **IGF-1/IGF-2** through pairing to their receptors IGF-1R and **IL-3** to IL-3R, respectively. Examples of death signals include the **FAS** ligand binding to the FAS receptor and **TNF- α** binding TNF-R1 [10].

Many signals that elicit apoptosis converge at the mitochondria, by **releasing cytochrome C**, a potent catalyst of apoptosis. Furthermore, members of the BCL-2 family of proteins, whose members have either **pro-apoptotic** (BAX, BAK, BID, BIM) or **anti-apoptotic** (BCL-2, BCL-XL, BCL-W) function, act in part by governing cytochrome C release through mitochondrial death signaling [1].

The **p53** tumor suppressor protein can also trigger apoptosis through the up-regulation of the pro-apoptotic **BAX** in response to extensive DNA damage, which in turn stimulates **cytochrome C** release. The two “gatekeeper” **caspases, CASP-8** and **CASP-9** are activated by death receptors such as **FAS** or by the **cytochrome C** release from mitochondria. **BCL-2 oncogene** was found up-regulated *via* chromosomal translocation in follicular lymphoma. Previous studies have demonstrated when co-expressed with **MYC** oncogene, the **BCL-2** gene is able to promote the formation of B-cell lymphomas [1].

The **p53 gene** (“guardian of the chromosome”) like the Rb gene, is a tumor suppressor. People with only one inherited functional copy of the p53 gene are predisposed to cancer. Usually they develop several independent tumors in a variety of tissues in early adulthood. However, this is a rare event (known as Li-Fraumeni syndrome) [11]. In contrast, acquired mutations in p53 are found in more than 50% of human tumor types, and so contribute to the complex network of molecular events

leading to tumor formation. One crucial effect of mutant p53 is that it can no longer bind DNA in an effective way, and as a consequence the p21 protein is not made available to act as the 'stop signal' for cell division. Thus cells divide uncontrollably and form tumors [1].

1.1.4 LIMITLESS REPLICATIVE POTENTIAL

Cultured cells exhibit a limited replication potential under normal conditions as a result of senescence, a phenomenon whereby cellular growth is stopped following a series of replication. This process can be manipulated by disabling tumor suppressor proteins like **pRb and p53**, resulting in cellular crisis. Massive cell death, karyotypic disarray, including end-to-end fusion of chromosomes, and immortalization may be observed as accompanying events. However, in culture the majority of tumor cells appears immortalized, leading to the suggestion that limitless replicative potential is an ability acquired during tumor progression *in vivo*, important for the development of malignant growth state [1].

In normal cells a progressive shortening of repeats of 6bp long elements (“telomers”) occurs at the end of chromosomes. Unprotected ends of chromosomes participate then in end-to-end fusions forcing affected cells to death. In contrast to normal cells, telomerase enzymatic activity appears maintained in all types of malignant cells, gaining the ability to restore telomeres by up-regulating enzyme expression. **Telomerase** serves to put hexanucleotide repeats onto telomeric ends of DNA or through activation of a specific mechanism, termed alternative lengthening of telomeres (ALT). This mechanism works by maintaining telomers through recombination-based, interchromosomal exchange of sequences. Most of the normal human cells have those two mechanisms strongly suppressed [12].

Whereas telomere maintenance is clearly a key component for unlimited replication the molecular process of senescence is only partially understood. Senescence is found to be induced in some cultured cells after high expression of genes such as the activated *RAS* oncogene. Senescence reflects a protective mechanism that can be induced by shortened telomeres or conflicting growth signals that lead aberrant cells irreversibly into G₀-like state [1].

1.1.5 SUSTAINED ANGIOGENESIS

In order to progress, neoplastic tissues must develop the ability to undertake **angiogenesis** which may be encouraged or blocked by the counterbalance of positive and negative signals including soluble factors, their receptors, integrins and adhesion molecules. The angiogenesis-initiating signals include **vascular endothelial growth factor (VEGF)** as well as acidic and basic **fibroblast growth factors (FGF1/2)**. The inhibition of angiogenesis is achieved through the binding of thrombospondin-1 to CD36, a transmembrane receptor on endothelial cells and subsequent coupling to intracellular SRC-like tyrosine kinases [1,13].

Tumors have the ability to either increase the expression of VEGF and/or FGFs in contrast to their normal tissue counterparts, or down-regulate the expression of endogenous inhibitors such as **thrombospondin-1** or **interferon-beta** [1,13].

1.1.6 TISSUE INVASION AND METASTASIS

The primary tumor masses release “pioneer” cells and metastasize to move out and settle at distant sites - a phenomenon responsible for 90% of deaths due to cancer. The ability for **invasion and metastasis** capacitates cancer cells to leave the primary tumor mass and colonize areas anywhere else in the body where nutrients and space are not limited. This capability depends on all other five acquired hallmarks as well [14].

Cellular mechanisms, which allow the invasion and development of metastasis, involve **cell-cell adhesion molecules (CAMs)** and **integrins**. The most observed changes involve **E-cadherin**, which is a homotypic cell-to-cell interaction molecule and ubiquitously expressed on epithelial cells. The function of E-cadherin is notably lost in the majority of epithelial cancers through mutational inactivation of E-cadherin or β -catenin genes, transcriptional repression, or proteolysis of the extracellular cadherin domain. An important suppressor of invasion and metastasis is depicted by E-cadherin in epithelial cancers. Another important contribution to the processes of

invasion and metastasis is the expression of **CAMs** belonging to the immunoglobulin superfamily (in particular **N-CAM**) [1].

The second part of promotion of invasiveness and formation of metastasis involves extracellular processes such as up-regulation of **protease genes**. Invasion by cancer cells into the stroma can be facilitated by docking of active proteases on the cell surface [15]. Digestion of barriers depicted by extracellular matrix components is mediated through **matrix metalloproteinases (MMP)**. In HCC patients, over-expression of MMP-2/ -9 is observed and associated with invasiveness [16].

1.2 The Hippo Pathway

The Hippo pathway got its name from Hippo (Hpo), which is a member of the core kinase complex in *Drosophila melanogaster*, where the pathway was first discovered [17,18].

It is comprised of tumor suppressors and oncogenes. Whereas the core components and upstream regulators are predominantly suppressive, the transcription co-activators YAP/TAZ and the transcription factors TEAD1-4 (TEF) are mostly involved in oncogenic events [19].

Several pathways are currently known to mediate cell fate decisions such as Notch, transforming growth factor beta (TGF- β), Hedgehog, Janus kinase (JAK)/signal transducer and activator of transcription (STAT) and the Hippo pathway [20]. There is also evidence that these pathways are involved in cross-talks with each other [21].

1.2.1 DISCOVERY

The Hippo pathway was initially characterized in *D. melanogaster* where the pathway was shown to be involved in tissue growth control. Originally, the genes involved in the Hippo pathway were identified through clonal genetic screens [17,22-24]. The pathway consists of **upstream regulators** at the **cell surface** including cell adhesion molecules and cell polarity complexes, a **kinase cascade** composed of two serine-threonine kinases with adaptors and regulators and a **downstream target** which functions as a transcription co-activator [21,22].

The kinase cascade was found to be composed of Hpo (Hippo) which is a Ste20-like kinase and NDR family kinase Wts (Warts). Hpo first associates via its C-terminal domain with the N-terminal domain of its adaptor protein, the scaffolding WW-domain containing protein Sav (Salvador) via their SARA (Sav/Rassf/Hpo) domain. Secondly, the complex is able to phosphorylate and therefore activate Wts which then interacts with its regulatory protein Mats. Phosphorylation of Mats by Hpo increases the affinity for Wts. Furthermore, after forming a complex with Mats, Wts is able to directly phosphorylate the transcription co-activator Yki (Yorkie) at three

HXRXXS consensus motifs which leads to cytoplasmic retention of this factor and interaction with the 14-3-3 protein [17-28].

Conversely, when the Hippo pathway is inactive, Yki is no longer phosphorylated by Wts and is able to translocate into the nucleus where it initiates gene expression. It therefore associates with the transcription factor Sd (Scalloped) which belongs to the TEAD/TEF family and promotes cell survival and proliferation. Yki promotes gene expression by interacting with other DNA binding proteins like Mad, Homothorax (Hth), and teashirt to promote gene expression. This co-transcription factor is negatively regulated by the pathway to restrict cell proliferation and promote cell death [24,26,29].

The Hippo pathway is regarded as a tumor suppressor pathway. Mutations in components which regulate the pathway result in an over-growth phenotype. Its main function is to govern diverse cellular processes, including cell survival, proliferation, differentiation and organ size [24]. Moreover, the Hippo pathway plays a fundamental role in organ growth control, stem cell function, regeneration and tumor suppression and is conserved throughout the animal kingdom [31].

Although most of the Hippo pathway components were initially identified in *Drosophila*, much research has recently been performed in mammalian cells and animal models, revealing this pathway's important contribution to tissue homeostasis, organ size control, cancer development and stem cell biology [24]. In human cancers, a dysfunction of the pathway is frequently detected and correlates with poor prognosis. However, it is very likely that altered pathway function underlies many human diseases besides cancer such as cardiac dysfunction or atherosclerosis [29].

All the components of the Hippo pathway in *Drosophila* are well conserved in mammals and include **Fat4** (Ft homolog), **FRMD6** (Ex homolog), **NF2** (Mer homolog), **MST1/2** (Hpo homolog), **WW45** (Sav homolog), **LATS1/2** (Wts homolog), **MOB1** (Mats homolog), **YAP** and **TAZ** (Yki homologs) and **TEAD** (Sd homolog) [18,22].

1.2.2 MECHANISM IN MAMMALS

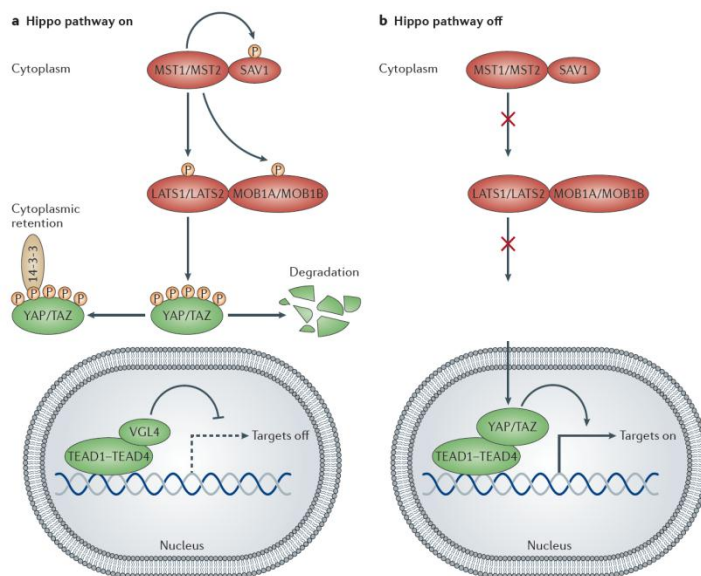


Figure 2: Hippo pathway ON and OFF in mammals [31]

a) Pathway on: LATS1/2 gets phosphorylated by MST1/2 which further is able to phosphorylate YAP/TAZ. This leads to cytoplasmic retention and degradation of respective co-transcription factors. VGL4 is able to bind TEAD1-4 and leads to a suppression of target genes. **b) Pathway off:** There are many factors that potentially lead to an inactivation of the Hippo pathway under physiologic conditions in particular during embryonic growth or tissue repair. In all cases MST1/2 gets inactivated and is not able anymore to phosphorylate LATS1/2. This leads to translocation of YAP/TAZ into the nucleus and the expression of YAP/TAZ and TEAD1-4 dependent genes, such as CTGF.

Mammalian homologues of the *Drosophila* Hippo pathway have been identified for nearly all components (Fig. 3) [29]. The Hippo core kinase cascade includes two serine/threonine kinases, MST1 (STE-20 like protein kinase 1) and MST2 in addition to LATS1 (large tumor suppressor homolog 1) and LATS2 kinase [23,31]. Other important components are represented by SAV-1 (Salvador homolog 1; also known as WW45), which interacts with MST1 and MST2, and MOB1A (MOB kinase activator 1A) and MOB1B, which associate with LATS1/2. The MST kinase first forms a complex with SAV-1 before it activates the NDR family kinases LATS1 and LATS2 and MOB1 co-factors through phosphorylation [31,32]. The targets of those kinases are the paralog transcription co-activators YAP, the mammalian ortholog of Yorkie [32] and TAZ also known as WWTR1 [33]. The phosphorylation of the transcription regulators by LATS1/2 promotes their cytoplasmic localization by facilitating their interaction with 14-3-3 proteins mediated through phosphorylation of Ser-89 of human TAZ and Ser-127 of human YAP. The phosphorylation of other serine residues also influences YAP/TAZ localization. Low LATS1/2 activity increases nuclear YAP/TAZ levels. These two proteins do not bind directly to DNA but rely on DNA binding factors. Their interaction is mediated through a small modular domain known as the WW domain, which is present in a number of Hippo pathway components [33,34]. YAP and TAZ are able to form complexes with the TEA domain containing sequence-specific transcription factors TEAD1 to TEAD4, their main

partners, but also SMADs, TBX5 (T-box transcription factor 5), RUNX1 (RUNT-related transcription factor 1), RUNX2 and p73. If YAP and TAZ are no longer present in the nucleus TEADs form complexes with VGL4 (transcriptional cofactor vestigial-like protein 4), which represses target gene expression [31]. Constitutively nuclear YAP or TAZ enhances cell proliferation and avoids contact-dependent growth inhibition. Different isoforms of YAP and TAZ possess either one or two WW domains that mediate interaction with a PPxY or PY motif. Interaction of YAP/TAZ with TEAD is able to drive cell transformation, whereby TEAD proteins bind the N-terminal region in YAP/TAZ in a region that is distinct from the WW domain [30-35].

The Hippo signal transduction pathway is negatively regulated and inhibits the nuclear translocation of YAP1 (Yes associated protein) and transcriptional co-activator TAZ both of which are homologs. Thus, if the pathway is on, the activity of YAP and TAZ is inhibited and gene expression driven by those components is suppressed. The main purpose of the Hippo pathway is to inhibit nuclear functions of YAP and TAZ [19,34].

1.2.3 REGULATION OF THE HIPPO PATHWAY

1.2.3.1 UPSTREAM REGULATORY ELEMENTS

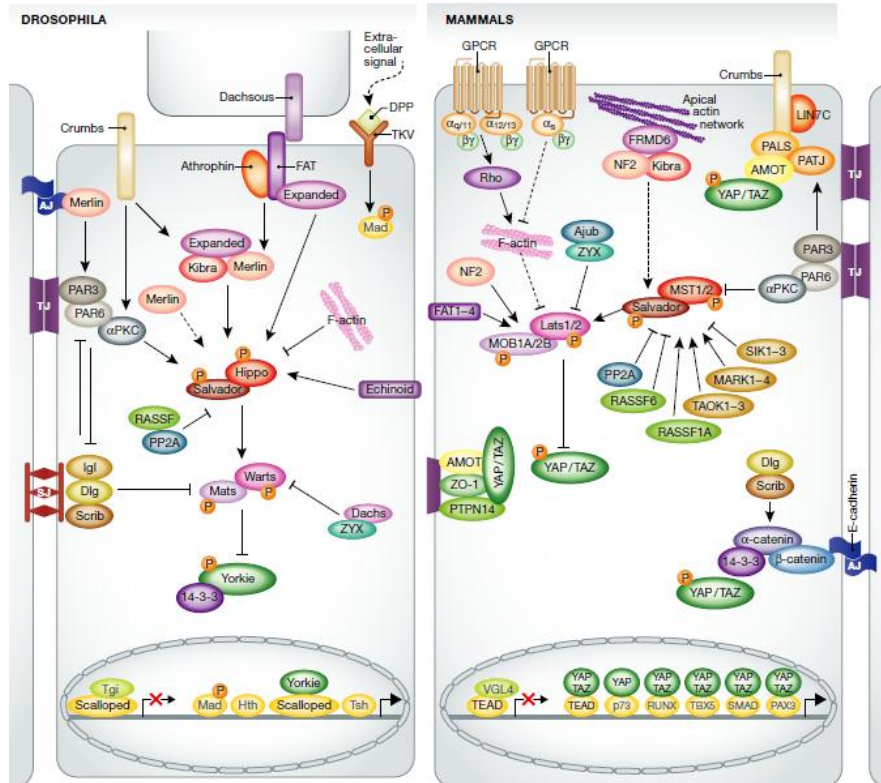


Figure 3: Regulation of the Hippo pathway in *Drosophila* compared to those in mammals [24]

Recent studies have revealed a complex network of Hippo pathway modulators. These upstream input factors include **cell density**, **mechanical sensation**, and **G-protein-coupled receptor (GPCR) signaling** [24,36,37]. In contrast to many other signal transduction pathways like EGF (epidermal growth factor), TGF- β (transforming growth factor-beta) or WNT signaling pathways, the Hippo pathway does not appear to have dedicated extracellular signaling peptides and receptors. Instead, a network of upstream components and mechanisms which are involved in regulating cell adhesion and cell polarity, were found to stimulate the signaling [31]. These mechanisms include dynamics of the **actin cytoskeleton** (RHO-GTPase proteins) through cell-cell contact, **transmembrane proteins composed** of Merlin/NF2 and FRMD6 (EX), α -catenin (**adherent junction-associated** protein), ZO-2 (**tight junction-associated** protein), the **polarity regulating** proteins of the Crumbs complex (PATJ, MPDZ, PALS1, LIN7c) and **Scrib** complex (SCRIB, DLG and LGL), **AMOT** (Crumbs complex associated protein) and the atypical **PKC kinases** [33].

1.2.3.1.1 ACTIN CYTOSKELETON

Key events that influence cell decisions in order to keep individual cells and whole tissues in a certain shape are cell-extracellular matrix (ECM) and cell-cell adhesion, the organization and tension forces. These elements are important for control of cell proliferation, cell migration, stem cell identity, differentiation and cell death [43]. One of the first stimuli described to influence the localization of YAP and TAZ was cell contact. Cells which grow with a high density display high cytoplasmic YAP/TAZ localization in contrast to low-density growing cells showing high nuclear YAP/TAZ activity [33].

1.2.3.1.2 KIBRA-EXPANDED-MERLIN IN *D.MELANOGASTER*

Ex and Mer, both of which contain a FERM-domain have been shown to act upstream of the Hippo pathway. Moreover, Kibra was identified to be another upstream regulator by interacting with several proteins including Mer, Ex and Hpo/Sav. Kibra is suggested to act as a key membrane scaffolding protein which not only promotes the assembly of the Ex-Kibra-Mer complex at the apical membrane but may also recruit Hpo-Sav and Wts-Mats onto that complex leading to the effective activation of the Hippo core machinery. The mammalian orthologs of Kibra, Expanded and Merlin are Kibra, Willin and NF2. Human Kibra (WWCI) was identified due to its enrichment in kidney and brain. Through its interaction with neurofibromin 2 (NF2), phosphorylation of LATS1/2 can be synergistically enhanced by co-expression of human Kibra and NF2 [38-41].

1.2.3.1.3 ADHERENT JUNCTIONS

Perhaps the most-well defined upstream branch that controls the Hippo pathway is composed of atypical cadherins, Fat and Dachous. However, it is currently only known to operate in *D. melanogaster* to repress tissue growth by promoting the abundance of Warts and Expanded [38].

The engagement of **E-cadherin** at adherent junctions regulates MST activity by suppressing nuclear localization and activity of YAP. The E-cadherin-associated protein α -catenin regulates YAP directly by sequestering YAP-14-3-3 protein. Furthermore, members of the junction-associated Ajuba protein family directly inhibit LATS kinase activity [31,49]

1.2.3.1.4 APICO-BASAL CELL POLARITY (ABCP) PROTEINS

These complexes of proteins include the mammalian Scribble (SCRIB), which is able to facilitate the activation of the core kinase cassette and the Crumbs complex, which binds and sequesters YAP and TAZ [33,38-41]. Crumbs (Crb) which is a large apical membrane protein with a short cytoplasmic region is a key regulator of epithelial cell polarity and also suggested to be important for apical membrane localization of Ex in epithelial cells [18]. It is also likely that Crb, by organizing the epithelial polarity and junctional complexes, is able to promote the apical membrane recruitment of Ex and therefore facilitating the formation of the Ex-Kibra-Mer complex. It in turn recruits the Hpo-Sav and Wts-Mats complexes to the apical membrane. There are three mammalian Crb homologs with Crb3 shown to act as a tumor suppressor [18].

CRB complex (Crumbs homolog)

The CRB complex contains CRB proteins, which are transmembrane proteins that localize to apical junctions. They are required to determine the apical plasma membrane domain [45]. Through their short intracellular domains with protein docking sites they are able to assemble multi protein complexes that have a great function in cell polarity and are also suggested to regulate the Hippo pathway by recruiting members of the angiomin (AMOT) family of adaptor proteins. Depending on the cellular and molecular context AMOT may have both growth-promoting and growth-suppressing functions. On the one hand AMOT is directly binding to YAP leading to inhibition of nuclear localization of this transcription co-factor, on the other hand it is activating LATS kinases that promote phosphorylation of YAP at serine 127 leading again to nuclear exclusion. However, there is also contradictory evidence that AMOT promotes the nuclear localization of YAP and that it forms a functional complex with YAP and TEADs on target gene DNA [31,43-45].

1.2.3.1.5 G PROTEIN-COUPLED RECEPTORS (GPCRs)

The signaling of several GPCRs is able to activate or inhibit YAP/TAZ dependent on the type G-protein used. G12/13 or Gq/11 stimulates YAP/TAZ whereby Gs inhibits the co-transcription factors [24]. G protein-coupled receptors are also proposed to modulate the Hippo pathway. For instance, it was shown that LATS1/2 is regulated by GPCRs [38]. In particular, GPCRs involved in cell proliferation stimulate the activity of YAP. GPCRs linked to Galpha-12/13 inhibit the activity of LATS, thereby relieving YAP from LATS-dependent inhibition, while receptors activating Galpha-s promote LATS activation thus inhibiting YAP [47]. Recent work by Gutkind and colleagues indicated that oncogenic mutations in the gene encoding Galpha-q activate YAP by a mechano-sensing pathway. The trigger seems to come from actin polymerization rather than by the inhibition of the Hippo pathway [48].

1.2.3.1.6 OTHER REGULATORS

Despite many different molecular mechanisms controlling or influencing the Hippo pathway, cross-talk among the regulatory branches is also suggested to exist [50]. In addition to the main regulators of the Hippo pathway, there are also other proteins that modulate its activity. Proteins like WBP2 (WW domain-binding protein 2), MASK (multiple ankyrin repeats single KH domain-containing protein), ZO1/2 (zona occludens protein 1/2), HIPK2 (homeodomain-interacting protein kinase 2), 14-3-3 protein, PTPN14 (protein tyrosine phosphatase non-receptor type 14), CSNK1 (casein kinase 1) and β -TRCP are also proposed to directly interact with or affect YAP and TAZ [51,52]. There are proteins that interact with the upstream kinase complexes such as the RASSFs (RAS association domain-containing family proteins) [53], PP2A (protein-phosphatase 2A) [54], SIKs (salt-inducible kinases) [55], Merlin [56], Scribble and the Scribble-associated proteins Dlg (discs large) and LgI (lethal giant larvae) [31,41,57]. In *D. melanogaster* the Hippo pathway is also regulated by a signaling axis from the atypical cadherin FAT, which regulates the levels and activity of Warts kinases. However, it is not clear whether there are also FAT homologs that are involved in the regulation of the Hippo pathway in vertebrates [31].

microRNA-375

MicroRNAs are important regulatory elements which control gene expression at post-transcriptional level. They especially have been linked to the regulation of oncogenes or tumor suppressors [107]. Example are the tumor suppressor tensin homolog (PTEN), which is regulated by **miR-21** [108] and oncogenes, such as *RAS* and *HMG2*, which are regulated by **let-7** families [109]. Interestingly, **miR-375** has been proposed to be involved in the regulation of oncogenic YAP by suppressing it. Ectopic expression of miR-375 in two different cell lines led to a decrease in YAP protein- and *CTGF* mRNA- level, which is a direct target of YAP [58].

Table 1: Core components of the Hippo pathway and its modulators [31]

Human proteins	<i>D. melanogaster</i> protein	Protein function	Domain composition
Core components			
MST1, MST2	Hpo	Serine/threonine kinase, STE 20 family	Kinase domain, SARAH domain
SAV1 (also known as WW45)	Sav	Adaptor protein	FERM domain-binding motif, two WW domains, SARAH domain
LATS1, LATS2	Wts	Serine/threonine kinase, NDR family	Kinase domain
MOB1A, MOB1B	Mats	Cofactor	MOB domain
YAP, TAZ	Yki	Transcriptional co-activator	Two WW-domains, 14-3-3 binding motif, TEAD-binding motif, PDZ-binding motif
TEAD1-TEAD4	Sd	Transcription factor	TEAD DNA-binding domain, vestigial binding domain
Pathway modulators			
CRB1-CRB3	Crb	Transmembrane receptor	EGF domains, four laminin AG domains, transmembrane domain
PATJ, MUPP1	Patj	Adaptor protein	Ribosomal protein L27, eight PDZ domains
MPP5 (also known as PALS1)	Sdt	Adaptor protein	Ribosomal protein L27, PDZ domain, SH3 domain, GUK domain
AMOT, AMOTL1, AMOTL2	-	Adaptor protein	Coiled coil domain, PDZ binding motif
NF2	Mer	Adaptor protein	FERM domain
KIBRA	Kibra	Adaptor protein	Two WW domains, C2 domain
FRMD6 (also known as EX1)	Ex	Adaptor protein	FERM domain
TAO1-TAO3	Tao	Serine/threonine kinase	Kinase domain
MARK1-MARK4	Par-1	Serine/threonine kinase	Kinase domain
E-cadherin	E-cadherin	Transmembrane receptor	Five cadherin domains, transmembrane domain
α -catenin	α -catenin	Adaptor protein	VH1-VH3 domains
Ajuba, LIMD1, WTIP	Jub	Adaptor protein	Three LIM domains
ZYX, LPP, TRIP6	Zyx	Adaptor protein	Three LIM domains
RASSF1-RASSF6	Rassf	Adaptor protein	RAS association domain, SARAH-domain
PP2A	STRIPAK-PP2A complex (sSTRIPAK)	Phosphatase	Phosphatase domain
SCRIB	Scrib	Adaptor protein	16LRP domains, 4PDZ domains
LGL1, LGL2	Lgl	Adaptor protein	Four WD40 domains
DLG1-DLG4	Dlg	Adaptor protein	Three PDZ domains, SH3 domain, GUK domain
PTPN14	Pez	Phosphatase	FERM domain, phosphatase domain
CSNK1	Dco	Serine/threonine kinase	Kinase domain
β -TRCP	Slimb	SCF-type E3 ubiquitin ligase	F-box domain, β -TRCP domain, WD40 domain
HIPK	Hipk	Serine/threonine kinase	Kinase domain
MASK1, MASK2	Mask	Adaptor protein	Two ankyrin domains, KH domain
WBP2	Wbp2	Cofactor	GRAM domain
VGL4	Tgi	Cofactor	Two tondu domains

1.2.3.2 EFFECTOR KINASES

Hippo (669A) and the shorter **MST1** (487AA) and **MST2** (491AA) polypeptides show the same domain structure as group II GCKs (germinal center kinases) with the exception of the specialized coiled-coil domain near the carboxy terminus known as the **SARAH domain**. This domain presents an acronym derived from the three gene families that contain homologous domains i.e. Salvador/SAV1-WW45, RASSF(1-6) and Hippo/MST1/MST2. The MST1 SARAH domain (AA432-480) forms a hairpin of helical segments, with the short N-terminal helical segment (AA433-437) bent back approx. $\sim 45^\circ$ towards the C-terminal helix (AA441-480). The **RASSF** polypeptides, 1-6 non catalytic polypeptides, contain a RAS-RAP association (RA) domain which is followed by a SARAH domain [32]. This enables them to hetero-dimerize with MST1 or MST2. The SARAH domain has also been implicated in Hpo binding and Wts was found to directly interact with the WW domains of Sav through its five PPXY motifs [18].

Another important feature of MST1/2 is the presence of cleavage sites for **caspase 3**, a basis for the hypothesis that catalytically active MST1/2 fragments are generated by caspase 3 cleavage of MST1. Whereas the SARAH domain mediated the binding to Hippo, SAV-1 also encodes tandem WW domains, which mediate the binding to LATS [32].

1.2.3.3 (CO-) TRANSCRIPTION FACTORS

YAP1 (Yes-1 associated or activated protein)

YAP was originally identified as a binding partner of **YES-1**, a member of the SRC family kinases, whereas other interacting partners include **TEADs**, **Smad1**, **RUNX**, **ErbB4** and **p73** transcription factors. TEAD family members were also found to be critical in the YAP regulation of gene expression [59].

YAP can be regulated in two different ways including phosphorylation-dependent and –independent mechanisms. The dependent route involves the phosphorylation of YAP on five **HXRXXS** motifs by core kinase cassette LATS1/2 on S-127, resulting in

cytoplasmic retention of YAP and 14-3-3 binding. The phosphorylation of YAP's HXRXXS motifs is facilitated by interaction of the WW-domain of YAP with the **PPxY** motifs in LATS. This phosphorylation creates a binding site for 14-3-3 proteins which provides the basis for the inhibition by the Hippo core components. Additionally, the phosphorylation on S-381 primes YAP to be subsequently phosphorylated by CKI delta/epsilon, which leads to ubiquitination and proteosomal degradation of YAP [19,60]. The second mechanism to inhibit the transcription co-activator in *Drosophila* is the direct binding of Ex to Yki which leads to re-localization from the nucleus into the cytoplasm which in turn regulates growth by reducing levels of Yki in the nucleus [61].

YAP was described as candidate oncogenic protein in mammals whereas *YAP* is amplified with **chromosome 11q22** [62]. Furthermore, this co-transcription factor was shown to be over-expressed and localized in the nucleus in a number of different human tumors like **colonic, ovarian, lung, hepatocellular, pancreatic, prostate, gastric** and **oral carcinomas** [63]. Another characteristic obtained from YAP over-expression includes cancer stem cell properties and cancer metastasis through induction of epithelial-mesenchymal transition (EMT) [19,62].

The protein domains of YAP (Fig. 4) consist of an N-terminal proline-rich region, a TEAD binding domain, two tandem WW-domains, an SH3 binding motif, a coiled-coil domain, a transcription activation domain and a C-terminal PDZ binding motif [19,60]. In contrast, the paralog of YAP, TAZ was originally identified as a 14-3-3 binding protein [64] and has a similar structure to YAP, with the exception of the proline-rich region, the second WW domain and the SH3 binding motif [65].

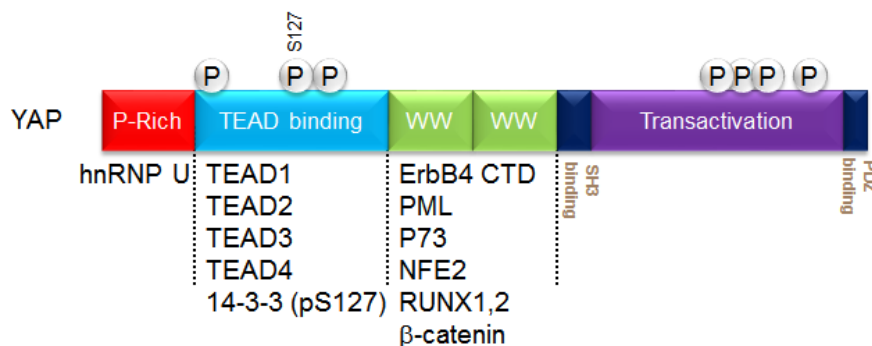


Figure 4: Protein domains of YAP and Interaction partners [18]

Proline-rich domain, TEAD binding domain, WW domain, a SH3 binding site, transactivation domain and a PDZ binding motif

Recent studies have shown that YAP can also be regulated via interaction with non-receptor tyrosine kinase PTPN14 through the WW domain of YAP and the PPxY domain of PTPN14. YAP was shown to be a direct substrate of PTPN14 which inhibits the transcription through protein interaction. Furthermore, the knockdown of PTPN14 leads to nuclear retention of YAP [66].

TAZ

TAZ (WWTR) was identified as 14-3-3 binding protein and has a similar structure to its paralog YAP with the exception of a proline-rich structure, a second WW domain and an SH3 binding motif. It was also shown to induce EMT and mediates TEAD dependent transcription. It is phosphorylated by LATS at serine 89 [18,19,64,65].

TEAD1-4

All four members of the transcription enhancer were found ubiquitously expressed in mice and humans but differentiate between their proline-rich regions and N-termini. While knockout of TEAD2 has no influence on mice, the double knockout (TEAD1/2) mice show reduced cell proliferation and increased apoptosis suggesting both having an overlapping role [67]. TEAD1 and TEAD4 are suggested to play the most important role for proliferation and cancer development [19,68]. The YAP/TEAD complex is formed by interaction of the C-terminal YAP-binding domains of TEAD (Fig. 5) with the N-terminal TEAD-interacting domain of YAP [69]. Nuclear magnetic resonance (NMR) studies have shown that the N-terminal TEAD-binding domain of YAP is natively unfolded and binding of TEAD forces YAP to undergo a conformation change [70].

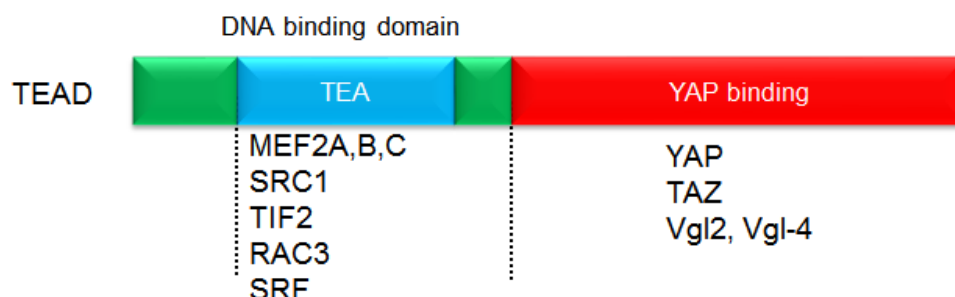


Figure 5: TEAD protein domains and interaction partners [19]

1.2.4 BIOLOGICAL FUNCTIONS OF THE HIPPO PATHWAY

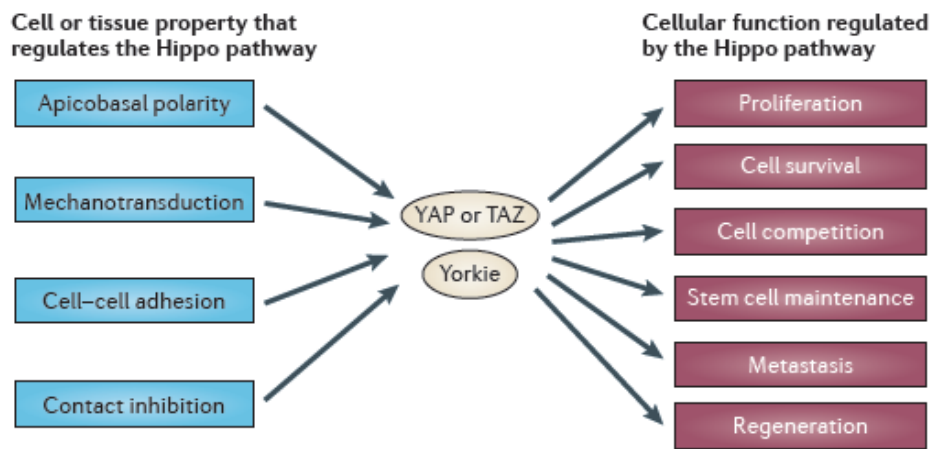


Figure 6: Biological functions of the Hippo pathway relevant to cancer [71]

1.2.4.1 CELL PROLIFERATION

As a result of the Hippo pathway being linked and regulated by several key mechanisms associated with tumorigenesis, the deregulation of this signaling leads to cell proliferation by causing neoplasia. Mutations in proteins of the Hippo pathway which lead to Yki hyper-activation in flies, or YAP or TAZ hyper-activation in mammals, are the cause for ectopic cell proliferation. Clones of cells with increased Yki activity in *D. melanogaster* imaginal discs were shown to progress through the cell cycle much faster than the wild-type control group; a phenomenon also proved in murine tissue. Following YAP over-expression or hyper-activation, excessive proliferation in multiple tissues has been observed including liver, gastrointestinal tract, skin and heart [71].

1.2.4.2 CELL SURVIVAL

Deregulation of the Hippo pathway contributes to tissue over-growth not only by promoting cell proliferation but also by developing insensitivity towards apoptosis. Both processes are central to carcinogenesis whereas YAP over-expression can

contribute to cell survival both *in vivo* and in cultured cells. YAP over-expression leads to the blockage of tumor necrosis factor- and Fas- induced apoptosis which contributes to apoptosis and drug resistance [71].

1.2.4.3 CELL COMPETITION

There is evidence that healthy cells can cause their neighbor cells to die. These are in particular factors that provide cells a relative survival advantage including increased translation efficiency, high expression of *MYC* or hyper-activation of Yki [71].

1.2.4.4 MAINTENANCE OF STEM CELL PHENOTYPE

Tumor cells have the ability to gain properties that are associated with stem or progenitor cells including substantial replicative potential, resistance to chemotherapeutic drugs and loss of mature differentiation markers. Several studies have suggested that the Hippo pathway is also linked to stem cell control. Both the YAP and TEAD transcription factors were shown enriched in multiple types of stem cells by promoting pluripotency of embryonic stem (ES) cells. Furthermore, TAZ regulates the mesenchymal stem cell differentiation [71].

1.2.4.5 PLANAR CELL POLARITY

In *D. melanogaster* planar cell polarity (PCP) and tissue growth is controlled via the Hippo pathway. However, there are no thoroughly explored links to mammals [71].

1.2.4.6 APICO-BASAL CELL POLARITY

Apicobasal cell polarity (ABCP) allows epithelial tissues to define and maintain functionally distinct membrane surfaces, the apical and basolateral side. In *D. melanogaster* epithelial tissues the loss of the ABCP proteins like Lethal giant larvae, Crumbs or Scribble lead to Hippo pathway repression and Yki-dependent hyperproliferation. Whereas Crumbs physically interacts with Expanded and therefore regulate its levels and subcellular localization, Lethal giant larvae has been shown to regulate the subcellular localization of Hpo and its inhibitor Rassf. Furthermore, Scribble was shown to bind to members of the Hippo pathway core kinase proteins in mouse cells and has been postulated to suppress YAP and TAZ. ABCP proteins have been shown to be mislocalized in some cancers [71].

1.2.4.7 CELL-CELL ADHESION

Adherent as well as tight junctions are the mediators of adherence of mammalian epithelial cells. One of the key components is E-cadherin and mutation in this protein leads to familial diffuse gastric cancer. Studies have shown that key junctional proteins such as Crumbs, PATJ, PALS, angiopotins, alpha-catenin and E-cadherin are able to form a complex with and also regulate YAP and TAZ by sequestering them at cell junctions. This prevents their entrance into the nucleus and access to phosphatases that antagonize the activity of YAP- and TAZ- inhibitory kinases. E- and α -cadherin have been shown to control proliferation of cultured cells and might play a role in tumors where the function of cell-cell adhesion proteins are compromised [71].

1.2.4.8 CONTACT INHIBITION

When cells come into physical contact with their neighbors they cease proliferation, a phenomenon which is called contact inhibition. Loss of this effect is a property of

transformed cells *in vitro* which can be achieved by artificial over-expression of YAP or loss of the upstream Hippo pathway protein NF2 [71].

1.2.4.9 MECHANOTRANSDUCTION

The Hippo pathway has previously been suggested to control organ size partly by responding to mechanical cues such as stretching and compression. YAP and TAZ were shown in mammalian cell culture to be active when cells are stretched and repressed or when they are compressed, a molecular event mediated by the actin cytoskeleton [71].

1.2.4.10 METASTASIS

A leading cause of patient death as a consequence of cancer is attributed to the formation of metastasis from advanced solid tumors. LATS1/2 expression has been shown to be significantly low in metastatic compared to non-metastatic, prostate cancers whereas loss of E-cadherin might also cause YAP and TAZ de-repression in metastatic cells, which might lead to EMT [71].

1.2.4.11 REGENERATION

Injury to tissue and chronic infection has been proposed to drive carcinogenesis, particularly in liver. The liver presents a highly regenerative organ in which the Hippo pathway has been identified to play an important role in its regenerative growth in *D. melanogaster* and mammalian epithelial tissues. Thus, it may be suggested that YAP and TAZ hyper-activation could be drivers of carcinogenesis in chronically regenerating tissues [71]. The Hippo signaling pathway plays a role in tissue homeostasis and organ size control by regulating tissue-specific stem cells. Moreover, this pathway plays a key role in tissue repair and regeneration [24].

1.3 Hepatocellular Carcinoma

The three main and prominent hepatic malignancies include hepatocellular carcinoma (HCC), cholangiocarcinoma (CC) and hepatoblastom (HB). Patients who are suffering from those cancers are characterized with poor prognosis. Treatment options are extremely limited mainly because of the lack of a detailed understanding of the complete mechanisms of pathogenesis. Studies have revealed that a deregulation in the Hippo pathway contributes to hepatocellular carcinoma formation where YAP/TEAD hetero-dimerization activates a number of genes involved in cell proliferation including *Survivin (BIRC5)*, *CTGF* and *Cyclin D1* [72].

1.3.1 LIVER PROGENITOR CELLS AND TUMORIGENESIS

The liver is the most important metabolic organ and is able to regenerate after more than 70% hepatectomy through its high regenerative capacity which depends on hepatocyte proliferation. Proliferation of liver progenitor cells give rise to both hepatocytes and cholangiocytes (biliary epithelial cells, BECs), which are the prominent epithelial cells of the bile duct [24].

There is a distinct ability to rapidly regenerate adult liver after acute injury and the generation of the organ is dependent on proliferation of hepatocytes and cholangiocytes (bile duct cells) where YAP, under the control of upstream Hippo pathway regulators, plays a crucial role. Interestingly over-expression of a nuclear localized YAP mutant in the mouse liver leads to rapid liver enlargement by increasing hepatocyte proliferation, a characteristic of hepatocellular carcinoma by providing cells with a resistance to apoptosis. These proto-oncogenic effects of YAP can be reversed by expressing a dominant-negative derivate of TEAD2 that lacks a DNA binding domain, which YAP is dependent on in order to fulfil its function. The disruption of this protein-protein interaction can also be mediated through a small molecule, Verteporfin, which was shown to suppress tumorigenesis following YAP expression in mice. SAV-1, MST1 and MST2, effectors of the Hippo pathway additionally have been characterized as negative regulators of YAP activity in liver whereby liver-specific deletion of *SAV-1*, or combined deletion of *MST1* and *MST2*

leads to increased liver mass and hepatocellular carcinomas. Furthermore, liver-specific deletion of *NF2*, another Hippo pathway component, was also able to initiate tumor formation in mice [33].

WNT and GPCR signaling pathways have also been recognized as important regulators of YAP/TAZ [73].

1.3.2 DEREGULATION OF THE HIPPO PATHWAY

A deregulated Hippo pathway is associated with cancer development [60,63,74]. Deregulation has been observed with a high frequency in a broad range of different human carcinomas, including lung, colorectal, ovarian, liver and prostate cancers. It is also correlated with a poor patient prognosis [71]. Immunohistochemical analysis showed YAP located in the nucleus of tumor tissue (60% of hepatocellular carcinomas, 15% of ovarian cancers and 65% of non-small-cell lung cancers) in contrast to infrequently nuclear localization in normal human tissues [71]. Compared to other well-known oncogenic signaling pathways, only a few cancers are known to be associated with a direct mutation of a Hippo pathway component [24].

TAZ has been shown to be a key regulator of cancer stem cells (CSCs) in breast cancer. Additionally, YAP and TEAD are highly expressed in CSCs of medulloblastoma. It has been suggested that tumor growth is dependent on CSCs, which represent a small subset of cells within a tumor but have the ability to self-renew, differentiate into other tumor cell types, and initiate tumor formation. CSCs are also thought to be resistant to chemotherapeutic agents and are responsible for cancer recurrence and metastasis [24].

YAP and TAZ are found hyper-activated in many human malignancies. Therefore, therapeutic intervention would involve reducing or inhibiting the oncogenic function of YAP and/or TAZ [31].

There is some evidence that loss of Hippo signaling or hyper-activation of YAP and TAZ promotes growth and cell pluripotency depending on the tissue type. The effect of YAP over-expression and hyper-activation on organ size and progenitor cell pools is dramatic. There are abnormally elevated levels of nuclear-localized YAP found in

various human cancers including liver, lung, breast, skin, colon and ovarian cancer. In addition, loss of Hippo pathway activity in mouse models can be shown to cause over-growth of various organs such as liver and heart. As a result of incorrect Hippo signaling development of cancer in the liver, skin and intestine is observed. In murine models it has been shown that attenuation of Hippo signaling or over-expression of YAP in liver, skin and colon is sufficient to promote tumor formation [31].

Although it is clear that nuclear YAP and TAZ lead to tumor formation the exact mechanism of transforming a cell into a malignant cell is not clear but likely to involve enhanced cell proliferation and survival coupled with the acquisition of additional cancer cell phenotypes such as cancer stem cell characteristics, epithelial to mesenchymal transition (EMT), drug resistance and inhibition of senescence [31].

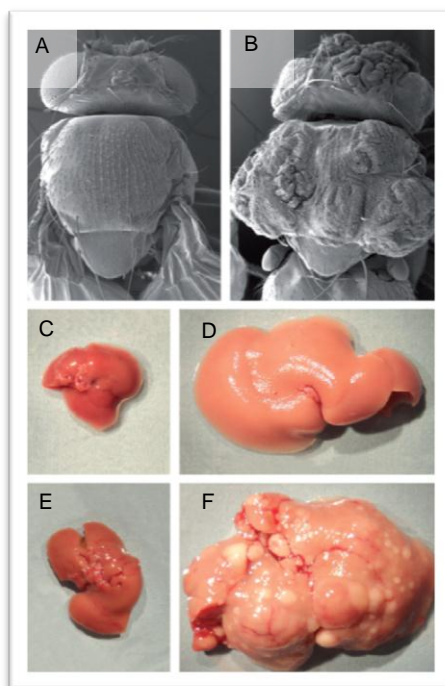


Figure 7: Hippo-mutant phenotypes in *Drosophila* and mice [31]

A) Scanning electron micrographs of a wild-type fruit fly **B)** Homozygous mutant for Hippo (*hpo*) gene **C)** Mouse liver wild-type animal (2 months of age) **D)** *Mst1/2* conditionally deletion in developing liver (2months) **E)** Normal mouse liver (6 months); **F)** Double mutant *Mst1* *-/-* *Mst2* *-/-* (6months) mouse liver

Over-expression of YAP and/or TAZ can lead to a mesenchymal phenotype in mammary epithelial cells, which suggests that Hippo signaling may have important roles in the suppression of EMT. Thus, YAP and/or TAZ activation *via* loss of cell polarity may engage a positive feed-forward loop in which YAP and/or TAZ promote EMT and the loss of cell polarity, which then further activates YAP and TAZ [31].

Loss of function of the Hippo or Warts kinases or over-expression of Yorkie in *D. melanogaster* results in severe tissue over-growth. Similarly, it was shown that over-expression of YAP or loss of MST or LATS kinase activities increased liver and heart size by increasing cell number in mice. In contrast, YAP over-expression in skin or intestine causes an enlargement of stem cell compartment but it does not lead to an overall increase in organ size [31].

1.4 Link between the Hippo Pathway and YES-1

1.4.1 FAMILY OF SRC KINASES

Transmembrane receptors spread the received extracellular signal to the internal control elements of the cell, which influences cell division, differentiation, survival, motility, adhesion, spreading and vesicular transport. Studies suggest that SRC family proteins can compensate for one another, in these pathways. One of the most important groups of non-receptor tyrosine kinases is the SRC-family. It is composed of nine partners including c-SRC, c-YES, FYN, LCK, LYN, HCK, BLK, FGR and YRK. They all carry a similar structural architecture made up of six functional domains including fatty acid acylation domain, SRC homology domain 4 (SH4), an unique domain, SH3 and SH2 domain, SH1 or catalytic domain and a carboxy-terminal regulatory region. The most similar kinases are c-SRC and c-YES, which according to sequence analysis show an overall 80% homology with a 90% homology within the catalytic domain. For this reason it is also not surprising that there are many common upstream signals binding and activating those kinases [75].

1.4.2 YES-1 KINASE

The proto-oncogene *c-YES-1* product, c-YES-1 belongs to the SRC-family protein-tyrosine kinases. The size is about 505-543 amino acid residues and they are highly conserved over a 460-residue contiguous region at the carboxyl terminus including SH2, SH3 and protein-tyrosine kinase domains. SRC kinases differ greatly in an 80-residue contiguous region at the amino terminus. It is known that the kinase activity of c-SRC is negatively regulated by phosphorylation of its C-terminal Tyr-527 residue, whose surrounding sequences are well conserved in c-YES. It has been suggested that the kinase activities are coordinately regulated by de-phosphorylation and phosphorylation of the C-terminal tyrosine by protein-tyrosine phosphatases and C-terminal SRC kinase or auto-phosphorylation. Other regulations can be mediated through auto-phosphorylation at Tyr-416 in c-SRC and Ca^{2+} -dependent inactivation of c-YES. The sequences of c-YES and c-SRC mainly differ in their N-terminal 80

amino acid residues. Both kinases begin with a myristoylated glycine, which allow them to associate with the inner surface of plasma membrane even though they lack a transmembrane domain. Through their unique N-terminal regions within the SRC-family tyrosine kinases they are able to interact with distinct cellular proteins, such as membrane receptors, unique effectors or specific substrates, and most likely play a crucial role in the physiological actions of those kinases [76]. There is evidence that c-YES promotes formation of the tight junction by phosphorylating occludin whereas c-SRC signaling down-regulates occludin formation in a RAF-1 dependent manner [75].

There is clear evidence of overlaps between β -catenin and TAZ or YAP: i) all are short-lived proteins in the cytoplasm and degraded by the same β -TrCP ubiquitin ligase complex, ii) they all control a number of epithelial and non-epithelial specific processes and iii) there is evidence that the same destruction complex which is responsible for β -catenin degradation also restrains TAZ protein levels. The latter effect is not due to direct phosphorylation of GSK3, but it rather seems that the GSK3-phosphorylated β -catenin serves as a scaffold for TAZ association with beta-TrCP/E3 ubiquitin-ligase complex. WNT is not only important for phosphorylation of β -catenin and therefore stabilizing it but is also proposed to be responsible for TAZ accumulation and activation of TAZ-dependent gene responses [77].

Yes-associated protein (YAP) was found to interact with YES-1 tyrosine kinase [29] and YES-1 down-regulation has a significant effect on the survival of basal-like breast cancer cell lines that over-express this gene [78].

1.4.3 STRUCTURES AND UPSTREAM ACTIVATORS

SH4 domain

The amino-terminal SH4 domain contains signals that allow myristoylation and palmitoylation, both of which contribute to the targeting of SRC family proteins to the cell membrane where interactions with growth factor receptors occur. The SH4 is the unique domain, which is heterogeneous across the SRC family protein kinases and is proposed to contribute to the specificity in SRC family signaling. It provides a docking site for specific cellular proteins and presents a unique phosphorylation site for protein serine/threonine kinases and auto-phosphorylation [75].

Activation of YES-1 (Table 1)

The SH3- and SH2-domain, SH2-kinase linker region, and C-terminal regulatory domain contribute to the intramolecular interactions that repress kinase activity. In the inactive kinase the C-terminal regulatory region is phosphorylated at tyrosine (Tyr-535 in c-YES). Intramolecular interactions are maintained by association of the tyrosine phosphorylated C-terminus and the SH2 domain. The deletion of these negatively regulated regions leads to constitutively activated kinases. In addition, the intramolecular interactions between the SH3 domain and the SH2-kinase linker region also contribute to the repression of kinase activity [75].

One class of upstream regulators comprises a group of receptor tyrosine kinases (RTKs) including PDGF-R, CSF-1-R, SCF-R, EGF-R (ErbB-1), NEU (ErbB-2), FGF-R and VEGF-R, respectively. If they get stimulated by a ligand the intrinsic kinase activity of these receptors becomes activated and thus leading to auto-phosphorylation. These phosphorylation sites provide the binding sites e.g. for c-YES. Binding is a prerequisite for activation and for phosphorylation of substrates and specific binding partners [75].

Furthermore, YES-1 was shown to be activated by another receptor class, the G protein coupled receptors (GPCRs) by binding of *G α* and *G β* to the catalytic domain of Src family kinases (SFKs). This results in a conformational change that allows increased substrate accessibility to the kinase [75].

Another form of activation is mediated through cytokine receptors, specifically oncostatin M (OSM), granulocyte macrophage colony-stimulating factor (MCSF/GM-CSF) and tissue factor (TF) [75].

Table 2: Activation of c-YES-1 [75]

Receptor Tyrosine Kinases		
Class I	ErbB1, ErbB2/Neu	Cell proliferation, Cell-Cell Interactions, Angiogenesis
Class III	PDGF-R, CSF-1R, SCF-R	
Class IV	FGF-R	
Class V	Flt-1-R	
G-Coupled Receptors		
	AT-1 Receptor	DNA Synthesis
	PECAM-1 Receptor	Migration, Integrin Interaction
Cytokine Receptors		
	Oncostatin M	IL-6 Induction/Myeloid Differentiation
	IL-11	Hematopoiesis
	TF-R	Cell proliferation, Migration
	GM-CSF	

1.4.4 CONTRIBUTION OF YES-1 TO YAP/TEAD-DEPENDENT TRANSCRIPTION

YES-1 was shown to be important for the growth of β -catenin-active colon carcinoma cell lines and suppression of YES-1 led to inhibition of proliferation. Furthermore, suppression of YES-1 led to reduced levels of *BIRC5* and *BCL2L1*. In addition, the group of Rosenbluh *et al.* [79] was able to show that shRNA against YES-1 did not affect expression of the closely related kinase SRC. They also confirmed interaction of YAP with YES-1 in β -catenin-active colon cancer cell line SW480 and failed to detect an interaction between YAP and other SRC related kinases like SRC or FYN. Furthermore, YAP phosphorylation requires the active form of YES-1 which could be inhibited by the tyrosine kinase inhibitor Dasatinib. SRC family members were found to phosphorylate tyrosine residues in the sequence motif YXXP. YAP harbors one tyrosine residue within such a motif at tyrosine 357. Rosenbluh *et al.* [79] was able to show that no phosphorylation took place when using a YAP Y357F mutant. They also confirmed that phosphorylation of YAP is important for rescue the phenotype after YES-1 shRNA-mediated knockdown by transfecting cells with YAP-wt and YAP Y357F mutated. Taking these results together, YES-1 was confirmed to be essential

for tumorigenicity of β -catenin-dependent cell lines and to regulate YAP activity by phosphorylation of Tyr-357 [79].

1.5 Hippo Pathway and the Therapeutic Concept

Cellular behavior can be described by a regulatory network of interaction between genes and proteins [78]. Targeted cancer therapies aim to neutralize specific proteins (strictly speaking the function of the respective proteins) that are necessary for the cancer cell to remain viable *in vivo* while exhibiting no dramatic effect on normal cells [78]. Ideally, the eradication of the respective gene (gene function) should have a major impact on the survival/fitness of the tumor cells [78].

Transcription co-activators YAP and TAZ have no catalytic function. For that reason inhibition of the protein-protein interaction may be the required target/therapeutic concept [31]. A critical issue of the therapeutic concept and the Hippo pathway is the fact that YAP and TAZ are required for tissue repair and regeneration in the context of injuries which may lead to deleterious side effects on normal tissue function and homeostasis when inhibiting those components [31].

1.6 Aim of the Project

Hepatocellular carcinoma (HCC) is the fifth most frequent cause of cancer worldwide whereas in China it is the second one due to infections with hepatitis B virus (HBV), which is the most significant risk factor for HCC. It is characterized as one of the most aggressive neoplasm, reflected by its highly metastatic potential which is the reason for poor prognosis in patients with HCC. Risk factors include viral infection, like chronic hepatitis, heavy alcohol intake, nonalcoholic steatohepatitis which cause liver damage and subsequent development of cirrhosis, dysplastic lesions and eventually invasive carcinoma [80]. YAP as an oncogene was shown to be over-expressed or hyper-activated due to YAP 11q22 amplification or genetic/epigenetic inactivation of tumor suppressors included in the Hippo pathway [80,81]. YAP transduction in hepatic progenitor cells (HPC) was also shown to lead to accelerated formation of liver carcinoma [80]. In the breast cancer cell line MCF-10 over-expression of YAP induces epithelial-to-mesenchymal transition (EMT). Furthermore, it leads to suppression of apoptosis and cells are able to grow anchorage-independently in soft agar [62]. A study of the group of Zhao *et al.* [60] has shown oncogenic effects of YAP as cells are able to overcome contact inhibition and de-differentiate during dysplastic progression [60]. In normal cells the Hippo pathway with its mediator kinases MST1/2 and LATS1/2 is responsible for YAP phosphorylation and inactivation following cell to cell contact inhibition in order to restrict organ size in adult tissue. In contrast, YAP has to be active during embryonic development and knockout of this co-transcription factor gene could lead to embryonic lethality [82]. In *Drosophila* as well as in mouse liver it could be shown that dysfunction of this pathway led to uncontrolled growth of organs. The group of Xu *et al.* [80] has investigated HCC cohorts in China, where a high prevalence of liver malignancy can be observed and has shown elevated levels of both YAP protein and mRNA transcription levels. By using Immunocytochemistry YAP accumulation in the cell nuclei of tumors could be observed [80]. Furthermore liver-specific WW45 (SAV-1) knockout led to a liver enlargement in mice due to deregulation of YAP. The phenotype of these mice was comparable to those achieved by over-expressing YAP [83] whereas combined MST1/2 deficiency results in loss of YAP Ser-127 phosphorylation and subsequently induces liver overgrowth and hepatocellular carcinoma formation.

Studies also revealed that ~30% of human HCCs display reduced phosphorylation of YAP at Ser-127 and a majority lack cleaved, activated MST1 kinase [84].

Even though YAP has been reported to bind to several DNA-binding transcription factors [34] the family of TEAD/TEF transcription factors was the best characterized. Therefore, inhibiting the TEAD-YAP interaction is a promising pharmacologically concept. By using a TEAD2 DN (dominant-negative) version of the transcription factor, which lacks its DNA binding domain it could be demonstrated that YAP-mediated transactivation of Gal-TEAD2 or Gal4TEAD4 was massively suppressed. Starting at the third week of age, induction of YAP over-expression led to expansion of liver size whereas starting the induction at birth HCC was developed. Furthermore, the expression of TEAD2-DN suppressed induced liver over-growth and YAP-induced HCC formation. At mRNA levels, TEAD2-DN reversed up-regulation of genes that have previously reported to be transcriptionally induced in YAP transgenic livers, including *Afp*, *Birc5/surviving*, *c-Myc*, *Sox4*, *Ctgf*, *Opn*, *Epcam* and *Gpc3* [81].

By knocking down TEAD an abort of expression of a majority of YAP-inducible genes, attenuation of YAP-induced over-growth, EMT and oncogenic transformation was demonstrated. Basically, the interaction between TEAD and YAP is mediated through a C-terminal region in TEAD whereas the N-terminal TEAD domain is necessary for DNA binding. YAP and TEAD form a heterodimer composed of four alpha helices and twelve beta-strands in TEAD and two alpha helices, one beta-strand and a coil in YAP (Figure 8A). Co-crystal structure analysis indicated three interfaces, interface 1 (Fig. 8D), interface 2 (Fig. 8E) and interface 3 (Fig. 8F) between those two proteins (Fig. 8C). By performing mutagenesis assays using Co-IP, interface 1 and 2 were shown not to be crucial for YAP-TEAD association whereas mutations S94A and F96A significantly reduced binding affinity between YAP and TEAD, indicating that under *in vitro* conditions interface 3 is the most important one. Furthermore, interface 3 is sufficient on its own to mediate interaction of YAP with TEAD. Also usage of a luciferase reporter assay driven by the *CTGF* promoter, which contains three TEAD binding sites and is strongly activated by YAP, revealed interface 3 as essential for its activity in contrast to the other two interfaces. Also critical residues necessary for TEAD binding are conserved in TAZ, which is a paralog of YAP [82].

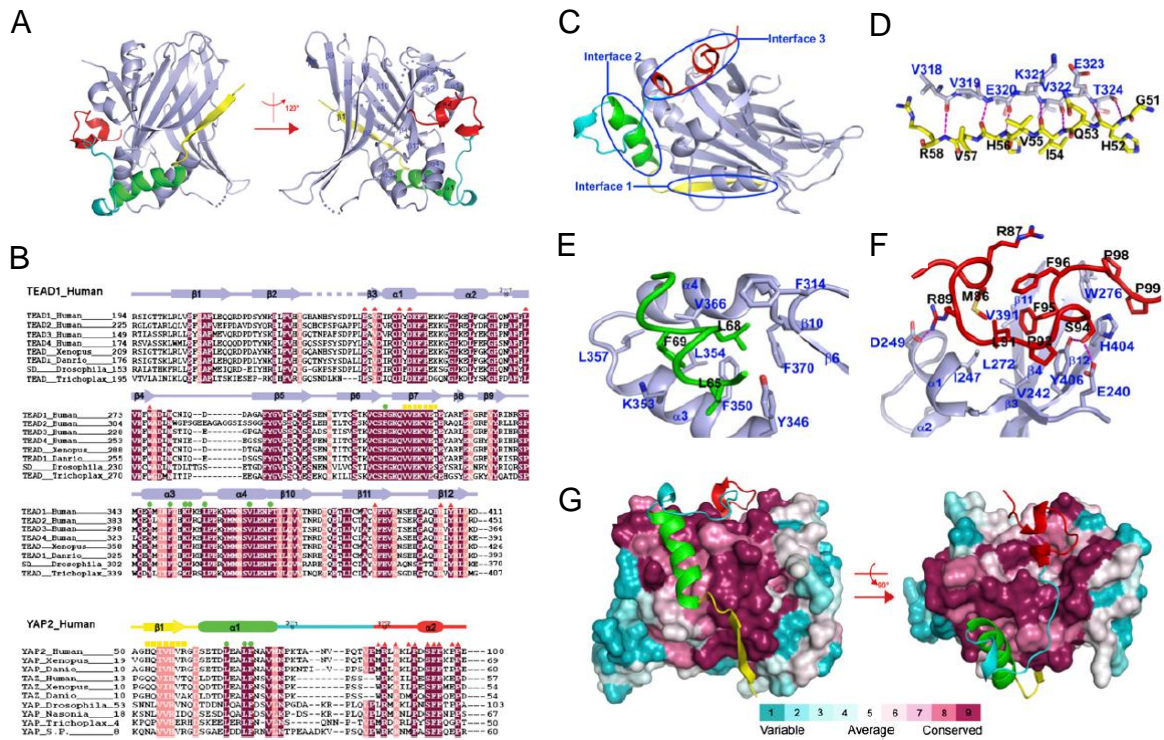


Figure 8: Structure of the YAP-TEAD complex, interfaces and sequence conservation [82]

A) Ribbon representation of YAP-TEAD complex. TEAD is illustrated in grey and interacting YAP elements are shown in red, green and yellow. The complex is shown from two orientations and the secondary structures are labelled. **B) TEAD and YAP sequences.** Yellow squares mark AA which are more variable across species in $\beta 1$, interaction of YAP and TEAD at interface 2 AA are completely conserved (green dots) **C) Interface YAP with its TEAD-binding domain** wraps around the globular structure of TEAD via three interfaces (1,2,3). **D) Interface 1:** Anti-parallel beta-sheet consisting of seven intermolecular hydrogen bonds. **E) Interface 2:** Marked by an alpha1 helix, binding occurs in a groove whereas the connection is mediated through hydrophobic interactions. Three residues of YAP interact with each other and also form a conserved LXXLF motif, which is well known as a binding module for a hydrophobic groove. **F) Interface 3:** Binding is mediated by side chains of YAP fitting in side chains into the deep pocket of TEAD. The interaction is strengthened by van der Waals contacts mediated by hydrophobic side chains of YAP and hydrogen bonds **G) Conserved regions of TEAD** are illustrated surrounded by YAP which is shown in the colors as described above.

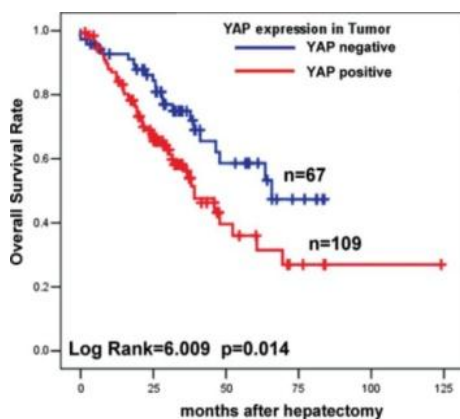


Figure 9: Poor overall survival of patients characterized as YAP positive based on YAP immunoreactivity by immunohistochemistry [80]

Patients suffering from HCC with accumulation of YAP have a much smaller chance of survival in contrast to patients which do not (Fig. 9). In 177 HCC samples investigated, significantly elevated levels of YAP were detected compared to non-tumor counterparts. It was also shown that the YAP protein was predominantly present in the nucleus of tumor cells but was also found in the cytoplasm although at lower levels. This suggests YAP to be an independent prognostic marker for the overall survival of HCC patients. To date, hepatic surgery is the most effective curative therapy and provides good survival outcomes. Unfortunately even patients which underwent surgery, 33% die because of tumor recurrence and spread within the first year [80]. Therefore, there is an urgent need for identifying new biomarkers for early detection of YAP dependent tumors and compounds which are able to inhibit YAP-TEAD complex formation and subsequent expression of proliferative and anti-apoptotic genes.

The group of Liu-Chittenden [81] screened the Johns Hopkins Drug Library in order to identify putative compounds for selective inhibiting YAP-TEAD complex formation and subsequent selectively inhibiting YAP-induced tumorigenesis. By using a luciferase reporter assay in which transcription is stimulated by YAP and TEAD, Verteporfin (VP), a clinically applied drug with little side effects was identified as a tool compound. After application of Verteporfin which belongs to the porphyrin family (10 μ M) the reporter gene activity was strongly impaired as Verteporfin binds to YAP and leads to a conformation change. Subsequently, YAP is no longer able to bind TEADs and as a consequence the reporter gene could not be expressed [81].

Furthermore, the group of Rosenbluh *et al.* [79] has demonstrated a contribution of YES-1 to tumorigenesis in colon carcinoma (1.4.4) and already suggested Dasatinib as an inhibitor of YES-1.

The master thesis is based on the assumption that YAP1 (YES-1 associated protein) has to be activated by YES-1 before it is able to move into the nucleus or before it can be inactivated through phosphorylation mediated by LATS1/2 (Fig. 10B). Furthermore, YAP1 is proposed to get phosphorylated by YES-1 at Tyr-357 giving it an active- and nuclear targeting signal (Fig. 10A). The idea is to inhibit YES-1 kinase (Fig. 10D) in order to inhibit YAP activation and therefore (independent of a deregulated Hippo pathway; (Fig. 10C)) leading to cytoplasmic retention of YAP1 co-transcription factor. The conceptual idea is to interrupt the YAP-TEAD complex by

inhibiting YES-1. In addition, inhibiting a kinase can be regarded as much more feasible than inhibiting proliferation through disruption of protein-protein interaction (YAP::TEAD) in the nucleus.

So far there are no robust data published linking YES-1 with HCC. Therefore, we focused on the investigation of YES-1 localization, its interaction partners and whether YES-1 actually contributes to human HCC formation and tumorigenesis. We further investigated whether the kinase activity of YES-1 or other functions of the protein are important for driving YAP/TEAD dependent transcription of target genes (Fig.11).

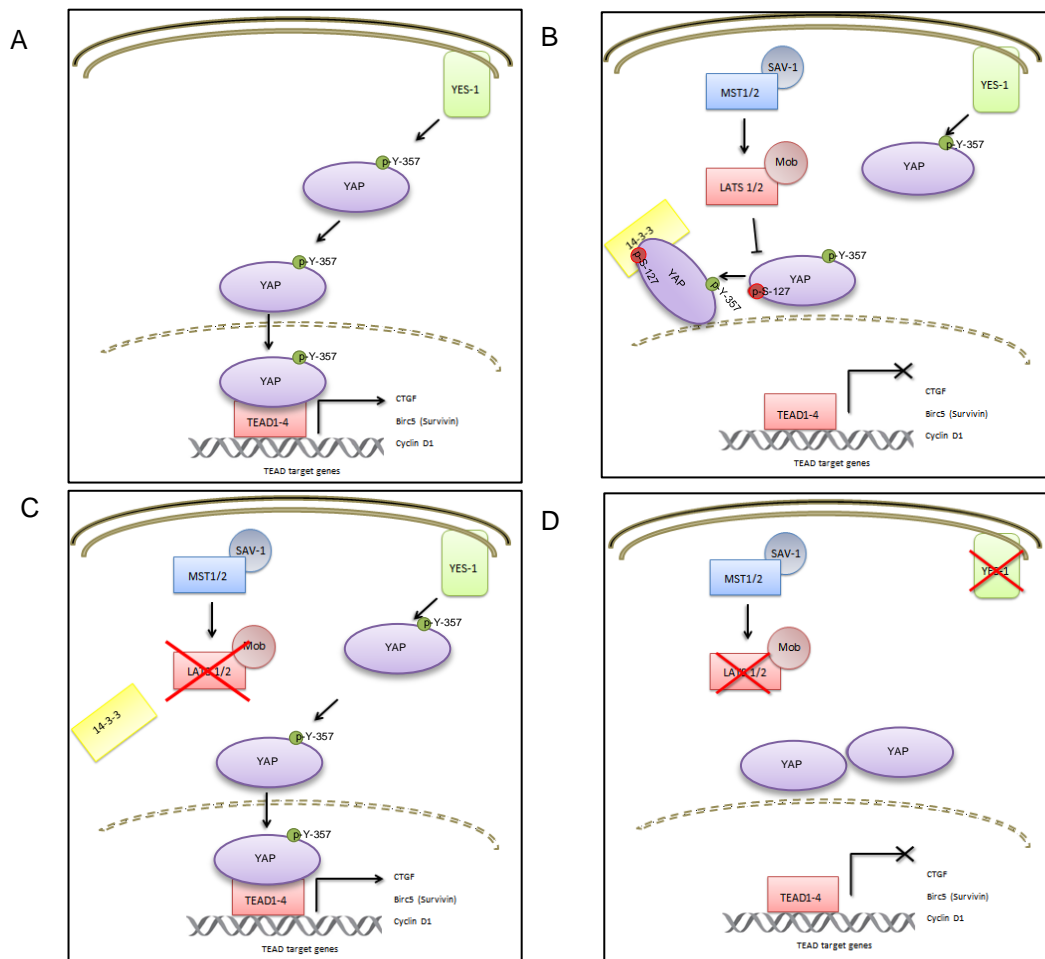


Figure 10: Hypotheses of contribution of YES-1 to YAP/TEAD dependent transcription activation

A) YES-mediated activation of YAP at tyrosine 357 leads to localization of YAP into the nucleus and drives proliferation **B)** active Hippo pathway cause phosphorylation of activated YAP at serine 127 giving it a repressive mark and leading to 14-3-3 protein binding, no transcription **C)** Phenomenon observed in many cancers YAP is able to accumulate in the nucleus because of a deregulated Hippo pathway **D) Hypotheses:** Even when the Hippo pathway is off, YAP cannot move into the nucleus because of YES-1 inhibition by compound and therefore lacking of its active phosphorylation mark.

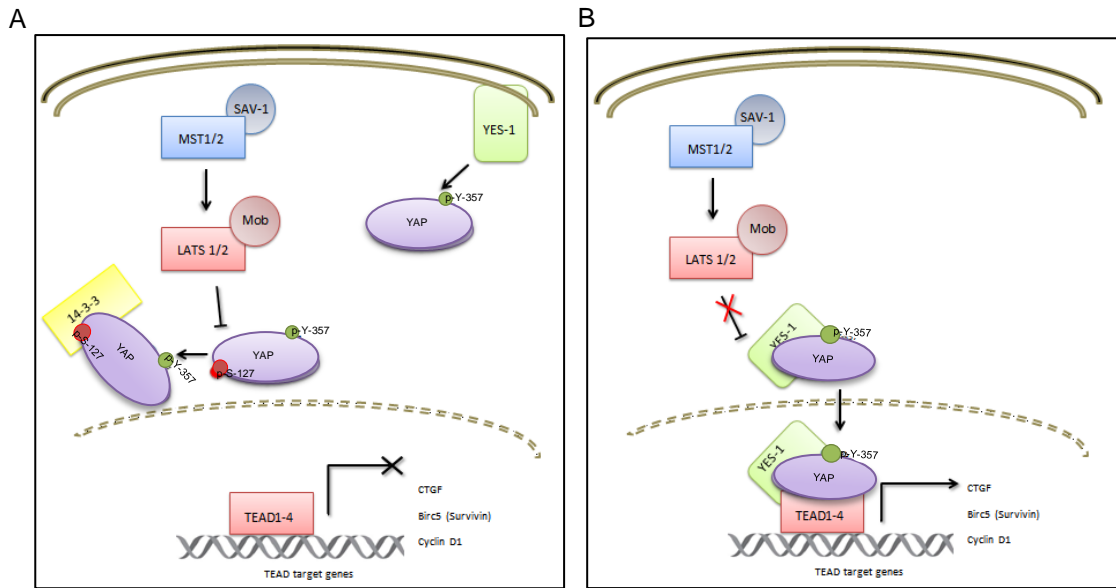


Figure 11: Hypothetical model of YES-1 location and contribution to YAP dependent transcription

A) YES-1 is located in the cytoplasm or is associated with the membrane and activates YAP at tyrosine 357 through phosphorylation **B)** YES-1 forms a complex with YAP and translocates into the nucleus where it drives YAP/TEAD/YES-1 dependent transcription.

Aims of the Master thesis

By analogy with known functions of YES-1 in colon carcinoma and based on our hypothetical model (Fig. 10+11) we framed seven aims to investigate the role of YES-1 in human HCC:

- 1) Description of the intracellular localization of YES-1 (cytoplasm vs. nucleus) by analyzing nuclear and cytoplasmic extracts on Western blot.
- 2) Analysis of 24 different human hepatocellular carcinoma cell lines with regard to their sensitivity towards YAP, TAZ or YES-1 knockdown by using RNAi.
- 3) Use AAV (adeno-associated virus) particles designed according to YAP-TEAD interaction amino acid sequence in order to confirm disruption of protein-protein interaction with the aid of a reporter gene assay.
- 4) Test different siRNAs and shRNA constructs for knockdown of YAP, TAZ, YES1 and TEADs and analyze the influence on a reporter gene assay using the promoter of *CTGF*, a target gene of TEAD.
- 5) Perform co-immunoprecipitation to identify interaction partners of YAP, TEAD and YES-1 to identify complexes which are essential for a TEAD promoter-driven transcription.
- 6) Perform rescue experiments by using codon optimized YES-1 plasmids aiming at the rescue of proliferation of cells where YES-1 has been knocked down. Utilizing also YES-1 kinase-dead constructs allows demonstration of kinase activity is indeed responsible for the proliferation and survival of human HCC cell lines.
- 7) Determine IC_{50} values for Dasatinib (=YES-1 inhibitor) or Verteporfin (=YAP-TEAD inhibitor) in different HCC cell lines.

2 MATERIAL AND METHODS

2.1 Cell Lines and Culture Conditions

Table: Cell lines and their cultivation conditions according to the producer's advice

	Morphology	Strain	Description	Source	Culture Conditions
C3A	Epithelial	Caucasian		ATCC No. CRL-10741	EMEM+ 10% FCS
Hep3B2.1-7	Epithelial	African		ATCC No. HB- 8064	RPMI1640 +2mM L-Glutamine
HepG2	Epithelial	Caucasian		ATCC No. HB- 8065	DMEM+ 10% FCS
HLE				JCRB No. JCRB0404	DMEM+ 10% FCS
HLF		Asian		JCRB No. JCRB0405	DMEM+ 10% FCS
HuCCT-1				JCRB0425	RPMI1640 + 10% FCS
huH-1	Epithelial- like	Japanese		JCRB0199	DMEM+ 10% FCS
HuH-6 Clone 5	Epithelial- like	Japanese		JCRB0401	EMEM+ 10% FCS
HuH-7		Asian		JCRB0403	DMEM+ 10% FCS
JHH-1	Epithelial- like	Japanese		JCRB1062	Williams' E medium
JHH-2	Spindle shaped	Japanese		JCRB1028	Williams' E medium + 10% FCS
JHH-4	Epithelial –like	Japanese		JCRB0435	Eagle's minimal essential medium
JHH-5	Epithelial-like	Japanese		JCRB1029	Williams' E medium
JHH-6	Epithelial- like			JCRB1030	Williams' E medium
JHH-7	Epithelial- like	Japanese		JCRB1031	Williams' E medium
SK-HEP-1		Caucasian	liver / ascites; adenocarcinoma	ATCC No. HTB-52	MEM+ 1% L-Glu, 1x NEAA, 2mM Hepes, 1x Na-Pyruvat
SNU-182		Asian		ATCC No. CRL-2235	RPMI+10%FCS +5ml Pyruvate (100x), +5ml 1M Hepes + 2,8ml 45% Glucose
SNU-387		Asian		ATCC NO. CRL-2237	RPMI+ 10% FCS
SNU-398		Asian		ATCC NO. CRL-2233	RPMI+ 10% FCS
SNU-423		Asian		ATCC NO.	RPMI+ 10% FCS, 2mM

				CRL-2238	L-Glutamine, 10mM HEPES, 1mM sodium pyruvate, 4,5g/L glucose, 1,5g/L sodium bicarbonate
SNU-449		Asian		ATCC NO. CRL-2234	RPMI+ 10% FCS
SNU-475		Asian		ATCC NO. CRL-2236	RPMI+ 10% FCS
RH-41	Epithelial-like				RPMI+ 10% FCS

2.1.1 MEDIUM AND ADDITIVES

Table 3: Medium and additional substances for production of a full medium

DMEM	Lonza, Basel
RPMI Medium 1640 (1x) + GlutaMax™-I	Gibco
EMEM	Lonza, Basel
Williams' E Medium	Gibco
FBS (heat inactivated 56°C/1h)	Gibco
1X DPBS	Gibco
Sodium Pyruvate 100mM (100X)	Gibco
HEPES 1M Solution pH=7,3	Affymetrix
MEM NEAA 100X	Gibco
Sodium Bicarbonate 7,5%	Gibco
GlutaMAX™ – I (100x)	Gibco
Trypsin	Gibco

2.1.2 INSTRUMENTATION

Table 4: List of Instruments

Fridge (+4°C)	Liebherr
Freezer (-20°C)	Liebherr
Freezer (-80°C)	Thermo Scientific
Incubator Heracell 240	Heraeus
Vi-Cell™ XR Cell viability analyser	Beckman Coulter
Centrifuge 5810R	Eppendorf
Centrifuge 5424	Eppendorf
Megafuge 3.0R	Heraeus
Microscope	Leica
Victor™ X5	Perkin Elmer 2030 multilabel reader
Laminar Flow	clanLAF
Amaxa biosystems Nucleofector® II	Lonza
Nanodrop 8000	Thermo Scientific
Clone Select Imager	Genetix
Pipettes 10µl, 100µl, 200µl, 1000µl	Eppendorf
Multichannel pipet 5-100µl	Biohit
Film processor Curix 60	AGFA
Ice maker AF100	Scotsman
Thermomixer comfort	Eppendorf
Trans-Turbo Blot	Bio-Rad

2.1.3 EQUIPMENT

Table 5: List of Equipment

96 well Micro titer plates	Corning/Costar
96 well white Micro titer plates	Corning/Costar
48 well plates	Corning/Costar
12 well plates	Corning/Costar
6 well plates	Corning/Costar
Pipette tips	Biohit
Pipettes 2ml, 5ml, 10ml, 25ml, 50ml	Costal
T-25 Flask	Becton Dickinson, Heidelberg
T-75 Flask	Becton Dickinson, Heidelberg
BD Falcon 15ml	BD Bioscience Discovery Lab ware
BD Falcon 50ml	BD Bioscience Discovery Lab ware
BD Falcon Cell strainer 40 μ M Nylon	BD Bioscience Discovery Lab ware
Reaction tubes (1.5,2ml)	Eppendorf
X-ray film	Amersham
Gel Criterion X5 4-12% Bis-Tris	Bio-Rad
PVDF membrane	Bio-Rad

2.2 Kits, Reagents and Buffers

Table 6: List of kits, reagents and buffers

Alamar Blue	Invitrogen
Loading buffer 4x	Roth
Gel Criterion™ X5 4-12% Bis-Tris	Bio Rad
Phenylmethanesulfonyl fluoride solution (PMSF) (100x)	Sigma
Amersham™ ECL™ Western Blotting Detection Reagents	GE Healthcare
Quick Start Bradford reagent	Bio-Rad
Lipofectamine™ RNAi MAX Reagent	Invitrogen
DharmaFECT®1 Transfection Reagent	Dharmacon
DharmaFECT®2 Transfection Reagent	Dharmacon
DharmaFECT®3 Transfection Reagent	Dharmacon
DharmaFECT®4 Transfection Reagent	Dharmacon
Protease inhibitors (100x)	Thermo Scientific
Complete Mini EDTA-free Phosphatase and Protease Inhibitor	Roche
5 x siRNA buffer	Thermo Scientific
Luciferase Assay System	Promega

AMAXA™ CELL LINE NUCLEOFECTOR™ KIT V

(LONZA)

NE-PER® NUCLEAR AND CYTOPLASMIC EXTRACTION REAGENTS

(THERMO SCIENTIFIC)

Table 7: Nuclear and cytoplasmic extraction reagents

Cytoplasmic Extraction Reagent 1 (CER 1)
Cytoplasmic Extraction Reagent 2 (CER 2)
Nuclear Extraction Reagent (NER)

Lysis buffer/wash buffer 1**Table 8: Components of lysis buffer/wash buffer 1**

Kit components	Final concentration (25ml)
5 ml core buffer	50mM Tris-HCL, pH 7.5
3.75 ml NaCl	150mM NaCl
2.5 ml detergent mix	1% Nonidet P40 0.5% sodium deoxycholate
1 Complete tablet	1 tablet/ 25-50ml
ad 25ml H ₂ O	

Wash buffer 2 (high salt)**Table 9: Components of wash buffer 2**

Kit components	Final concentration (50ml)
10ml core buffer	50mM Tris-HCl, pH 7,5
25 ml NaCl	500 mM NaCl
0.5 ml detergent mix	0,1% Nonidet P40 0,05% sodium deoxycholate
ad 50 ml H ₂ O	

Wash buffer 3 (low salt)**Table 10: Components of wash buffer 3**

Kit components	Final concentration (25ml)
1ml core buffer	10mM Tris-HCl, pH 7.5
0.25 ml detergent mix	0.1% Nonidet P40 0.05% sodium deoxycholate
ad 25ml H ₂ O	

Hepex Lysis Buffer:

Table 11: HEPEX lysis buffer

	Stock	Dilution	1L
20mM Hepes pH 7.4	1M	1:50	20ml
100mM NaCl	5M	1:50	20ml
5mM EDTA pH 7.4	500mM	1:100	10ml
1mM Na ₃ VO ₄	200mM	1:200	5ml
30mM NaF	500mM	1:16.67	60ml
5% Glycerol	100%	1:20	50ml
0.1% SDS	10%	1:100	10ml
1% Triton X-100	10%	1:10	100ml
1mM β-Glycerophosphat	1M	1:1000	1ml
1mM DTT	1M	1:1000	1ml
H ₂ O			723ml
1 Complete Mini EDTA free Protease Inhibitor Cocktail Tablet / 10 ml (Roche # 04693159001)			
1:100 PMSF			

TBS-T:

Table 12: Composition of TBS-T buffer

1L 10x TBS	Bio Rad
100ml Tween 20 (10%)	Bio Rad
8.9L H ₂ O	

XT-MOPS:

Table 13: Dilution of 20x XT MOPS

500mL 20x XT MOPS	Bio Rad
9.5L H ₂ O	

Blocking Milk (5%)

Table 14: Composition of blocking milk

Milk powder	Fluka
in TBS-T	See above

BSA (5%)

Table 15: Composition of BSA blocking solution

Bovine Serum Albumin	SERVA
in TBS-T	See above

2.2.1 PROTEIN MW MARKERS

Table 16: List of protein ladders

Full Range Rainbow™	GE Healthcare
Page Ruler Prestained (21616)	Thermo Scientific
Page Ruler Prestained (21619)	Thermo Scientific

2.2.2 ANTIBODIES

2.2.2.1 PRIMARY ANTIBODIES

Table 17: List of primary antibodies

	Supplier
GAPDH	Abcam
LATS1 (C66B5) #3477P	Cell Signaling
p-LATS1 (T1079) # 8654P	Cell Signaling
LATS2 (D83D6) #5888S	Cell Signaling
TAZ (V386) Ab	Cell Signaling
MST1#3682S	Cell Signaling
MOB1 #3863P	Cell Signaling
p-MOB1 (Thr35) (D2F10)	Cell Signaling
p-MST-1 T183	Cell Signaling
SAV1 #3507	Cell Signaling
TEF-1	BD Transduction Laboratories
PLK1 (208G4)	Cell Signaling
YAP sc-14199	Santa Cruz
YES-1 133314	Abcam
p-YES-1 (S-127)	Abcam
c-MYC	Clontech
β -catenin #9587S	Cell Signaling
p-YAP1-Y357 (ab62751)	Abcam
Anti-Axin-2	Millipore
YAP	Cell Signaling

2.2.2.2 SECONDARY ANTIBODIES

Table 18: List of secondary antibodies

Polyclonal goat Anti-mouse IgG/ HRP	(Deko, Denmark)
Polyclonal goat Anti-rabbit IgG/ HRP	(Deko, Denmark)

2.2.2.3 siRNAs

Table 19: List of siRNAs

ON-TARGET plus Non-targeting siRNA #1	Cat # D-001810-01	Thermo Scientific
ON-TARGET plus SMART pool Human PLK1	Cat # L-003290-00 Lot# 130318	Thermo Scientific
ON-TARGETplus Human TEAD1 (7003) siRNA - SMARTpool, 20 nmol	L-012603-00-0020	Thermo Scientific
ON-TARGETplus Human TEAD2 (8463) siRNA - SMARTpool, 20 nmol	L-012611-01-0020	Thermo Scientific
ON-TARGETplus Human TEAD3 (7005) siRNA - SMARTpool, 20 nmol	L-012604-00-0020	Thermo Scientific
ON-TARGETplus Human TEAD4 (7004) siRNA - SMARTpool, 20 nmol	L-019570-00-0020	Thermo Scientific
ON-TARGET plus HUMAN YES1 (7525) siRNA -SMARTpool, 20nmol	L-003184-00-0020	Thermo Scientific
ON-TARGETplus SMARTpool Human WWTR1, 20nmol	Cat # L-016083-00 Lot # 130715	Thermo Scientific
ON-TARGET plus SMART pool Human YAP1, 20nmol	Cat# L-012200-00 Lot# 130710	Thermo Scientific

2.2.3 sHRNAs

(SIGMA-ALDRICH)

Product Name: Mission™ Lentiviral Transduction Particles

Product Number: SHCLNV

Table 20: PLK-1 shRNA

Construct	Number	Sequence	Region	Kd efficiency
PLK-1	TRCN0000121325	CCGGCCCGAGGTGCTGAGCAAGAACTCGAGTTTCTTGCTCAGCACCTCGGGTTTTTG	CDS	92%

Non-targeting

Product Name: MISSION Non-TARGET shRNA Control Transduction Particles

Product Number SHC002V

Table 21: List of shRNAs

Construct	Number	Sequence	Region	Kd efficiency
YES-1	TRCN000001607	CCGGCCAGCCTACATTCACCTTCTAACTCGAGTTAGAAGTGAATGTAGGCTGGTTTTT		70%
	TRCN000001608	CCGGGCAGTTAATTCAGCAGTCTTCTCGAGAAGACTGCTGAAATTAAGTCTTTTT		90%
	TRCN000001609	CCGGCTGCACTGTATGGTCGGTTTACTCGAGTAAACCGACCACATACAGTGCAGTTTTT		85%
	TRCN000001610	CCGGTTACTATATTTGTGGCCTTACTCGAGTAAAGCCACAAAATATAGTAACTTTTT		61%
	TRCN000001611	CCGGACCACGAAAGTAGCAATCAAACCTCGAGTTTGATTGCTACTTTCTGGTTTTTT		98%
YAP	TRCN0000107265	CCGGCCAGTTAAATGTTACCAATCTCGAGATTGGTGAACATTTAACTGGGTTTTTG	3UTR	82%
	TRCN0000107266	CCGGGCCACCAAGCTAGATAAAGAAGCTCGAGTTCTTTATCTAGCTTGGTGGCTTTTTG	CDS	91%
	TRCN0000107267	CCGGCAGGTGATACTATCAACCAAACCTCGAGTTTGGTTGATAGTATCACCTGTTTTTG		88%
	TRCN0000107268	CCGGGACCAATAGCTCAGATCCTTTCTCGAGAAGGATCTGAGCTATTGGTCTTTTTG	CDS	76%
	TRCN0000107269	CCGGCGACCAATAGCTCAGATCCTTCTCGAGAAGGATCTGAGCTATTGGTCGTTTTTG	CDS	58%
TAZ (WWTR1)	TRCN000019469	CCGGGCGATGAATCAGCCTCTGAATCTCGAGATTCAGAGGCTGATTCATCGCTTTTT	CDS	97%
	TRCN0000319149	CCGGGCGATGAATCAGCCTCTGAATCTCGAGATTCAGAGGCTGATTCATCGCTTTTTG	CDS	83%
	TRCN0000319150	CCGGCAGCCAAATCTCGTATGAATCTCGAGATTCATCAGAGATTTGGCTGTTTTTG	CDS	61%
	TRCN0000319224	CCGGCCAGGAACAACGTTGACTTACTCGAGTAAAGTCAACGTTTGTCTGGTTTTTG	CDS	61%
	TRCN0000370006	CCGGTAAGCTTTATGGGTGTTAATTCTCGAGAATTAACACCATAAAGCTTATTTTTG	3UTR	62%
TEAD-1	TRCN0000278040	CCGGGCTCAAACACTTACCAGAGAAGCTCGAGTTCTCTGGTAAGTGTGGAGCTTTTTG		95%

	TRCN0000297070	CCGGGCCCTGTTTCTAATTGTGGTACTCGAGTACCACAATTAGAAACAGGGCTTTTTG	3UTR	79%
	TRCN0000015799	CCGGCCAGAAGGAAATCTCGTGATTCTCGAGAATCACGAGATTCCTTCTGGTTTTT	CDS	97%
	TRCN0000015800	CCGGCCGATTTGTATACCGAATAAACTCGAGTTTATTCGGTATACAAATCGGTTTTT	CDS	98%
	TRCN0000015801	CCGGGCTCAAACACTTACCAGAGAACTCGAGTCTCTGGTAAGTGTGAGCTTTTT	CDS	91%
TEAD-2	TRCN0000013203	CCGGGCTCACCTCATGCTTCTTATTCTCGAGAATAAGAAGCATGAGGTGAGCTTTTT	3UTR	
	TRCN0000013204	CCGGCCCCGAAGGAAATCAAGGGAACTCGAGTTTCCCTTGATTCCTTCGGGTTTTT	CDS	
	TRCN0000013205	CCGGCCGCGAGATCTACGACAAATTCTCGAGAATTTGTCGTAGATCTGCCGTTTTT	CDS	
	TRCN0000013206	CCGGGCTGAGCGATACATGATGAACCTCGAGTTCATCATGTATCGCTCAGGCTTTTT	CDS	
	TRCN0000013207	CCGGCCAAGTTGAAGGACCAGGTTTCTCGAGAACTGGTCCTTCAACTTGGTTTTT	CDS	
TEAD-3	TRCN0000015952	CCGGGAGTTGATTGCACGCTATATTCTCGAGAATATAGCGTGCAATCAACTCTTTTT	CDS	93%
	TRCN0000015948	CCGGGCCACTGTTCTGCGCTTAACTCGAGATTAAGCGCAGAACAGTGGCTTTTT	CDS	82%
	TRCN0000015949	CCGGCCATGTCTACAAGCTCGTCAACTCGAGTTGACGAGCTTGAGACATGGTTTTT	CDS	85%
	TRCN0000015950	CCGGCCTGGAGTATTCAGCCTTCATCTCGAGATGAAGGCTGAATACTCCAGGTTTTT		73%
	TRCN0000015951	CCGGCTCTGCTGATAGCATGACCATCTCGAGATGGTCATGCTATCAGCAGATTTTT		72%
TEAD-4	TRCN0000285156	CCGGGAGACAGAGTATGCTCGCTATCTCGAGATAGCGAGCATACTCTGTCTTTTTG	CDS	83%
	TRCN0000274223	CCGGCGAGATCCAGGCCAAGCTAAACTCGAGTTAGCTTGGCCTGGATCTCGTTTTTG	CDS	72%
	TRCN0000015875	CCGGGAGACAGAGTATGCTCGCTATCTCGAGATAGCGAGCATACTCTGTCTTTTTT	CDS	84%
	TRCN0000015876	CCGGCCTTCTCTCAGCAAACCTATCTCGAGATAGGTTTGTCTGAGAGAAAGTTTTT	CDS	80%
	TRCN0000015877	CCGGGCTGTGCATTGCCTATGTCTTCTCGAGAAGACATAGGCAATGCACAGCTTTTT	CDS	76%

2.2.4 PLASMIDS

Table 22: List of plasmids¹

Reporter gene plasmids	Promega
pGL4_16 <i>CTGF</i> -wt	
pGL4_16 <i>CTGF</i> -mut	
pGL4_16 <i>CTGF</i> -wt (-Smad)	
pGL4_16 <i>CTGF</i> -6x	
pGL4_16 <i>CTGF</i> -del (TB1-3)	
pGL4_28 <i>CTGF</i> -wt	
pGL4_28 <i>CTGF</i> -mut	
pGL4_28 <i>CTGF</i> -wt (-Smad)	

¹ Graph of pGL4 plasmids see attachments

pGL4_28 CTGF-6x	
pGL4_28 CTGF-del (TB1-3)	
YES-1 plasmids	Invitrogen
pCDNA-YES1_wt_opti (Amp)	
pcDNA-YES1-K330M_opt (Amp)	
pcDNA-YES1_T348I_opt (Amp)	

2.2.5 ANTIBIOTICS

Table 23: List of antibiotics

Puromycin	Sigma
Hygromycin	Invitrogen
G418 Geneticin	Gibco
Ampicillin	Sigma

2.2.6 COMPOUNDS

Table 24: List of Compounds

Dasatinib	BI Vienna (in-house)
Verteporfin	Sigma-Aldrich

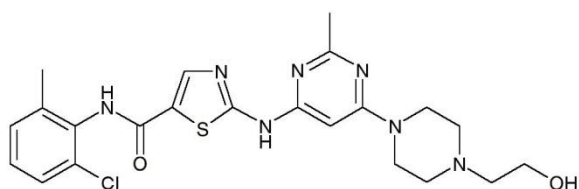


Figure 12: Structural formula of Dasatinib

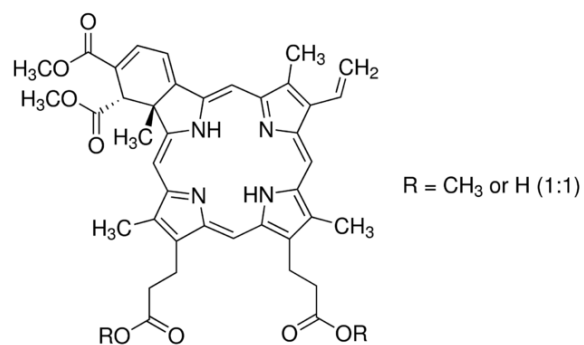


Figure 13: Structural formula Verteporfin

2.2.7 AAV-PARTICLES

Table 25: AAV Particles

CMV _YAP1pep_FLAG_sc	Dr.D. Mennerich's lab at BI/Biberach
CMV-NLS_YAP1pep_FLAG_sc	Dr.D. Mennerich's lab at BI/Biberach

2.2.8 SEEDING OF CELLS

For the assays, T-75 flasks of cells with a confluence of 60-80% were used. First of all the medium was aspirated and cells were washed with 10ml 1xPBS. Cells were detached by adding 1ml of trypsin and incubated for three minutes at 37°C in a humidified incubator in an atmosphere of 5-7% CO₂. At least 9 ml medium were added after incubation in order to inhibit trypsin through the FCS in the medium. Cell suspension was transferred through a cell strainer to avoid lumps and cells were counted afterwards by Vi-cell. The number of viable cells was determined and cells were diluted in order to gain the desired cell density.

2.2.9 siRNA TRANSFECTION WITH RNAIMAX OR DHARMAFECT (ALAMAR BLUE)

siRNA (final concentration 20nM) was mixed with transfection reagent (0.1-0.3µl) at the ratio of 1:1 and incubated at room temperature for 20 minutes. 20µl of transfection mixture were added to each well (96-well plate) as well as 80µl cell suspension (1000-5000 cells/well) and incubated for 24-72h at 37°C, 5-7% CO₂. The proliferation was measured by adding 1/10 of total volume Alamar blue reagent and incubated for 3-10h until absorbance was measured.

2.2.10 LENTIVIRUS TRANSDUCTION

Two Lentivirus transduction protocols have been established to evaluate shRNAs and characterize cell lines according to their sensitivity towards YAP, TAZ or YES-1 knockdown.

Puromycin selection (killing curves)

The concentration which was necessary to kill most of the untransduced cells was determined by setting up puromycin killing curves.

Therefore 1000 cells per well (96-well plate) were seeded in a volume of 100 μ l. 10 μ l puromycin (11x) were titrated from 4 to 0.0625 μ M and added after the cells were incubated for 24 hours. Alamar blue was added after 72 hours incubation with puromycin and the necessary concentration for killing almost all, not transduced cells was determined.

Protocol 1:

On **day 0** 30000 cells in 1ml appropriate medium were seeded in a 12-well plate and incubated over night at 37°C in a humidified incubator in an atmosphere of 5-7% CO₂. On **day 1** lentiviruses were added carefully with an MOI of 4. Depending on the titer given by the producer of the particles and the seeded cell number different volumes of virus particles were added.

$$(\text{Total number of cells per well}) \times (\text{Desired MOI}) = \text{Total transducing units needed (TU)}$$

$$(\text{Total TU needed}) / (\text{TU/ml reported on C of A}) =$$

$$\text{Total ml of lentiviral particles to add to each well}$$

Figure 15: Formula for calculation of ml lentiviral particle needed for a certain MOI and cell number

Samples were again incubated over night at 37°C in humidified incubator in an atmosphere of 5-7% CO₂.

On **day 2** the medium had to be exchanged due to traces of the viruses in the supernatant. On **day 3** the selection with puromycin was started with a concentration

determined by puromycin killing curves. Cells were incubated at the same conditions as before and counted on **day 8** by washing cells with 1xPBS and detaching them with trypsin. Cell suspension was diluted in order to achieve 3000 cells per 150µl and seeded in a 96-well plate. The confluence measurement was started on **day 8** until the confluence of non-targeting shRNA treated cells reached approximately 80%. On that day, 15µl of Alamar blue reagent were added to the cells to measure proliferation. The last steps included washing with 1xPBS and lysis of cells in 15µl Hepex lysis buffer. Samples were frozen at -20°C until used for Western blot analysis.

Protocol 2:

On **day 0** 500 and 1000 cells in 100µl appropriate medium were seeded in a 96-well plate and incubated over night at 37°C in humidified incubator in an atmosphere of 5-7% CO₂. After 24h incubation, lentiviruses were added carefully with an MOI of 4 (8 for SK-HEP-1 cell line). Depending on the titer- defined by the producer and the cell number, different volumes of virus particles were added. See calculation of µl needed in protocol 1 (Figure 13). Samples were incubated over night at 37°C in humidified incubator in an atmosphere of 5-7% CO₂. On **day 2** the medium was changed and on **day 3** the selection with puromycin was started. By evaluating the puromycin killing curves, the concentration of puromycin necessary for killing almost all not transduced cells, was calculated. The medium (still containing puromycin) was changed on **day 8** and the confluence measurement was started. Alamar blue reagent was added when the confluence of non-targeting shRNA treated cells reached about 80%. After the measurement, cells were washed with PBS, lysed in 15µl Hepex lysis buffer and stored at -20°C.

2.2.11 BACTERIAL TRANSFORMATION

Transformation

First, 10µl H₂O were added to all constructs to produce a stock concentration of 500ng/µl, which was further diluted 1:20 to reach a final concentration of 25ng/µl. Afterwards the concentration was verified by OD measurement with Nanodrop 8000. A 2ml Eppendorf tube was chilled on ice and competent cells (1001 bacteria) from -80°C were thawed by placing the tube on ice before they were portioned à 100µl into pre chilled culture tubes. An amount of 50ng of DNA (1-50ng in a volume not greater than 10µl per 100µl competent cells) was added to 100µl competent bacteria and the tube was quickly flicked several times. The tube was returned on ice for 10 minutes. A heat shock was induced by putting the cells into a 42°C warm water bath for 45-50 seconds without shaking. Samples were immediately placed back on ice for another 2 minutes and 900µl of cold SOC medium were added to each transformation reaction. Samples were incubated for 60 minutes at 37°C and 225rpm and cells were then centrifuged at 6000rpm. Cell pellets were resuspended in 200µl medium and plated in different concentrations on Amp containing LB-plates. Samples were incubated for at least 24 hours at 37°C and put on 4°C until needed for further cultivation.

Preculture

To 2.5ml LB medium, Amp (1:1000) was added. A colony was picked from the plates and transferred to a prepared tube and incubated for three hours at 37 degrees and 225rpm.

Main Culture

After an incubation period, the 2.5ml pre-culture were transferred to a 250ml LB medium+ AMP (1:1000) containing flask and again incubated over night at the same conditions as for pre-culture.

2.2.12 MIDI-PREP

RNAseA solution was added to buffer P1, mixed and stored at 4°C. Also LyseBlue® reagent was added to buffer P1 at a ratio 1:1000. Buffer P3 was put on ice and 96-100% ethanol was added to endotoxin-free water supplied with the kit. Also endotoxin or pyrogen-free plastic ware was used.

Overnight LB culture was harvested by centrifuging cells at 4200 x g for 20 minutes at 4°C. The bacterial pellet was resuspended in 10ml buffer P1. Afterwards 10ml buffer P2 were added and thoroughly mixed by inverting the tube 4-6 times and incubated at room temperature for 5 minutes. Then 10ml chilled buffer P3 were added and samples were inverted 4– 6 times. The lysate was poured into the barrel of the QIAfilter Cartridge and incubated at room temperature for 10 minutes. The plunger then was inserted and the cell lysate was filtered into a 50ml tube. 2.5ml of buffer ER were added to the filtered lysate, mixed again by inverting the tube approximately 10 times and incubated on ice for 30 minutes. QIAGEN-tip 500 was equilibrated by applying 10ml buffer QBT and allowed to drain by gravity flow. Filtered lysate was then applied to the QIAGEN-tip, which was washed two times with buffer QC. DNA was eluted with 15ml buffer QN into a 30ml endotoxin-free or pyrogen-free tube. Afterwards DNA was precipitated by adding 0.7 volumes of room-temperature isopropanol and centrifuged at 4000 rpm for 40 minutes at 4°C. Supernatant was carefully decanted without compromising the pellet. Then it was washed with 5ml endotoxin-free room temperature 70% ethanol and centrifuged at 4000 rpm for 10 minutes. Again supernatant was carefully decanted without disturbing the pellet, which was air-dried for 5-10 minutes and redissolved in endotoxin-free buffer TE. The concentration of DNA was determined by Nano Drop measurement.

2.2.13 DNA PURIFICATION (STERIL)

Appropriate amount of plasmid was taken and transferred to a fresh 1.5ml Eppendorf tube and 1/10 3M NaAc (pH=5.5) was added. Tube was shaken and afterwards two volumes of 96% EtOH were added. Eppendorf tube was inverted and incubated for

30 minutes at -20°C. It was subsequently centrifuged for 15 minutes at 4°C at full speed. After the pellet was washed with 70% EtOH and centrifuged again, the supernatant was removed. The pellet was dried by leaving the lid of the Eppendorf tube open and allowing the alcohol to evaporate. 400µl of sterile water were added to achieve a final concentration of 1µg/µl.

2.2.14 AMAXA PLASMID TRANSFECTION

The wells of a 6-well plate were filled up with 2.5ml culture medium and pre-incubated/ equilibrated in a humidified 37°C/ 5% CO₂ incubator. Required number of cells (1×10^6 cells per transfection) was centrifuged at 120 x g for 8 minutes at room temperature. The supernatant was completely removed and the cell pellet was resuspended in 100µl room-temperature Nucleofector Solution V. 100µl of cell suspension were combined with 5µg plasmid DNA (1µg/µL) in a cuvette. The lid was closed and Nucleofector program T-028 was selected before cuvette with the cell-DNA suspension was inserted into the nucleofector cuvette mounting and the selected program was applied. Immediately, ~500µl of the pre-equilibrated culture medium were added to the cuvette. The suspension was gently transferred to a prepared 6-well plate by using supplied pipettes, avoiding repeated aspiration of the sample. Cells were incubated for at least 24h until a change of medium was performed.

2.2.15 RESCUE EXPERIMENT

For the Rescue Experiment cells were transfected with appropriate plasmids by AMAXA (see 2.2.14) and incubated for at least 24h after medium was changed and Geneticin selection was started by using a concentration of 500µg/ml. Medium was changed every fourth day for a total time period of 9 weeks until stably transfected cells were used for shRNA mediated knockdown by using Lentivirus transduction method 2 (2.2.10) and measured via CSI till day 13. On the same day Alamar Blue Assay was carried out and cells were lysed in 15µl Hepex lysis buffer.

2.2.16 ALAMAR BLUE PROLIFERATION ASSAY

1/10 of the total volume Alamar blue reagent was added and the assay was incubated for at least 6h before measurement at 544/590nm, 0,2s.

2.2.17 REPORTER GENE ASSAY

Validation of plasmids

SK-HEP-1 cell line was transfected according to AMAXA transfection protocol (2.2.14) and incubated for 48 hours in a 12 well plate. After incubation, the supernatant was transferred to an Eppendorf tube, centrifuged at 400 x g for 4 minutes and washed with PBS. Afterwards cells of supernatant were centrifuged again. Cells left in wells were also washed with PBS and 60µl of lysis buffer were added (10µl lysis buffer to cell pellet of the supernatant) before lysates were mixed together. After a freeze (-20°) and thaw cycle 3 x 20µl of the lysate mix were transferred to a white 96-well plate and 100µl of room temperature substrate were added. Samples were mixed by putting the plate on a rocking platform for a few seconds and immediately measured.

Reporter gene assay by using compounds or si/shRNAs

SK-HEP-1 cell line was transfected according to AMAXA transfection (2.2.14) and selected with 500µg/ml hygromycin whereby a pool of stably transfected cells was generated and frozen at -80°C.

The assay was set up according to the compound treatment or si/shRNA assay with the exception of using white 96-well plates. After 24-72 hours incubation, supernatant was evacuated and cells washed with PBS. Then 20µl of 1 x Reporter gene lysis buffer were added and plate was frozen at -80°C. Afterwards cells were thawed and 100µl of room temperature substrate was added, mixed and luminescence was measured immediately.

2.2.18 CYTOPLASMIC AND NUCLEAR EXTRACTS

Cells were washed with PBS and detached from the flask by adding trypsin. After incubation for 3 minutes at 37°C, appropriate medium was added and cells were centrifuged at 500 x g for 5 minutes. Then cells were resuspended in PBS and 1-10 x 10⁶ cells were transferred to an Eppendorf tube and again centrifuged at 500 x g for 2-3 minutes. Supernatant was removed completely and ice-cold CER I was added (see table 25).

Table 26: Necessary reagent volumes according to cell packed volumes (Thermo Scientific)

Packed Cell Volume (µl)	CER I (µl)	CER II (µl)	NER (µl)
10	100	5.5	50
20	200	11	100
50	500	27.5	250
100	1000	55	500

Tubes were vigorously vortexed for 15 minutes at the highest setting and incubated on ice for 10 minutes and ice-cold CER II was added to the Eppendorf tube. They were vortexed again for 5 seconds on the highest setting and incubated for another minute. After another step of vortexing for 5 seconds on the highest setting samples were centrifuged for 5 minutes at maximum speed (~16,000 x g). Supernatant (cytoplasmic extract) was immediately transferred to a clean pre-chilled tube and was placed on ice until usage. The insoluble fraction (pellet) which contained the nuclei was resuspended in ice-cold NER and vortexed on the highest settings for 15 seconds. Samples were put on ice and vortexed for 15 seconds every 10 minutes, for a total of 40 minutes. Finally, samples were centrifuged at high speed for 10 minutes and supernatant (nuclear extract) was immediately transferred to a pre-chilled tube and placed on ice until further usage.

2.2.19 IMMUNOPRECIPITATION

Whole cell lysates

Cells were cultivated in 10cm PD's and harvested when they reached a confluence of 80%. Therefore medium was aspirated and cells were washed with PBS. Cold lysis buffer was added to the monolayer and cells were scraped and transferred to an Eppendorf tube. 50µl of homogenous protein A agarose suspension were added to approximately 1ml cell suspension and incubated for at least 3h (or overnight) at 4°C on a rocking platform. Beads were pelleted by centrifugation at 12,000 x g for 20 seconds and supernatants were transferred to fresh tubes. Antibodies were added in varying concentrations (1µg for monoclonal, 5µg for polyclonal) and incubated for 1 hour at 4°C on a rocking platform. Afterwards 50µl of homogenous protein A suspension were added and incubated for at least 3h (or overnight) at 4°C on a rocking platform. Complexes were collected by centrifuging the samples at 12,000 x g for 20 seconds and supernatant was removed carefully. Pellets were washed with 1ml of wash buffer 1 by resuspending the beads and incubated for 20 minutes at 4°C on a rocking platform. Washing with buffer 1 was repeated once before the same procedure was carried out twice with washing buffer 2, followed by a washing step with buffer 3 (total time of washing 1 hour and 40 minutes). After the last step of centrifugation, the last traces of the final wash from agarose pellet were removed. Therefore, 25-75µl of gel-loading buffer were added and proteins denatured by heating the samples to 96°C for 3 minutes. Protein A agarose was removed by centrifugation of samples at 12,000 x g for 20 seconds and supernatant was transferred to fresh tubes and then analyzed by Western Blot (2.2.20).

CYTOLASMIC AND NUCLEAR EXTRACT IMMUNOPRECIPITATION

For immunoprecipitation with cytoplasmic or nuclear extract, samples produced in (2.2.18) were filled up with wash buffer 1 to a total volume of 1ml before further steps were carried out according to the whole cell lysate immunoprecipitation protocol.

2.2.20 WESTERN BLOT

DETERMINATION OF PROTEIN CONCENTRATION (BRADFORD ASSAY)

The concentration of proteins was determined via photometric measurement by using Bradford assay. 1ml of the reagent was mixed with 2 μ l of the sample and measured at a wavelength of 595nm. The amount of total protein in the sample was calculated by using a standard curve, for which different amounts of BSA were diluted in Bradford reagent and OD was measured.

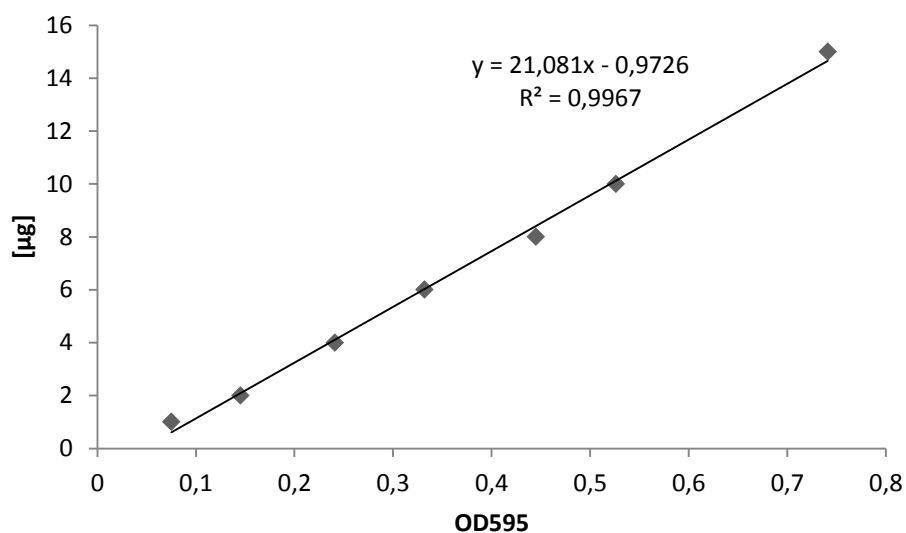


Figure 16: Standard curve for determination of protein concentration

BSA was used in different amounts (1-15 μ g) for Bradford assay and OD595 was determined. Afterwards a standard curve was generated with Microsoft Excel and the formula of $y=21,081*x- 0.9726$ was used for calculating the μ g of protein in the sample after OD595 measuring.

LYSIS

Cells were lysed in Hepex lysis buffer, pooled if possible and centrifuged for 20min at maximal speed and 4°C. Afterwards supernatant was transferred into a fresh Eppendorf tube and filled up with loading buffer. Proteins were denatured at 94°C for 5min before loaded on the 4-12% Gel in XT MOPS buffer. Depending on the used Voltage 120-180V the Gel ran for 90- 120min.

BLOTTING ON THE MEMBRANE

Proteins were blotted using a PVDF-membrane and a Turbo Blot Instrument.

BLOCKING

After blotting of proteins, the membrane was blocked with 5% milk solution for 1 h.

ANTIBODY INCUBATION

Primary antibodies were generally diluted 1:1000 in 5% milk or 5% BSA solution according to producer's recommendation and membranes were incubated over night at 4°C. Traces of antibody were removed by washing three times with TBS-T buffer for at least 10 minutes. The second antibody was diluted 1:2000 in 5% milk and membranes were incubated at room temperature for at least 1h. The membranes were washed three times in TBS-T Buffer and membranes were covered with detection reagent (ECL or Visualizer) and films were processed.

2.2.21 COMPOUND TREATMENT

3000 cells were seeded in 190µl of the appropriate medium and incubated for 24h at 37°C. On day 1 the compound was diluted 1:4, starting with a concentration of 50µM and 10µL of 20 fold concentrated compound were added. On day 3 or 4 Alamar blue reagent was added and dose response curves were generated using GraphPad Prism.

2.2.22 AAV-PARTICLE EXPERIMENT

SK-HEP-1 Clone-wt3 generated by AMAXA plasmid transfection was used for the AAV particle experiment. 1×10^4 cells/ well in a 96-well plate were seeded and incubated for 24h until AAV particles with a MOI of 100,000 were added. Cells were incubated for another 48h until reporter gene assay was carried out.

3 RESULTS

3.1 Protein Levels of Hippo-relevant Genes in a Panel of Human HCC Cell Lines

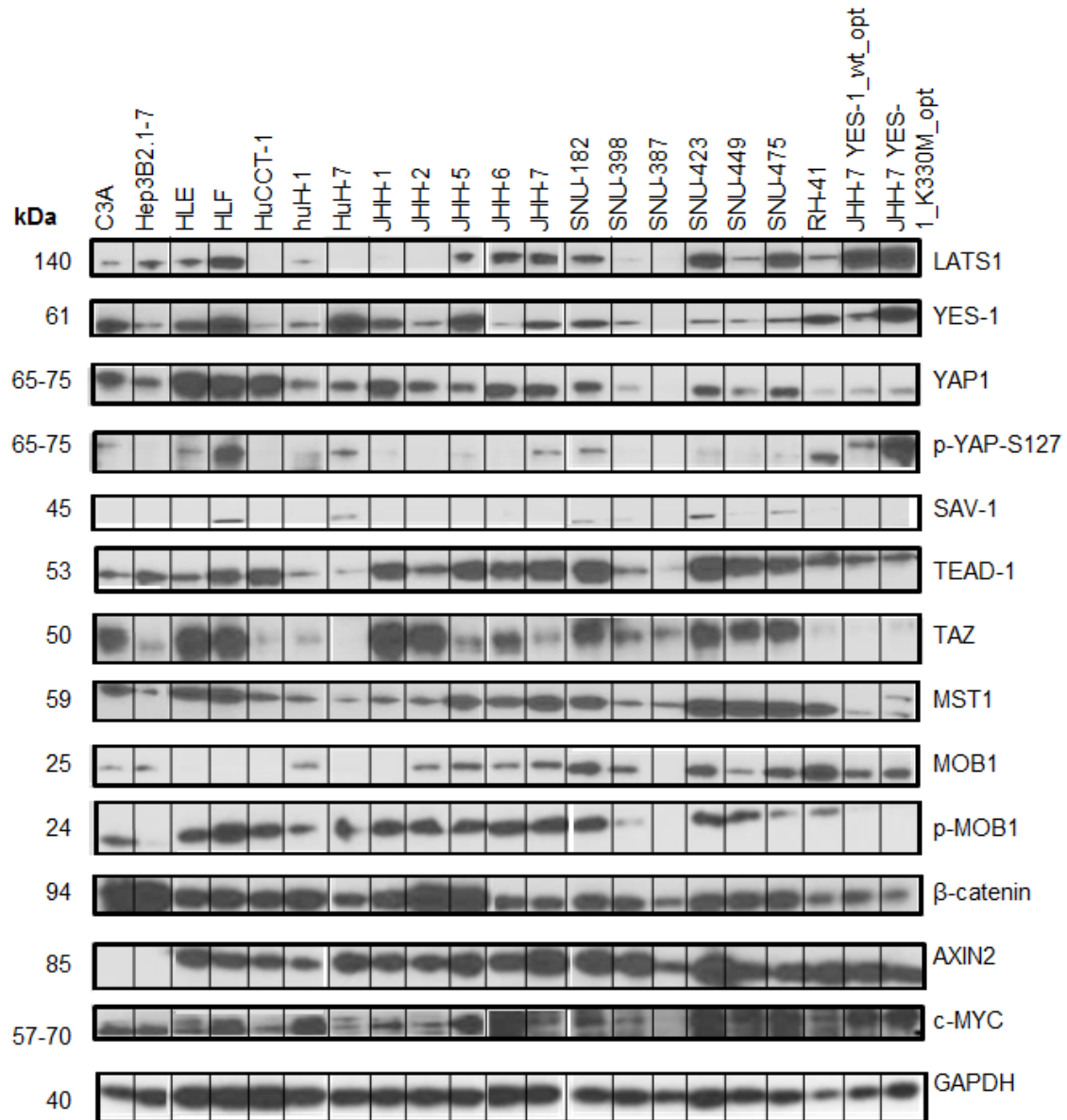


Figure 17: Western blot analysis of Hippo-relevant proteins in 21 HCC cell lines

Cells at a confluence of ~70% were lysed and the proteins of interest were analyzed on Western blot. The left column of the figure depicts the molecular weight in kDa of the different proteins. Gene names are displayed on the right side. Cell lines are shown at the top. The last two columns depict two recombinant JHH-7 cell lines, one of which is transiently expressing YES-1_wt the other YES-1_K330M.

Note: The absence of AXIN2 signal in C3A and Hep3B2.1-7 might be caused by an inappropriate covering of the membrane with detection reagent.

In order to analyze the Hippo-specific protein repertoire of hepatocellular cell lines, a detailed Western blot analysis was performed. In addition, the change in protein levels of those proteins was analyzed under conditions of over-expression of either wt- or kinase dead- (K330M) YES-1 in cell line JHH-7 (JHH-7 YES-1_wt or YES-1_K330M).

Elevated levels of c-MYC, which is proposed to be a target gene of the Hippo pathway [106], can be seen in the majority of cell lines. This particularly holds true for **HLF**, **huH-1**, **JHH-5**, **JHH-6**, **SNU-423**, **SNU-449** and **SNU-475** whereas **SNU-387**, **JHH-2** and **HuCCT-1** have only low c-MYC levels. Interestingly, in cell lines that over-expressed YES-1_wt or YES-1_K330M, the protein levels of c-MYC are increased compared to the un-transfected JHH-7 cell line. It might be the case that over-expression of YES-1, regardless of its kinase function, triggers the expression of c-MYC and/or stabilizes the c-MYC protein.

Both WNT-pathway associated proteins, β -catenin and AXIN2, exhibit no great variance between the cell lines tested.

With regard to Hippo pathway related proteins, the cell lines show a more heterogeneous expression profile. TEAD1 is increased in **HLF**, **HuCCT-1**, **JHH-1**, **JHH-5**, **JHH-6**, **JHH-7**, **SNU-182**, **SNU-423**, **SNU-449** and **SNU-475** whereas **SNU-387**, **HuH-7** and **huH-1** only express very low levels of TEADs. Additionally, cells which were transfected with YES-1 plasmid show a decrease in TEAD1, YAP and TAZ levels compared to the parental cell line JHH-7 (Fig. 17).

With regard to YAP and phosphorylated YAP at position 127 (p-YAP-S-127) levels, a huge variation is observed. P-YAP-S-127 is hardly detectable in many cell lines indicating that most of them seem to have an inactive Hippo pathway (at least from the point of view of the inhibitory phosphorylation pattern of YAP). However, the intracellular localization (nucleus vs. cytoplasm) of p-YAP-S-127 has also to be taken into account (for details see Fig. 18). High levels of p-YAP-S-127 are only seen in **HLF**, **RH-41** and **JHH-7_K330M**. Interestingly, in some cases p-YAP-S-127 appears as a double band (e.g. huH-1) or as the faster migrating band only (e.g. RH-41). The biologic meaning of these variants and the molecular mechanism leading to the formation of these variants (clipped protein, alternative splice variants, isoforms etc.) is not known. In contrast, YAP levels are high in approximately one third of analyzed

cell lines but YAP is expressed at moderate levels in most of the other cell lines. A low expression is found in **SNU-398**, **RH-41** and the two JHH-7 recombinant sub-lines, **JHH-7 YES-1_wt** and **JHH-7 YES-1_K330M** mutant, respectively. **SNU-387** exhibits no expression of YAP at all.

A strong signal for expression of one of the two negatively regulating kinases, LATS1 is detected in **HLF**, **JHH-6**, **JHH-7**, **SNU-423**, **SNU-475** and in the two modified cell lines **JHH-7 YES-1_wt** and **JHH-7 YES-1_K330M**. It is noteworthy, that levels of LATS1 are increased after transiently transfecting cells with both YES-1 expression plasmids whereas a concomitant drop in protein levels of MST1 can be observed.

MST1 is efficiently expressed in more than half of the HCC cell lines. Lower expression is found in **SNU-387/398**, **JHH-1/-2/-7**, **huH-1**, **Hep3B2.1-7** and the two recombinant **JHH-7 sub-lines**.

In *Drosophila* Mats (human MOB) was shown to be essential for control of proliferation and death. Loss of this tumor suppressor protein is lethal for flies. It was described to be specifically phosphorylated on Thr-12 and Thr-35 by MST1/2 [86] whereas for our studies an antibody against the p-MOB-Thr-35 was used. The binding of members of the MOB (Mps one binder) protein family, is essential for LATS kinase to fulfil its function and subsequently contributes to the inhibition of YAP and TAZ [86]. In our studies a huge difference in the phospho-specific and the pan-signal was observed. In some cell lines there is no or only a minor pan-signal visible but a strong signal with the corresponding phospho-specific antibody including cell lines **SNU-387**, **JHH-1/-7**, **huH-1**, **HLF**, and **HLE**. In contrast to the parental cell line JHH-7, over-expression of both YES-1 variants in JHH-7 lead to induction of MOB1. It therefore, cannot be excluded that over-expression of both active and inactive YES-1 can modulate the Hippo pathway, a phenomenon which also can be observed with p-YAP-S-127 and LATS1 (see above).

SAV-1, a protein interacting with MST1/2 is also regarded to inhibit YAP and TAZ. In general, the protein levels of this regulatory protein are rather low or even undetectable on Western blot in most of the HCC cell lines.

In summary, based on the complex Western blot data the following conclusions can be drawn: Firstly, with regard to the expression level of YAP, TAZ and TEADs, cell lines **SNU-182/423/475**, **JHH-1/2/5/6/7**, **HuCCT-1**, **HLF**, **HLE**, **C3A** and **Hep3B2.1.7** respectively, exhibit an over-expression. Secondly, according to the expression level of YES-1, this kinase may contribute to the activation in **SNU-182**, **JHH-1/5/7**, **HLE**, **HLF** and **C3A**. Thirdly, the level of counteracting proteins such as LATS1, MOB1 and MST1 remains to be analyzed in knockdown studies. It may be easily conceivable that activation/over-expression of YAP, TAZ and TEADs may also lead to an increase in the levels of counteracting proteins such as LATS1, MOB1 and MST1. Fourthly, the induction of the putative target gene *c-MYC*, in most cases goes hand in hand with expression levels of YAP/TAZ/TEADs. Fifthly, expression levels of AXIN2 and β -catenin do not allow discrimination between the analyzed cell lines. To further address the contribution of selected proteins, the sub-cellular localization was analyzed in more detail (see 3.2.) and knockdown studies for the activating proteins were performed (see 3.3. and 3.4).

mean activation level) and <0.2 (red: low activation level). Similarly the activation status was determined for the N/C ratio of TAZ and YES-1. The assumption that YES-1 can most efficiently contribute in its nuclear-localized form is purely speculative and based on the observation in colon cancer cell lines [79]. A comparison of the ratio p-YAP-S-127 with pan YAP is not feasible as the affinity of the detection antibodies is different for pan-YAP and p-YAP-S-127. As TEF-1 (TEAD1) is exclusively detected in the nucleus (Fig. 18) the calculation of a distribution ratio is not meaningful. TEAD1 is one of the major transcription factors of the Hippo pathway and its presence in the nucleus points to the activation of this pathway [18]. However, it is currently not known if the ratio of nuclear vs. cytoplasmic presence has any influence on the level of induction of this pathway. The analysis of p-YAP-S-127 and GAPDH serves as a quality control of the preparation of nuclear and cytoplasmic extracts, whereas both proteins are expected to be found exclusively in the cytoplasm.

In general, the protein levels of TEF-1 (TEAD1) are very high except in JHH-6. Almost all cell lines which had been already shown to highly express TEAD1 in whole cell lysates (Fig. 17) including **HLF**, **JHH-1/-5/-7** and **SNU-423/-449** were also identified as high expressers by results obtained from C and N extracts (exceptions are JHH-6 and HuCCT-1). The differences in the latter two cell lines might be due to an inappropriate extraction of nuclear proteins by using whole cell extractions or losing protein during cytoplasmic and nuclear separation. Different pathways might be turned on at different time points and also confluence might influence the stability of the respective proteins.

With regard to the distribution of YAP, **JHH-5**, **SK-HEP-1**, **C3A**, **huH-1**, **HuH-7** and **SNU-398** are characterized as Hippo-activated cell lines and are expected to be sensitive to YAP RNAi-mediated knockdown. Cell lines which depict elevated levels of YAP1 are **SK-HEP-1**, **HLE**, **HuCCT-1**, **JHH-4/-6**, **C3A**, **huH-1** **HuH-7** and **SNU-398/-475** which in part correlates with the analysis of whole cell lysates (Fig. 17).

Interestingly, some cell lines like **SK-HEP-1**, **HLE**, **JHH-4**, **huH-1**, **Hep3B2.1-7**, **JHH-1**, **SNU-423** and **JHH-2** exhibit high amounts of TAZ, which is a paralog of YAP. There is evidence that YAP and TAZ can substitute for each other which might be the reason why cell lines are still able to proliferate after knockdown of one of the homologs (see 3.3. and 3.4.).

YES-1 was shown to interact with YAP, β -catenin and TBX5 in the nucleus of colon carcinoma cell lines [79]. In total, we investigated 21 HCC cell lines with regard to distribution of YES-1 kinase and found that this kinase is present in the cytoplasm as well as in the nucleus. According to our assumption that nuclear YES-1 is necessary for YAP activation, **HepG2**, **JHH-1/-2/-4/-5** and **SNU-423** are suggested as representatives of YES-1 dependent cell lines. Interestingly, YES-1 appears as a two-band pattern on the Western blot (Fig. 18) most likely due to the reported splice variants (<http://omim.org/entry/164880>). The reason why some cell lines show either the lower- or the upper- band in one of the two fractions (e.g. JHH-6, C3A, huh-1) is unclear. Furthermore, YES-1 can exclusively found in the nucleus of **HepG2**, **HLE**, **JHH-1**, **SNU-423** and **JHH-2**. Conversely in **SK-HEP-1**, **HuCCT-1** and **SNU-449** it can be detected in the cytoplasm.

Based on the distribution pattern of either YAP or TAZ (N/C ratio higher than 0.5; see Fig. 18), the following HCC cell lines can be regarded as potentially Hippo-pathway dependent: **JHH-1,-2,-4,-6**, **SK-HEP-1**, **HLE**, **C3A**, **HuH-1,-7**, **SNU-398,-423**, and **HEP3B2.1-7**. Provided that YES-1 in the nucleus of HCC cell lines equally contributes to the Hippo activation as shown for colon cancer [79] the cell lines **HepG2**, **JHH-1,-2,-4,-6**, **HLE** and **HEP3B2.1-7** (N/C ratio of YES-1 higher than 2) might also be YES-1 dependent. Since it could not be ruled out that the change in the protein pattern is subjected to the cultivation conditions, we next performed a detailed knockdown study of the essential downstream Hippo proteins such as TAZ, YAP, TEADs and YES-1.

3.3 siRNA-mediated Knockdown of TAZ, YAP, TEADs and YES-1 in HCC Cell Lines

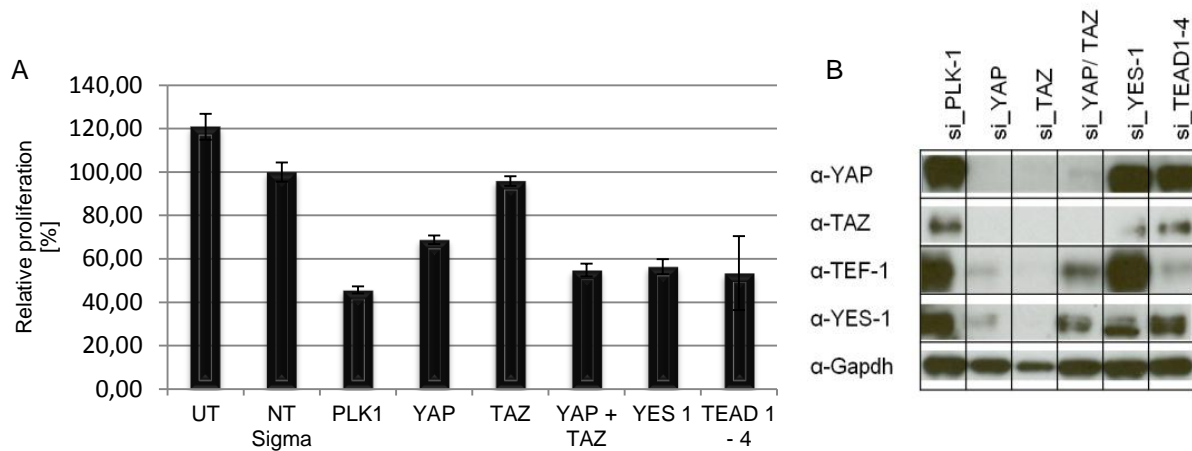


Figure 19: SK-HEP-1 after 72 hours of siRNA treatment

A) Alamar blue: Cell proliferation was measured by using the Alamar blue assay. Assays were performed in triplicate values ($n > 3$) were normalized to the negative non-targeting control (NT Sigma), which was set to 100% proliferation. The untreated cell line served as an additional negative control (UT). Knockdown of PLK-1 represents the positive control **B) Western blot:** GAPDH was used as a loading control. At the top of the Western blot image the respective siRNAs are depicted. The description at the left side of the image indicates the specific antibody used for detection.

Due to the accumulation of YAP and TAZ in the nucleus (Fig. 18), SK-HEP-1 was suggested to be a YAP- as well as TAZ- dependent cell line. In contrast, YES-1 was shown to be localized preferentially in the cytoplasm (Fig. 18) and therefore SK-HEP-1 was regarded to be YES-1-independent.

HCC cell lines are known to be either resistant or extremely sensitive to manipulation in particular to transfection procedures (pers. commun. W.Mikulits/ Medical University Vienna). Therefore, transfection conditions had to be optimized individually for each HCC cell line. As a positive control of knockdown (kd) PLK-1 was used throughout all experiments. In SK-HEP-1 kd of YAP has a pronounced influence on proliferation. The same holds true for YES-1 and TEAD1-4. Kd of TAZ had no effect but the double kd of YAP+TAZ exhibited a similar reduction in proliferation as the kd of PLK-1. It has to be taken into account that even the kd of PLK-1 lead to the reduction in proliferation of 60% only. Although PLK-1 had already an influence on proliferation, the protein status of the Hippo proteins is still maintained. Therefore, a reduction in the same range as seen with kd of PLK-1 can be regarded as significant. On Western

blot, a 50% reduction in protein for YES-1 was observed whereas the kd of YAP, TAZ, YAP+TAZ and TEAD1-4 were almost complete (Fig. 19B).

As the efficient kd of TAZ had no effect on proliferation but that from the paralog gene YAP, it can be concluded that YAP plays an essential role in proliferation of SK-HEP-1. The same holds true for TEAD1-4 and YES-1 even though kd of YES-1 was not complete (Fig. 19B).

Interestingly, the amount of TAZ protein was greatly decreased after YES-1 kd. A similar effect was observed with TEAD1 (=TEF-1) upon kd of YAP and/or TAZ. Whenever YAP and/or TAZ were knocked down a dramatic decrease in TEAD1-4 levels was observed. These data set not only prove SK-HEP-1 as YAP, YES-1 and TEAD1-4 dependent but it also shows how these genes/proteins are wired. If this “wiring” takes place at transcriptional or (post)-translational level, remains to be determined.

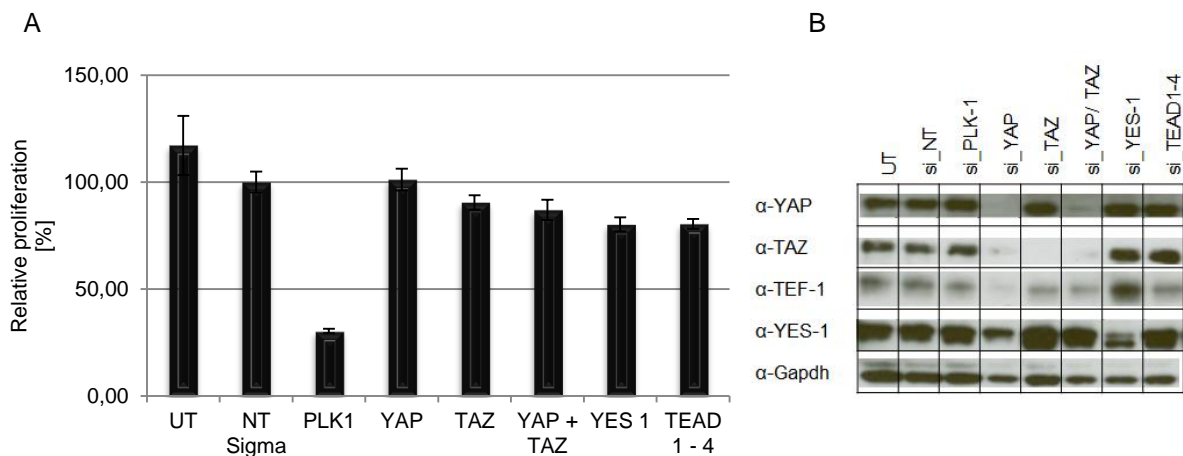


Figure 20: HLF after 72 hours of siRNA treatment

Details of the experiment are stated in Figure 19 A) Alamar blue B) Western blot

In identically designed experiments further HCC cell lines were analyzed (HLF, HLE, huH-1 and JHH-4 (Figs. 20-23)). Based on the data which had been obtained from the detailed Western blot analysis on the nuclear vs. cytoplasmic distribution of key proteins of the Hippo pathway, HLF was suggested to be a non-dependent cell line. In general, the HLF cell line exhibits YAP, TAZ and YES-1 over-expression (Fig. 17). For all analyzed proteins only a partial inhibition of proliferation was observed upon

knockdown although the kd was incomplete in the case of TEAD1-4 and YES-1, respectively (Fig. 20B). According to these results, HLF can be regarded as a YAP and/or TAZ and most likely also YES-1 independent cell line whereas shRNA-mediated kd revealed different results (Fig. 38). Again, kd of YAP lead to a decrease in TAZ, TEAD1-4 and YES-1 levels. Interestingly, kd of TAZ lead only to a decrease in TEAD1-4 but not in YAP or YES-1 perhaps indicating a different “wiring” as in the SK-HEP-1 cell line.

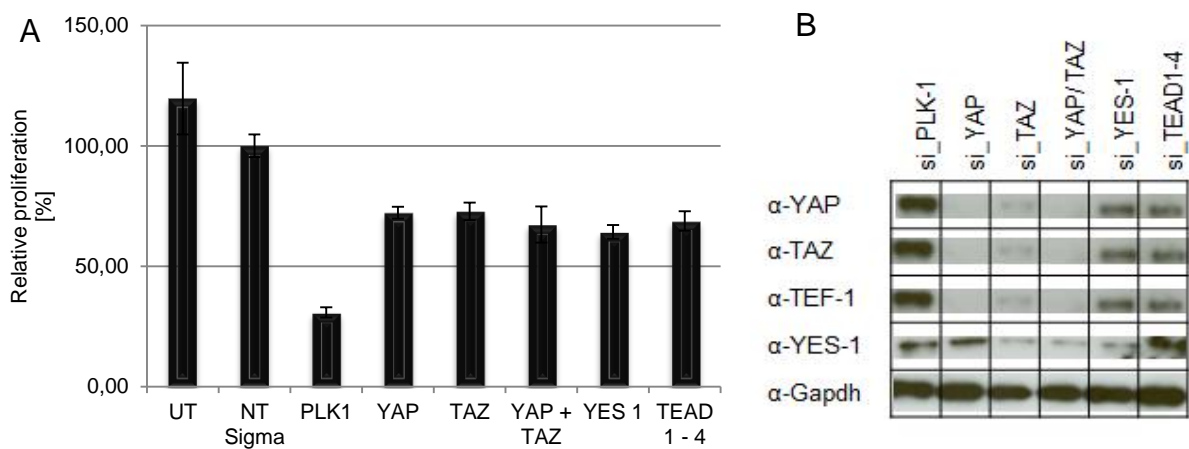


Figure 21: HLE after 72 hours of siRNA treatment

Details of the experiment are stated in Figure 19 A) Alamar blue B) Western blot

Cell line HLE was suggested to be partially dependent on YAP and dependent on TAZ and YES-1 (Fig. 18). The efficient kd of YAP, TAZ and YES-1 had a mediocre effect on the proliferation of HLE whereas a kd of TEAD1-4 was not achieved. Again, YAP as well as TAZ and the combined kd lead to decreased levels of the respective other co-transcription factor but also to significant reduced levels of YES-1 and TEAD1-4, respectively. To summarize, HLE exhibits only a weak dependency on YAP, TAZ and YES-1.

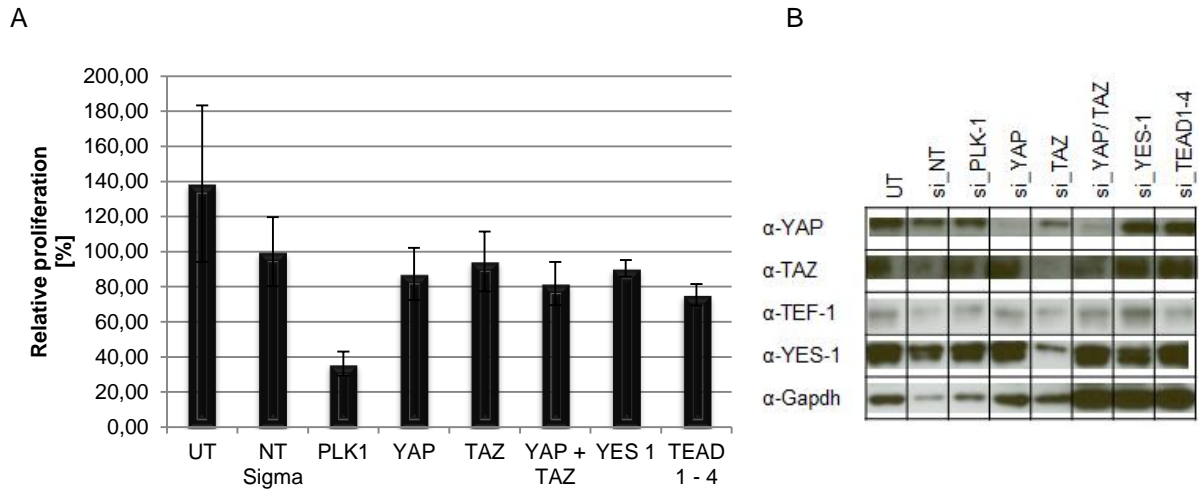


Figure 22: huH-1 after 72 hours of siRNA treatment

Details of the experiment are stated in Figure 19 A) Alamar blue B) Western blot

In addition to HLE, also huH-1 cannot be regarded as a cell line being dependent on any of the analyzed proteins. Although the GAPDH levels suggest an inappropriate loading for some samples (Fig. 22B) a few conclusions can still be drawn. Neither an efficient kd of YAP or TAZ nor the combined kd has any significant effect on proliferation of huH-1. As YES-1 and TEAD1-4 could not be efficiently knocked down no conclusive results could be obtained. Kd of YAP does not influence the protein levels of TAZ, TEAD1 (=TEF-1) or YES-1. However, kd of TAZ massively reduces YES-1 but not YAP or TEAD1.

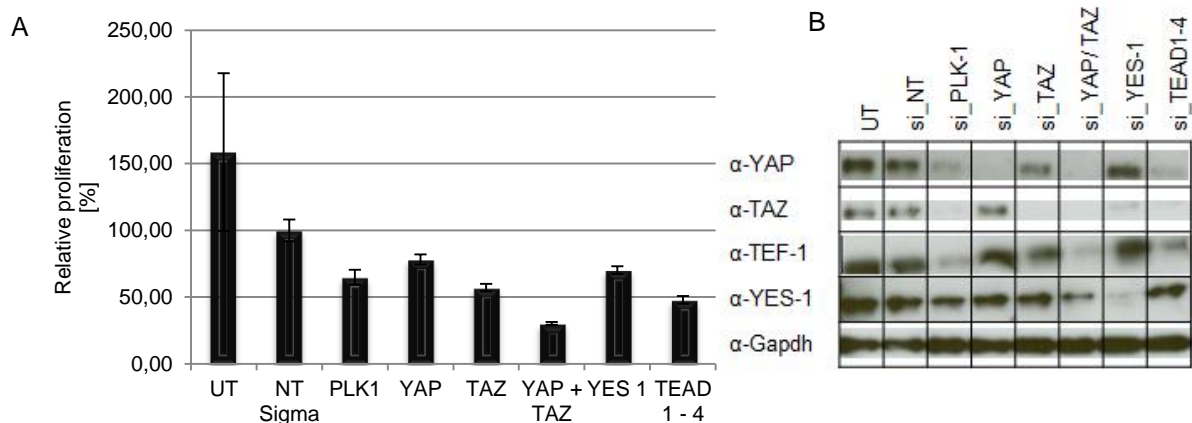


Figure 23: JHH-4 after 72 hours of siRNA treatment

Details of the experiment are stated in Figure 19 A) Alamar blue B) Western blot

Based on our previous studies, cell line JHH-4 was suggested to be YES-1 and TAZ dependent and partially dependent on YAP (Fig. 18). JHH-4 is a representative example of the reported different behavior of HCC cell lines. Kd of PLK-1 had a severe inhibitory influence on YAP, TAZ and TEAD1 levels although the loading control GAPDH stays unaffected. However, kd of YAP, TAZ, YAP+TAZ, YES-1 and TEAD1-4 had a pronounced inhibitory effect on the proliferation (between 40 to 75% reduction). As observed with other YAP, TAZ, YES-1 and TEAD1-4 dependent cell lines, the combined kd of YAP+TAZ lead to reduction in TEAD1 levels and kd of YES-1 and TEAD1-4 lead to a reduction in TAZ and YAP+TAZ levels, respectively.

Due to the fact that transfection conditions for siRNA-mediated kd could only be successfully optimized for six HCC cell lines, it was decided to use shRNAs for gene specific kds.

3.4 Lentivirus- based shRNA-mediated Knockdown of TAZ, YAP, TEADs and YES-1 in HCC Cell Lines

To overcome the problems of siRNA-mediated kd, in particular the fact that the majority of HCC cell lines could not be efficiently transfected with siRNA (see 3.3), we made use of a lentiviral delivery of shRNAs (for details see Material and Methods). Lentiviral constructs can easily transduce typically “challenging” cell lines and readily integrate the shRNA into the genome of these cells for stable gene silencing. In order to select for lentivirus-transfected cell lines a puromycin selection has to be performed. Therefore we first generated puromycin killing curves to identify the optimal concentration for selection after transduction to enrich for positively transfected cells. In a next step, we tested five different shRNAs for each gene of interest (YAP, TAZ, YES-1 and TEAD1-4) in one representative cell line JHH-7 before we performed shRNA-mediated kds in ten HCC cell lines. Usually the validating experiments were conducted according to lentiviral transduction method 1 whereas for the specific kds in the different HCC cell lines method 2 seemed to be more beneficial (for details see Material and Methods).

3.4.1 PUROMYCIN KILLING CURVES

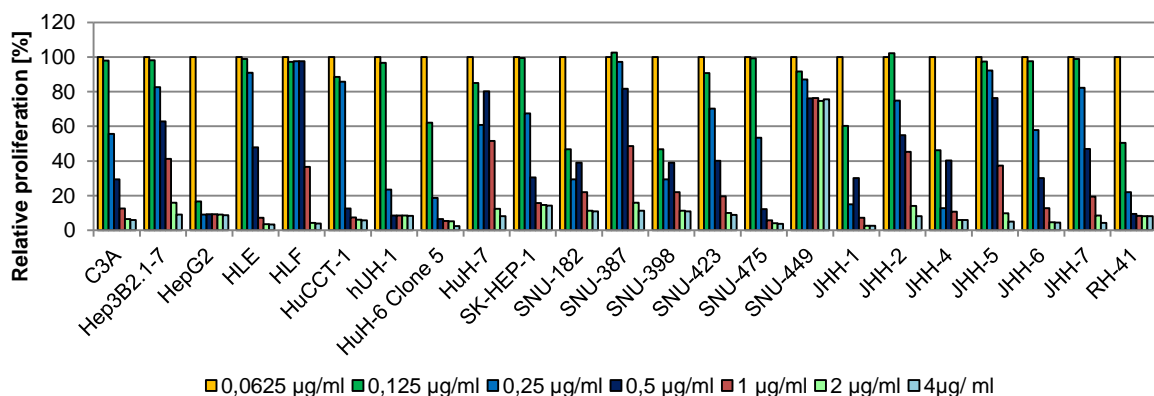


Figure 24: Puromycin titration from 4-0.06 µg/ml in 23 HCC cell lines

The different cell lines are indicated. The first bar always represents 100% proliferation (yellow) normalized to the non-toxic treatment with 0.0625 µg/ml puromycin. All other values were set in correlation to that value.

Table 27: Lethal concentration [$\mu\text{g/ml}$] of Puromycin for 23 different HCC cell lines

Cell Line:	C3A	Hep3B2.1-7	HepG2	HLE	HLF	HuCC-T-1	hUH-1	HuH-6 Clone 5	HuH-7	SK-HEP-1	SNU-182	SNU-387	SNU-398	SNU-423	SNU-475	SNU-449	JHH-1	JHH-2	JHH-4	JHH-5	JHH-6	JHH-7	RH-41	
Puromycin [$\mu\text{g/ml}$]	2	4	0,25	2	2	2	1	0,5	4	4	4	4	4	4	2	>4	2	4	4	4	4	2	4	0,25

The range of lethal concentration of Puromycin for 23 analyzed cell lines lies between 0.25 and 4 $\mu\text{g/ml}$. For most cell lines treatment with 2-4 $\mu\text{g/ml}$ seemed to be appropriate except for HepG2 and RH-41 (0.25 $\mu\text{g/ml}$), HuH-6 Clone 5 (0.5 $\mu\text{g/ml}$) and SNU-449 (>4 $\mu\text{g/ml}$).

3.4.2 VALIDATION OF SHRNAs IN CELL LINE JHH-7

The validation of the different shRNAs was carried out according to lentivirus transduction method 1. Briefly, 3000 cells were transferred into a 96-well plate and proliferation was monitored. In contrast, using lentivirus transduction method 2 cells were initially seeded in 96-well plates and not transferred into another plate after puromycin selection.

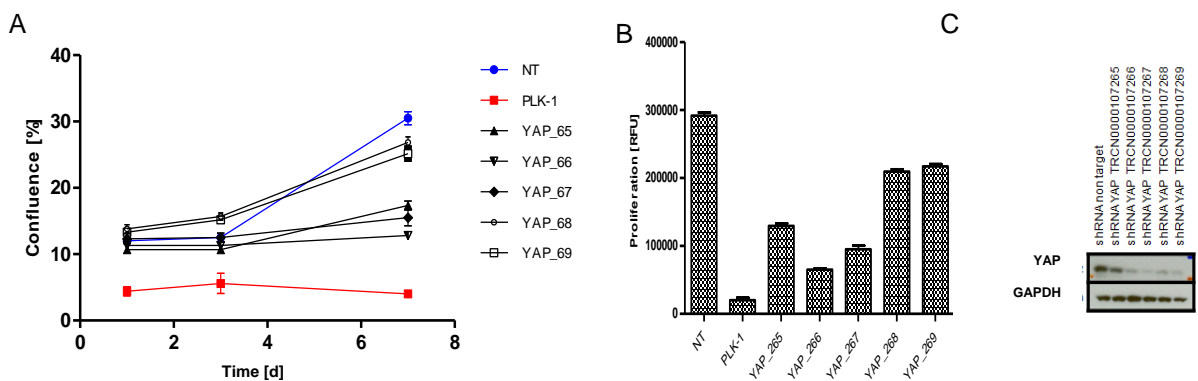


Figure 25: Characterization of five different YAP shRNA lentiviruses in cell line JHH-7 (7 days)

Transduced cells (3000 per well) were transferred into a 96-well plate and the proliferation was measured over a time period of 7 days. Five different constructs (see 2.2.3 shRNAs) were used and efficiency of kd was determined on Western blot
A) Confluence measurement (proliferation) B) Alamar blue C) Western blot

α -YAP: sc-101199 Santa Cruz; α -GAPDH: ab8245 Abcam

The knockdown was equally efficient for each construct except for shRNA_YAP_265 (Fig. 25C). Since for shRNA_YAP_265 there was still an influence on proliferation (Fig. 25A+B) detectable, it was regarded to act off-target. The usage of shRNAs YAP_266 and 267 lead to a great drop in proliferation as shown by confluence measurement (clone select imager, CSI; Fig. 25A) and Alamar blue assay (Fig. 25B). For further experiments **sh_YAP_266²** and **sh_YAP_268** were chosen.

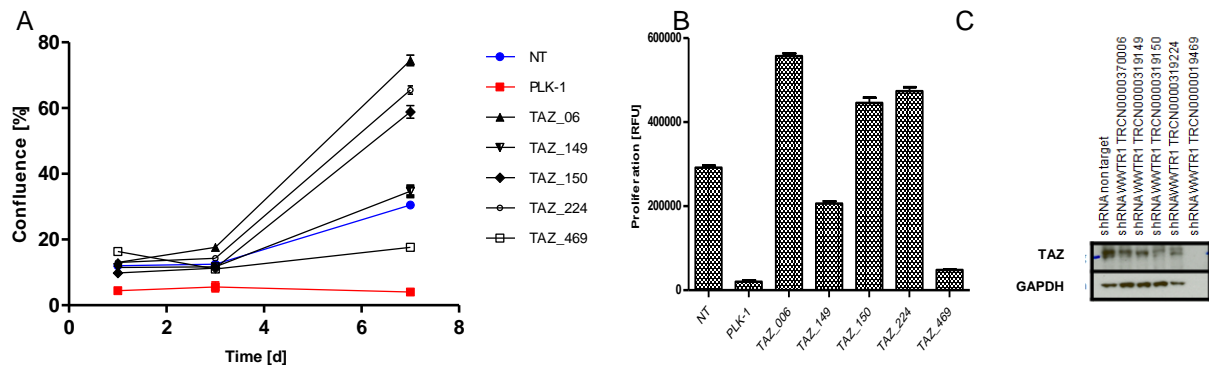


Figure 26: Characterization of five different TAZ shRNA lentiviruses in cell line JHH-7 (7 days)

Experimental details are described in Figure 25 **A) CSI confluence measurement** over a time period of 7 days after shRNA-mediated TAZ knockdown by using 5 different constructs **B) Alamar blue C) Western blot**

α -TAZ: #2149 Cell Signaling; α -GAPDH: ab8245 Abcam

In a similar way, protein levels of TAZ were compared after shRNA-mediated kd to the non-targeting control. Due to an invalid loading control of GAPDH (Fig. 26C) no conclusion about the kd efficiency could be drawn for sh_TAZ_469. Even though there is no pronounced effect on proliferation (Fig. 26A+B) the kd could be confirmed on Western blot for **sh_TAZ_150** and **224**. Both shRNAs were therefore chosen for further experiments. According to the provider (see 2.2.3 shRNAs) sh_TAZ_150 and 224 are less efficient than sh_TAZ_469. Therefore, it might be conceivable that sh_TAZ_469 already killed most of the cells, explaining why GAPDH was not detectable.

² Numbers of shRNAs always refer to the last 3 numbers of the original number listed in 2.2.3 shRNAs

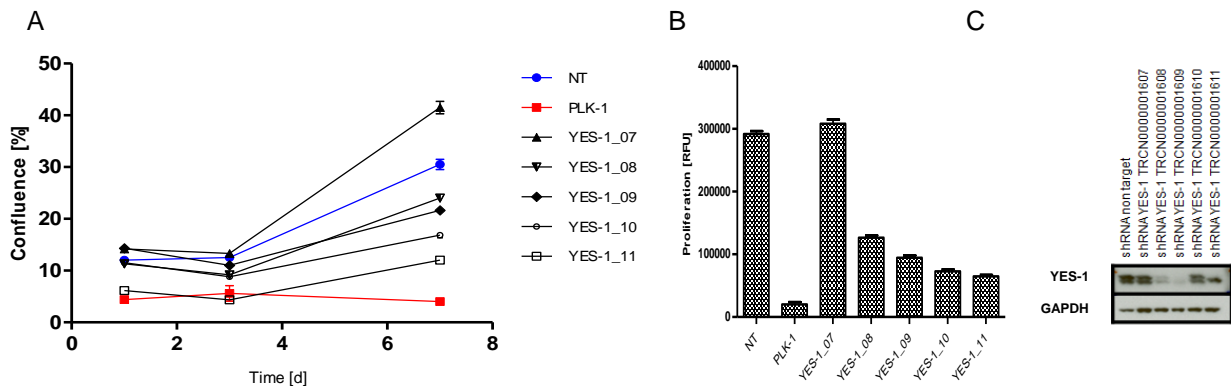


Figure 27: Characterization of five different YES-1 shRNA lentiviruses in JHH-7 cell line (7 days)

Experimental details are stated in Figure 25 **A) CSI confluence measurement** over a time period of 7 days after shRNA-mediated YES-1 knockdown by using 5 different constructs **B) Alamar blue C) Western blot**

α -YES-1: ab133314 ; α -GAPDH: ab8245 Abcam

The Western blot for YES-1 kd showed a pronounced reduction of protein levels after treatment of cells with sh_YES-1_08, 09 and 11. These data correlate well with the kd efficiency given by the provider. As concluded from the proliferation data (Fig. 27B) the sh_YES-1_07-mediated kd did not work (Fig. 27C). For sh_YES-1_10 an off-target effect might be the cause of the drop in proliferation as the protein could still be detected on the Western blot (Fig. 27C). For further experiments sh_YES-1_09 and sh_YES-1_11 were chosen.

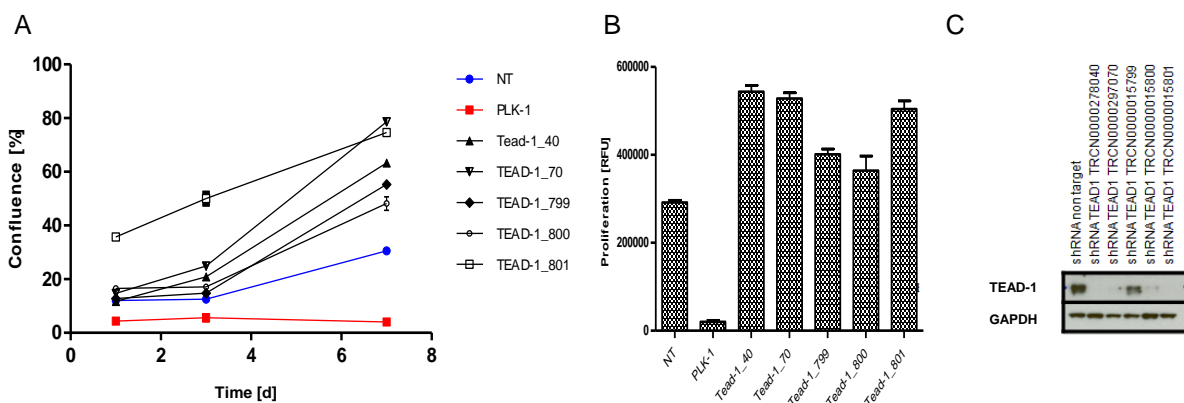


Figure 28: Characterization of five different TEAD1 shRNA lentiviruses in cell line JHH-7 (7 days)

Experimental details are stated in Figure 25 **A) CSI confluence measurement** over a time period of 7 days after shRNA-mediated TEAD1 knockdown by using 5 different constructs **B) Alamar blue C) Western blot**

α -TEAD1: #122292 Cell Signaling; α -GAPDH: ab8245 Abcam

Except for sh_TEAD1_799 a kd of TEAD1 was confirmed on Western blot for all shRNAs. According to efficiency values enumerated by the provider all of the shRNAs are described to have more than 90% kd efficiency with the exception of sh_TEAD1_070. No effect of any of the TEAD1 shRNAs on the proliferation (Fig. 28A+B) of cell line JHH-7 was observed. Most likely the growth of JHH-7 cell line is not dependent on TEAD1. Taken the results from the Western blot **sh_TEAD1_800** and **sh_TEAD1_801** seemed to generate the most efficient kd of TEAD1.

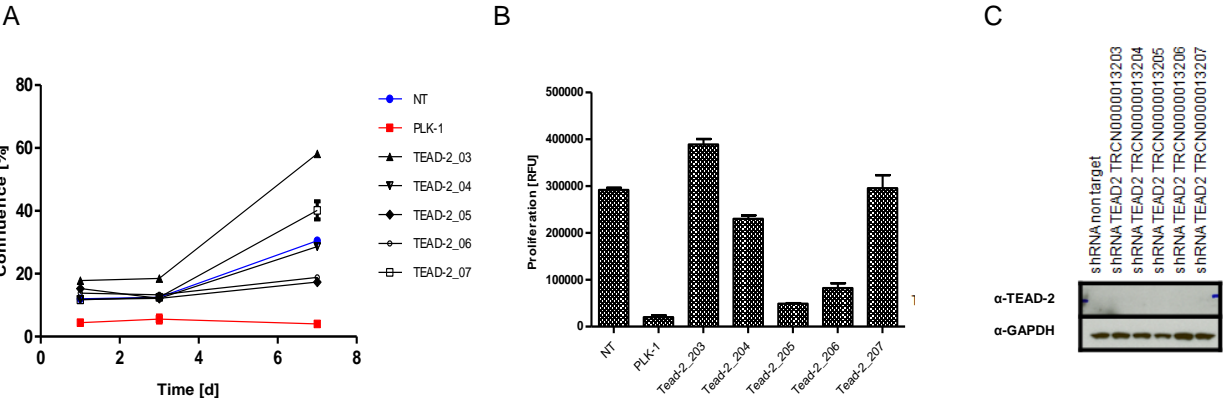


Figure 29: Characterization of five different TEAD2 shRNA lentiviruses in cell line JHH-7 (7 days)

Experimental details are stated in Figure 25 A) **CSI confluence measurement** over a time period of 7 days after shRNA-mediated TEAD2 knockdown by using 5 different constructs B) **Alamar blue** C) **Western blot**

α-TEAD2: #8870 Cell Signaling; α-GAPDH: ab8245 Abcam

The TEAD2 antibody exhibited no signal on the Western blot at all. Therefore, the selection of shRNAs was based on proliferation only. Two out of five TEAD2 shRNAs induced a pronounced drop in proliferation (**sh_TEAD2_205** and **206**).

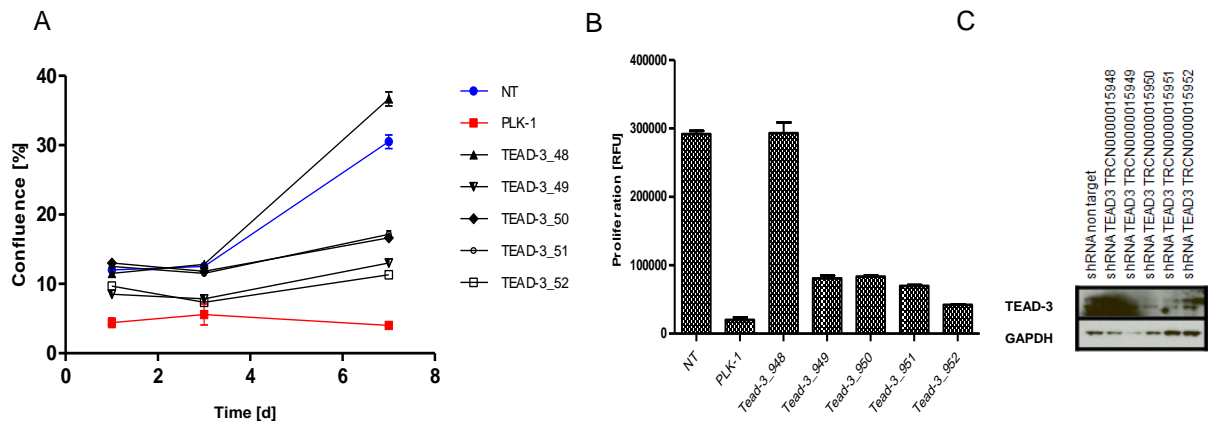


Figure 30: Characterization of five different TEAD3 shRNA lentiviruses in cell line JHH-7 (7 days)

Experimental details are stated in Figure 25 **A) CSI confluence measurement** over a time period of 7 days after shRNA-mediated TEAD3 knockdown by using 5 different constructs **B) Alamar blue C) Western blot**

α -TEAD3: ab75192; α -GAPDH: ab8245 Abcam

Knockdown of TEAD3 triggers a pronounced inhibitory effect on the proliferation (Fig. 30A+B) of cell line JHH-7. Based on both the kd efficiency and the inhibition of proliferation **sh_TEAD3_949** and **950** were chosen for further experiments.

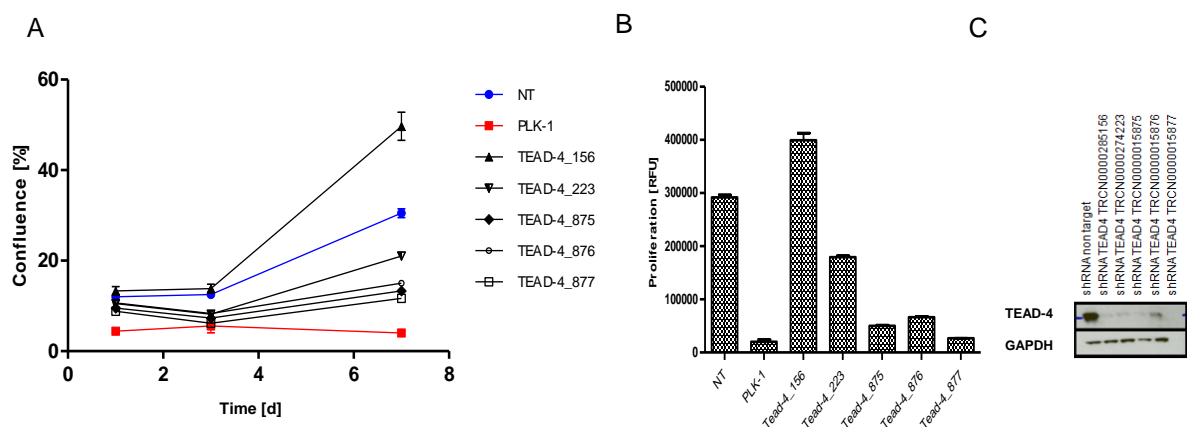


Figure 31: Characterization of five different TEAD4 shRNA lentiviruses in cell line JHH-7 (7 days)

Experimental details are stated in Figure 25 **A) CSI confluence measurement** over a time period of 7 days after shRNA-mediated TEAD4 knockdown by using 5 different constructs **B) Alamar blue C) Western blot**

α -TEAD4: ab58310; α -GAPDH: ab8245 Abcam

The kd of TEAD4 worked quite efficiently for each of the shRNA tested (Fig. 31C). Based on the most inhibitory effect on proliferation **sh_TEAD4_223** and **sh_TEAD4_875** were selected for further experiments.

3.4.3 LENTIVIRAL TRANSDUCTION

Based on the results obtained from the validation of shRNAs (see 3.4.2), two constructs for each protein were chosen and used for lentiviral transductions of 10 HCC cell lines. In the case of a combined knockdown (kd) of more than one gene, only one shRNA lentiviral construct per gene was used (YAP_66, TAZ_150 and YES-1_09). As the regulation of the Hippo pathway depends on cell density [73], we also included cell confluence as a third parameter. In general, an increase in kd was observed at a lower cell density. Interestingly, combination of several shRNA lentiviral constructs lead sometimes to a decrease in the kd efficiency [112]. One reason for these phenomena might be the unspecific interaction of the various shRNA constructs thereby reducing their kd potential. In general, the negative controls such as the untreated cell lines (UT) and treatment with non-targeting lentivirus shRNAs (NT) can be compared to each other. In this way effects generated by the treatment itself can be determined. In an optimal scenario the NT setting should not show a great difference compared to the untreated control. However, some of the analyzed HCC cell lines exhibited already a negative influence on their proliferation upon treatment with non-targeting shRNA lentiviral constructs, a phenomenon particularly known for HCC cell lines [112]. In addition, the positive controls (treatment with Puromycin and kd of PLK-1) can be compared to each other. Both treatment modalities lead to induction of cell death (apoptosis). Puromycin is a protein synthesis inhibitor causing premature release of nascent polypeptide chains and kills all untransfected cells not expressing the resistance gene [85]. PLK-1 which is essential during mitosis leads to massive cell death after kd [86]. All of the HCC cell lines analyzed were equally sensitive towards both treatment modalities.

3.4.3.1 HEP3B2.1-7

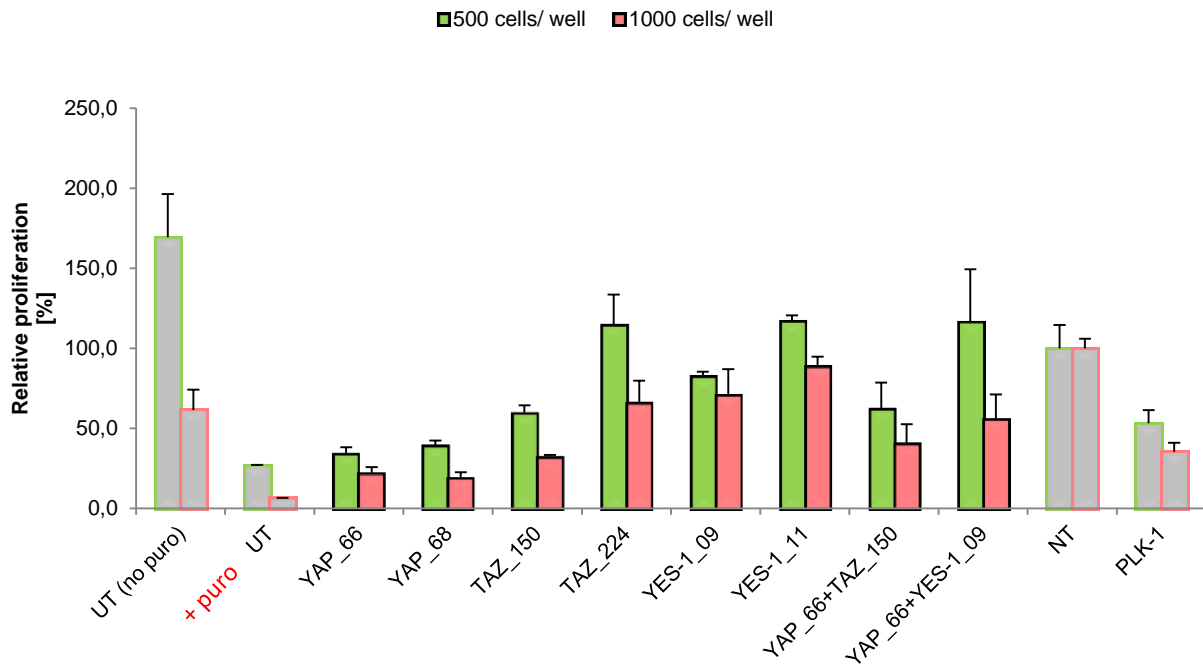


Figure 32: Hep3B2.1-7 proliferation data

A) 500 cells/ well (green) **B)** 1000 cells/ well (red); readout: Alamar blue

Negative controls: untreated (UT), non-targeting (NT); Positive controls: Puromycin treatment and kd of PLK-1. The targets of the respective shRNA lentivirus constructions are indicated.

Hep3B2.1-7 (Fig. 32) exhibited sensitivity towards YAP kd at both cellular density set ups as well as for both constructs (sh_YAP_66/68). Kd was confirmed on Western blot (Fig. 33). Results for the TAZ kd are controversial (Fig. 32A+B) which is due to an incomplete kd by shRNA_TAZ_224 as shown on Western blot (Fig. 33B+E). Based on these data, Hep3B2.1-7 can be regarded as a YAP- as well as a TAZ-dependent cell line. The combination also decreases proliferation but combined treatment (YAP+TAZ) does not have a more pronounced effect than single treatment, which was previously shown in siRNA experiments (different cell line). Compared to those results obtained in cytoplasmic and nuclear extracts (Fig. 18), Hep3B2.1-7 was suggested to be partially sensitive towards YAP- and sensitive towards TAZ-kd which correlates with our data set retrieved from lentiviral transduction.

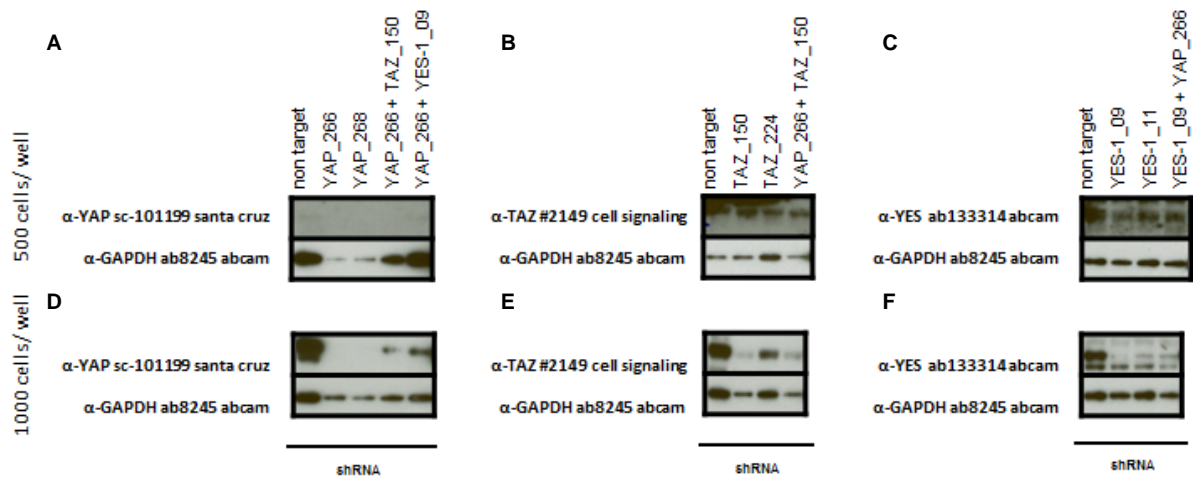


Figure 33: Hep3B2.1-7 Western blot data

Protein levels of YAP, TAZ and YES-1 after lentiviral shRNA- mediated knockdown A-C) 500 and D-F) 1000 cells/ well

Based on the results obtained by Western blot analysis of cytoplasmic and nuclear extracts, Hep3B2.1-7 cell line was suggested to be insensitive towards YES-1 kd. Similar results were obtained for the lentiviral shRNA-mediated kd of YES-1 (Fig. 32) as well as for the treatment with Dasatinib, a YES-1 inhibitor, for which the IC_{50} value was determined as $24.44\mu M$ (Table 29).

3.4.3.2 HLE

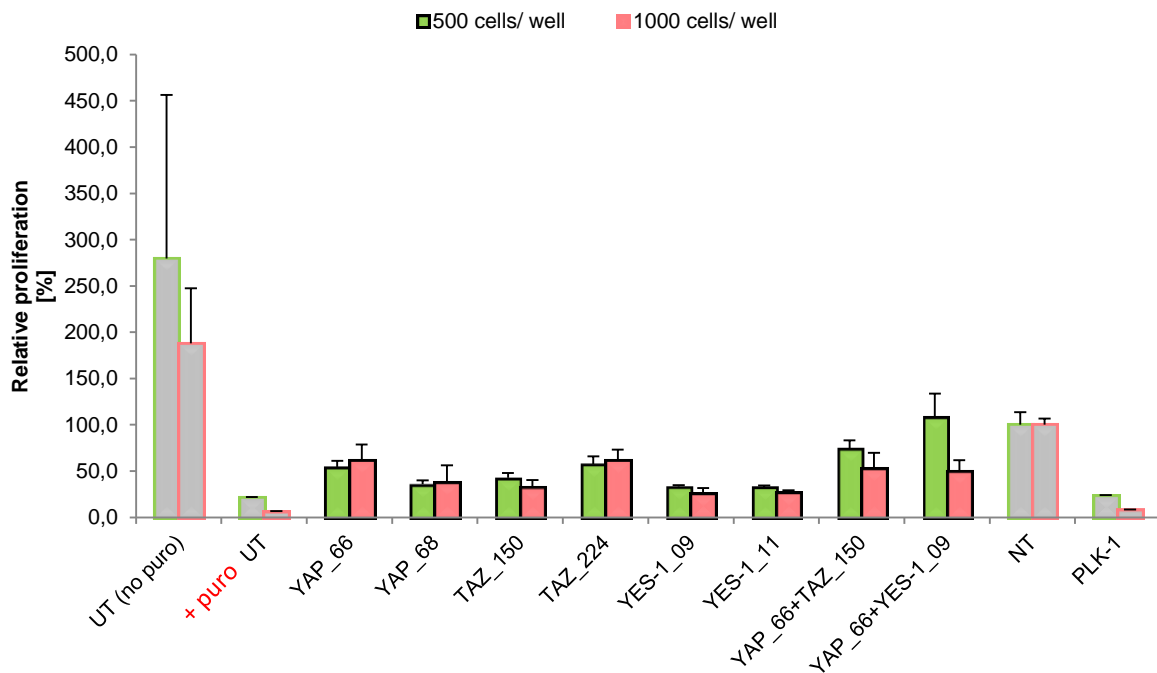


Figure 34: HLE Proliferation data relative to non-targeting- including untreated control

A) 500 cells/ well (green) **B)** 1000 cells/ well (red); readout: Alamar blue

Cell line HLE has been shown to produce huge amounts of YAP, YES-1, TAZ, p-MOB and c-MYC and decreased protein levels of SAV-1 in whole cell protein analysis (Fig. 17). Mutations have been found in FAT4 and SAV-1 (see attachments 8.5) which might indicate a deregulated pathway as SAV-1 and FAT4 influence Hippo pathway activity. The mutations can be characterized as loss-of-function mutations which would explain elevated levels of YAP, TAZ and subsequently c-MYC. With regard to the cytoplasmic and nuclear distribution, cell line HLE showed a high amount of YAP, TAZ as well as YES-1 in the nucleus and was therefore suggested to be sensitive towards kd of these genes which could be confirmed by using lentiviral transduction.

Even there was a great difference between UT and NT control (Fig. 34A), there is still a window between NT- and PLK-1-shRNA-treated cells (Fig. 34B). HLE was shown to be sensitive towards YAP-, TAZ- and YES-1- kd whereas combined treatment was less efficient due to mainly incomplete kd of TAZ (Fig. 35B). Nevertheless, YAP and YES-1 kd could be confirmed for both constructs as well as for combined treatment

whereas TAZ kd did not work at all. Therefore, impaired proliferation after shRNA_TAZ_150/ 224 mediated kd might be caused due to an off-target effect and cannot be regarded as a specific effect.

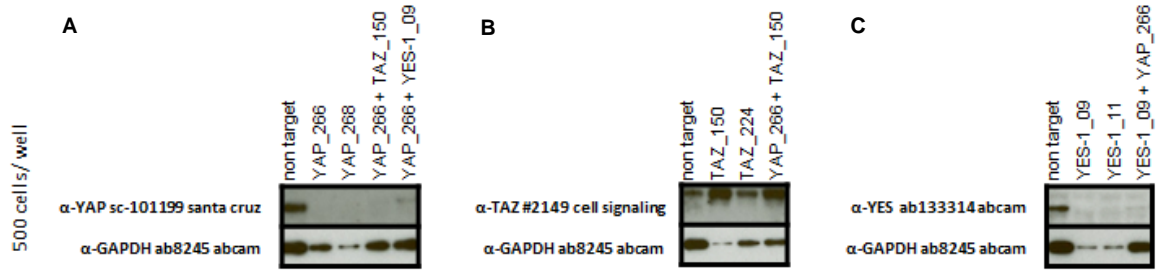


Figure 35: HLE Western blot data (500 cells/ well)

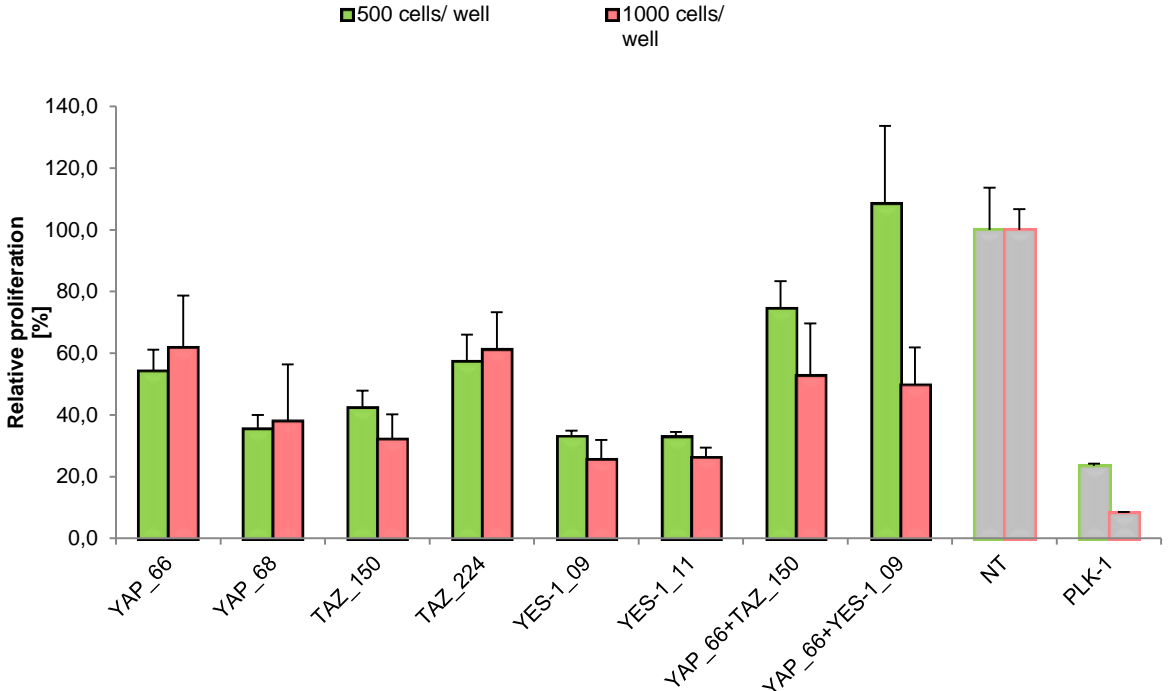


Figure 36: HLE Proliferation data relative to non-targeting- without untreated control

A) 500 cells/ well (green) B) 1000 cells/ well (red); readout: Alamar blue

Similar results could be obtained for HLE at a higher cell density. Efficient kd of YAP and YES-1 could again be confirmed on Western blot (Fig. 37) whereas TAZ kd did not work and - as shown for the lower cell density - the drop in proliferation might be a result of an off-target effect. Our former siRNA studies had already suggested cell line HLE as partially dependent on YAP, TAZ and YES-1. In summary, HLE was characterized as being sensitive at least to kd of YAP and YES-1.

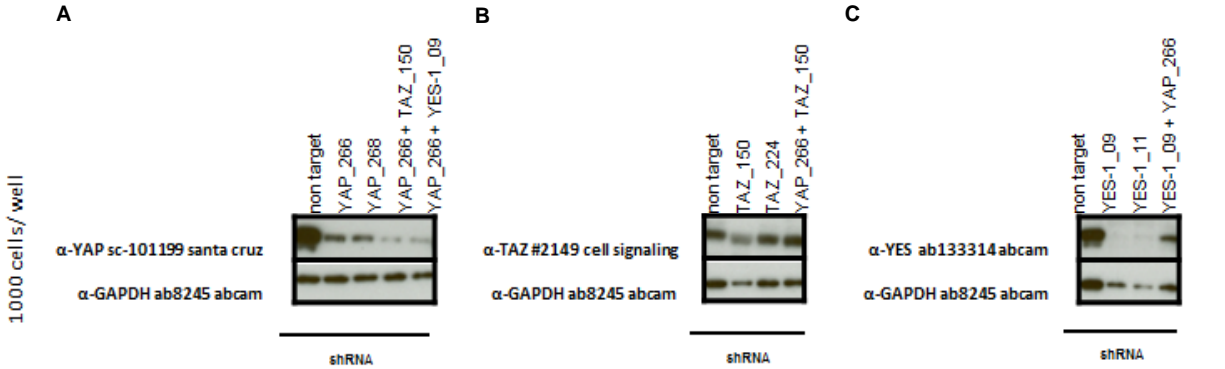


Figure 37: HLE Western blot data (1000 cells/ well)

3.4.3.3 HLF

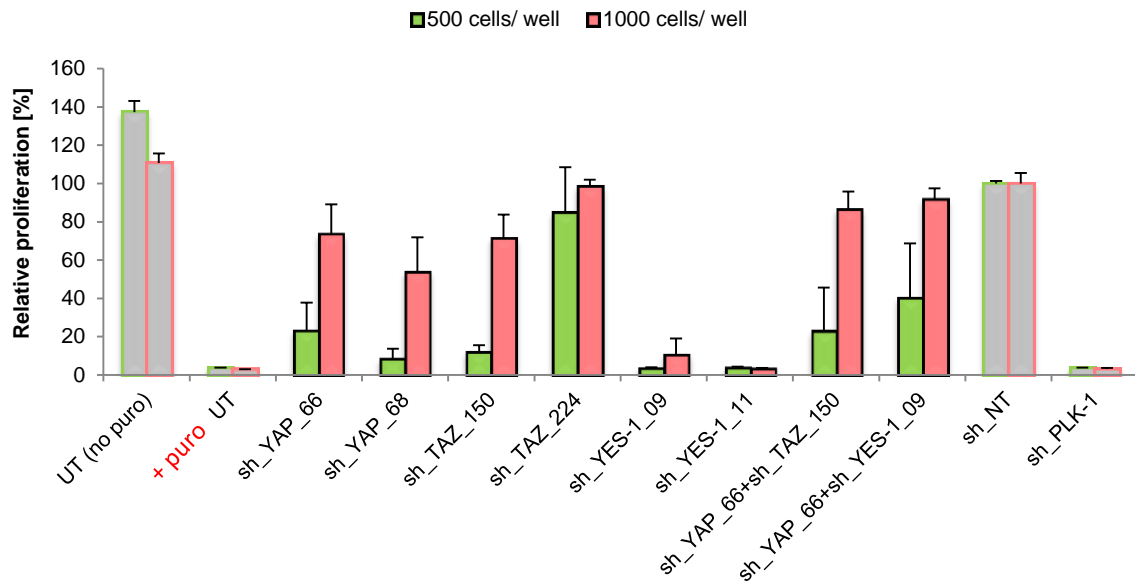


Figure 38: HLF Proliferation data

A) 500 cells/ well (green) **B)** 1000 cells/ well (red); readout: Alamar blue

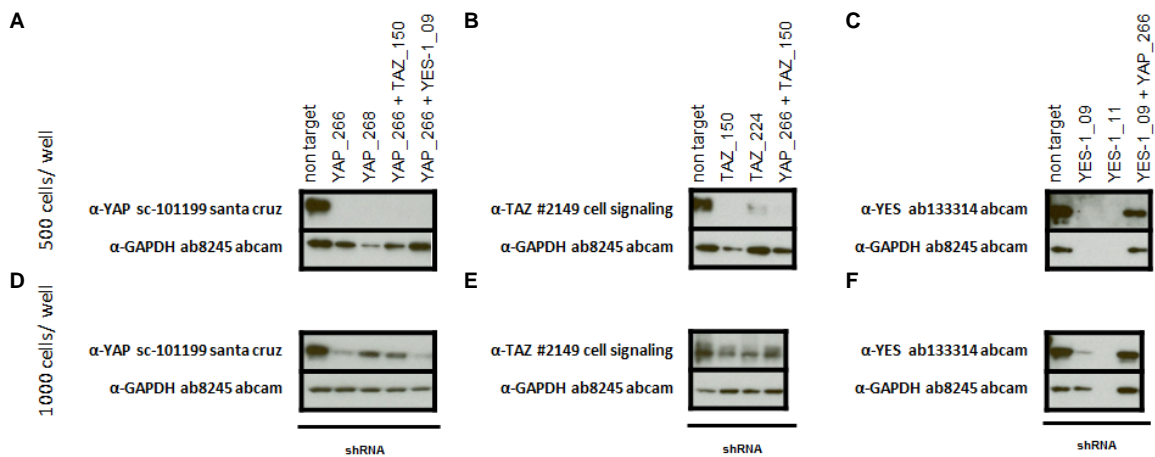


Figure 39: HLF Western blot data

Protein levels of YAP, TAZ and YES-1 after shRNA- mediated knockdown **A-C)** 500 and **D-F)** 1000 cells/ well

According to the data set retrieved from previous experiments including whole cell extraction (Fig. 17), cytoplasmic versus nuclear extracts (Fig. 18) and siRNA-mediated kd (Fig. 20), Hippo pathway related protein levels in general were increased in HLF. HLF cell line was characterized as YAP-, YES-1- as well as TAZ-independent. Preliminary experiments using siRNA already confirmed this

assumption with the exception of YES-1, for which the kd was not complete therefore another shRNA-mediated kd was performed using lentiviral transduction.

Regarding the results obtained from lentiviral shRNA-mediated kd HLF can be described as YAP-, partial TAZ- and YES-1- kd sensitive. In contrast to YAP and TAZ, kd of YES-1 was equally efficient leading to a pronounced anti-proliferative effect also at higher cell numbers. Combined treatment again did not result in a more efficient kd. YES-1 kd could not be confirmed in this setting. However, the dependency of cell line HLF on YES-1 was also confirmed by treatment with Dasatinib (IC_{50} value for Dasatinib is 590 nM (see 3.6.1 IC_{50} values)).

In summary, cell line HLF was characterized as sensitive towards kd of YAP, TAZ and YES-1. In comparison to HLE a different protein pattern was identified; in HLF higher protein levels of LATS1 and p-YAP-S-127 could be detected. However, in both cell lines a mutation in SAV-1 was identified (see 8.6 mutation analyses). It still has to be determined whether higher levels of LATS1 and p-YAP-S-127 in HLF might serve as a biomarker for the independency on the Hippo pathway.

3.4.3.4 HuCCT-1

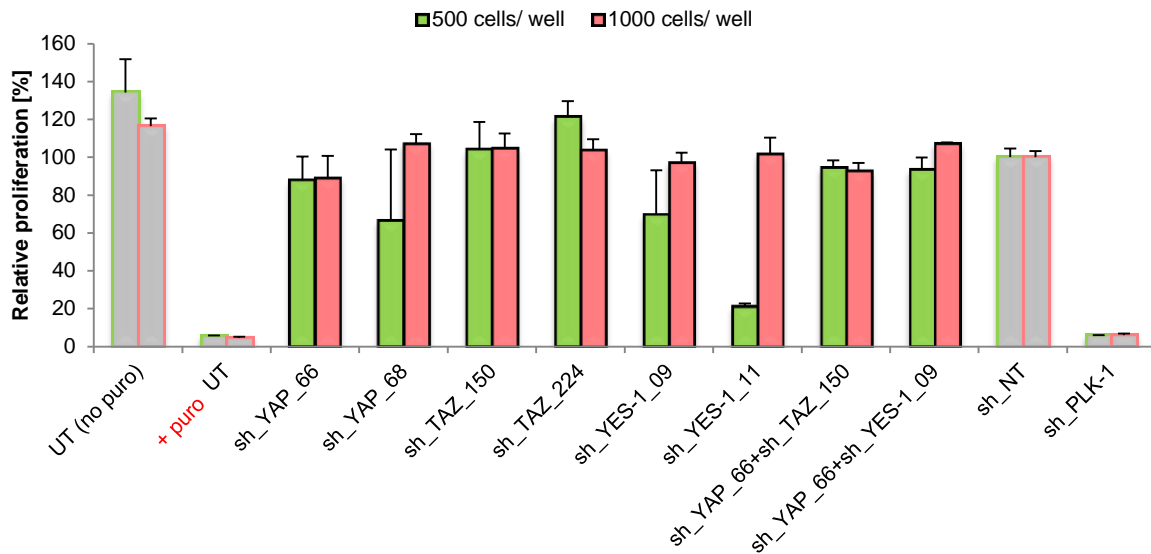


Figure 40: HuCCT-1 proliferation data

A) 500 cells/ well (green) B) 1000 cells/ well (red); readout: Alamar blue

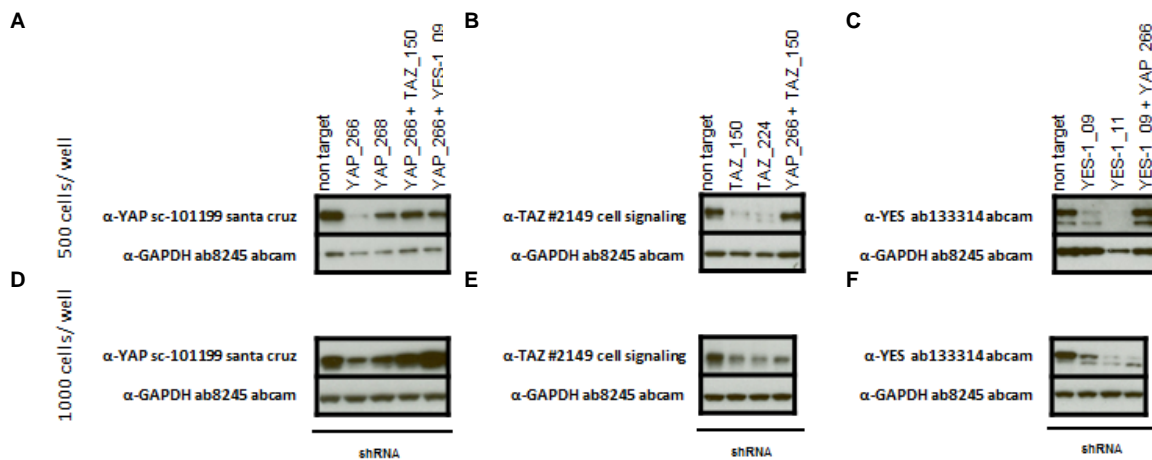


Figure 41: HuCCT-1 Western blot data

Protein levels of YAP, TAZ and YES-1 after shRNA- mediated knockdown A-C) 500 and D-F) 1000 cells/ well

The sensitivity of HuCCT-1 depends very much on the cell density as it was shown to be dependent on YES-1 and partially on YAP at a cell density of 500 cells/ well. However, no dependency at all was observed after increasing the cell number (Fig. 40B). Former results obtained from cytoplasmic and nuclear extracts suggested cell line HuCCT-1 as YES-1 independent and partially reliant on YAP and TAZ which could be confirmed by results obtained from lentiviral shRNA- mediated kd (1000 cells/well). Interestingly, YES-1 could not be detected in the nucleus (Fig. 18). In

general, YES-1 as well as c-MYC levels (Fig. 17) are low. Also the amount of MST1, SAV-1, LATS1 and MOB1 are very low or not present which leads to the assumption that this cell line is dependent on other signaling pathways apart from the Hippo pathway. It also has to be kept in mind that the protein distribution might be different by using different cell densities.

3.4.3.5 JHH-6

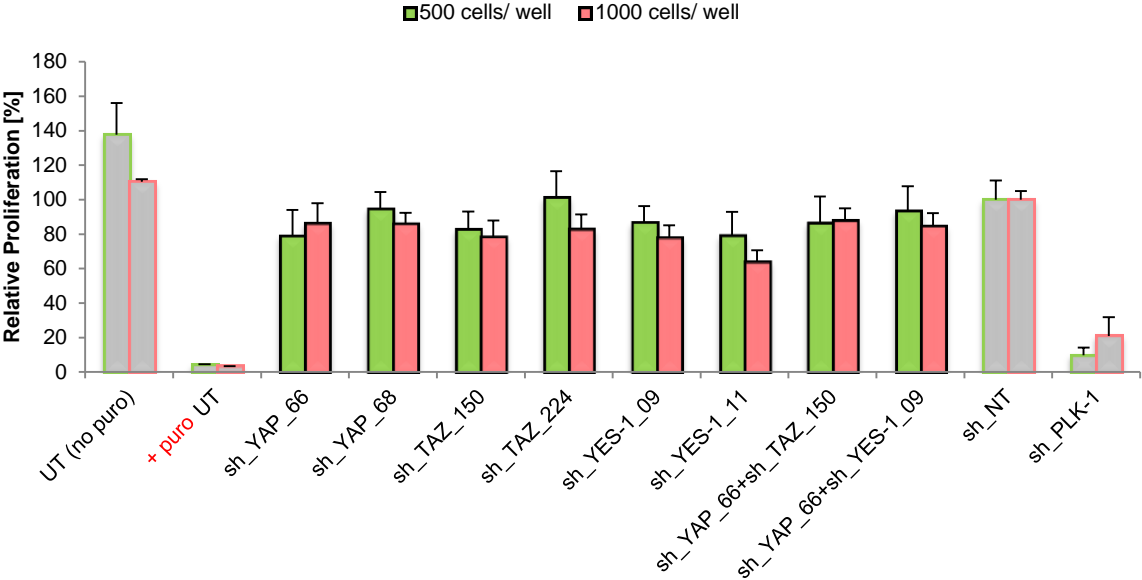


Figure 42: JHH-6 proliferation data

A) 500 cells/ well (green) B) 1000 cells/ well (red); readout: Alamar blue

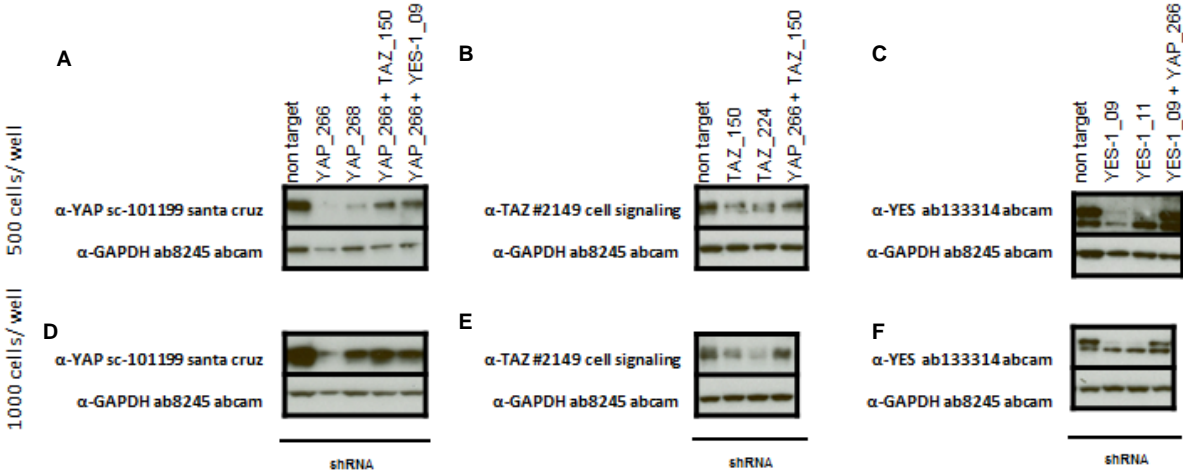


Figure 43: JHH-6 Western blot data

Protein levels of YAP, TAZ and YES-1 after shRNA- mediated knockdown A-C) 500 and D-F) 1000 cells/ well

Mutation analysis of cell line JHH-6 (attachment 8.3) revealed no mutation in Hippo pathway-related genes or their regulators and the protein pattern of whole cell lysate did not allow any speculation on the Hippo pathway dependency (Fig. 17). Based on the comparison of expression levels of proteins of the Hippo pathway in cytoplasmic and nuclear extracts (3.2), JHH-6 was regarded as partially dependent on YAP, TAZ and YES-1. In contrast, the lentiviral shRNA-mediated kd of YAP, TAZ and YES-1 in JHH-6 exhibited no effect on proliferation (Fig. 42). However, efficient kd was only confirmed for YAP_266/268 (1000 cells/ well), for both TAZ constructs and YES-1 but not for the combined treatment. Interestingly, JHH-6 contains a two band pattern (Fig. 18) for YES-1 whereas the lower band is found in the cytoplasm and the upper one in the nucleus. By performing a YES-1 kd only the upper band, which had been previously detected in the nucleus, disappeared. The specific function of these two YES-1 molecules is currently unknown.

3.4.3.6 JHH-7

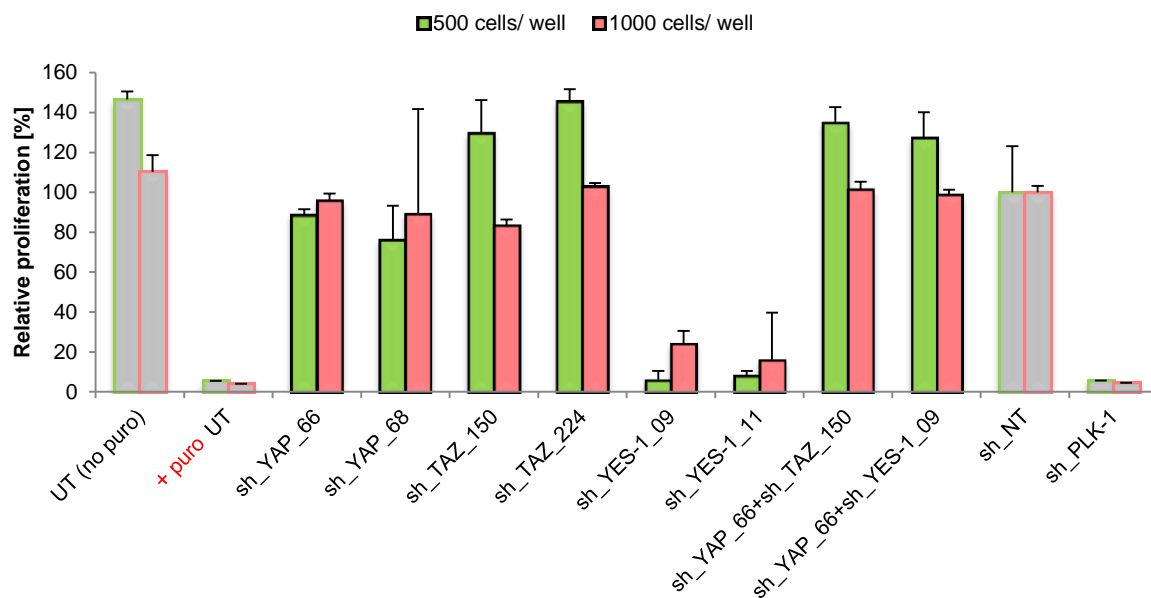


Figure 44: JHH-7 proliferation data

A) 500 cells/ well (green) **B)** 1000 cells/ well (red); readout: Alamar blue

JHH-7 is an excellent example for a YES-1 dependent HCC cell line. At both cell densities a massive drop in proliferation after treatment with shRNA_YES-1_09 or shRNA_YES-1_11 was observed. The drop in proliferation is in agreement with the kd efficacy shown on Western blot (Fig. 45C+F). In former studies JHH-7 was proposed to be partially dependent on YES-1 (Fig. 18).

In contrast to kd of YES-1, JHH-7 was not sensitive towards kd of YAP or TAZ (Fig. 44A+B and 45D). The kd was almost complete at lower cell numbers (Fig. 45A-C) whereas at higher cell numbers only a partial kd was observed. For YES-1 the kd worked efficiently at both cell densities (Fig. 45C+F). It is of interest that a combined kd of YES-1 and YAP (Fig. 45C+F) reverted the effect of YES-1 kd but not *vice versa*. In summary, JHH-7 can be regarded as a YES-1 dependent HCC cell line whereas proteins of the Hippo pathway are not essential for JHH-7.

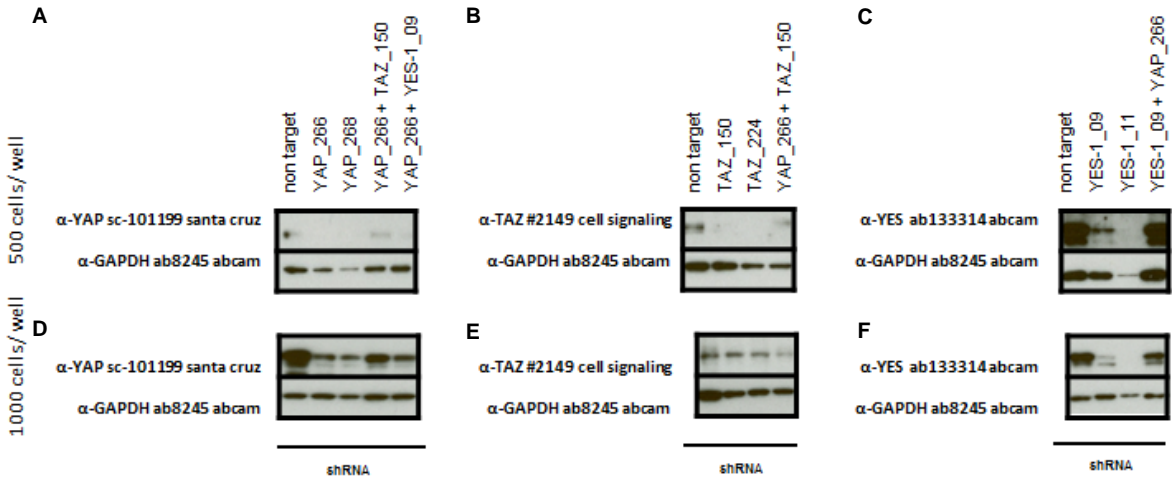


Figure 45: JHH-7 Western blot data

Protein levels of YAP, TAZ and YES-1 after shRNA- mediated knockdown A-C) 500 and D-F) 1000 cells/ well

3.4.3.7 SK-HEP-1³

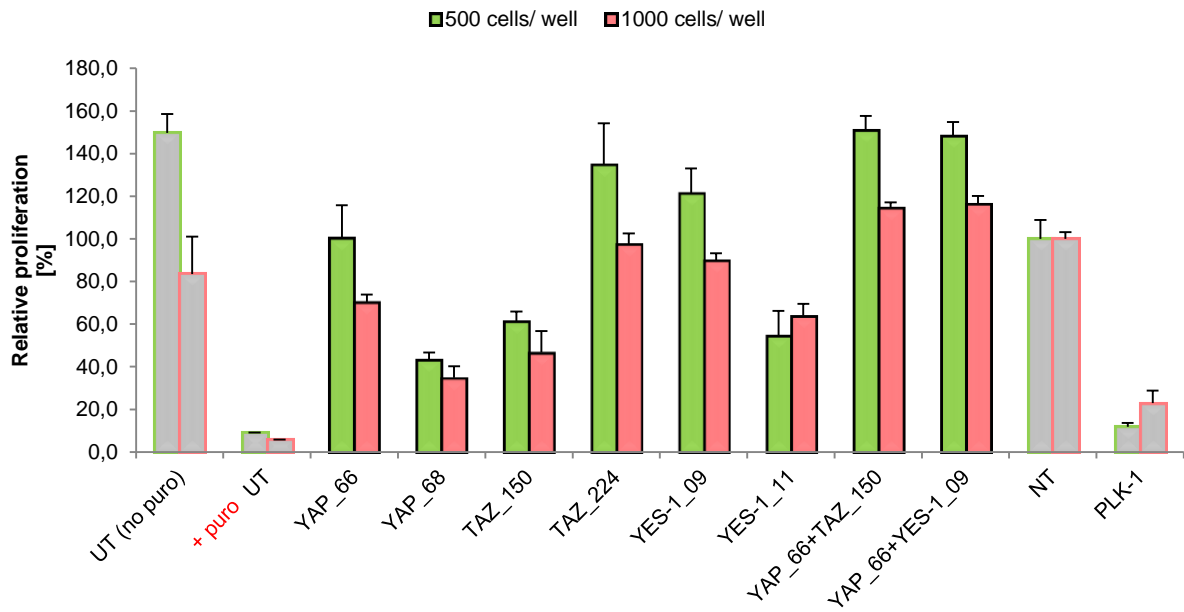


Figure 46: SK-HEP-1 proliferation data

A) 500 cells/ well (green) **B)** 1000 cells/ well (red); readout: Alamar blue

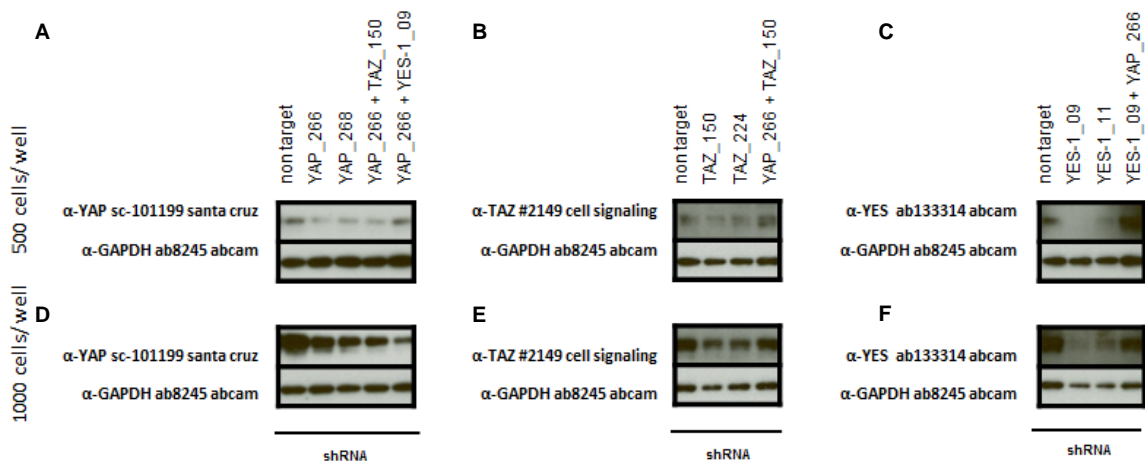


Figure 47: SK-HEP-1 Western blot data

Protein levels of YAP, TAZ and YES-1 after shRNA- mediated knockdown **A-C)** 500 and **D-F)** 1000 cells/ well

³ MOI=8 instead of MOI=4

According to preliminary experiments (data not shown) cell line SK-HEP-1 requires a higher MOI of 8 for appropriate transduction efficiency. YAP kd (Fig. 46) generated a minor drop in proliferation which might be due to the incomplete kd as shown on Western blot (Fig. 47D). In general, the kd efficiency for YAP is more pronounced at a lower cell number (Fig. 47A+D). Based on previous siRNA- (Fig. 19) and the present shRNA kd studies SK-HEP-1 seems to be (at least partially) dependent on YAP.

The kd mediated by shRNA_TAZ_150 massively impaired the proliferation although at the protein level (Fig. 46A+B) only a small reduction of TAZ was detected. Treatment of SK-HEP-1 with the second lentiviral TAZ shRNA construct could not achieve a considerable kd on the protein level (Fig. 47B+E).

Only in the case of shRNA_YES-1_11 (Fig. 46A+B) a 40% decrease in proliferation was observed although the amount of YES-1 protein was efficiently reduced by both shRNA constructs independent of the cell number (Fig. 46 and Fig. 47C+F).

As observed in previous experiments, the combined treatment of shRNA_YAP_66 with shRNA_TAZ_150 or shRNA_YAP_66 with shRNA_YES-1_09 exhibited no reduction of the specific protein on Western blot but rather positively affects the proliferation compared to the non-targeting control.

Based on previous results from nuclear and cytoplasmic extractions, SK-HEP-1 was proposed to be YES-1 independent but dependent on YAP/TAZ (Fig. 18). Taking all results into account, SK-HEP-1 can be regarded as YAP/TAZ dependent and as partially sensitive towards kd of YES-1 (Fig. 46). The dependency of this cell line on the deregulated Hippo pathway is supported by the fact that SK-HEP-1 exhibits an inactivating mutation in the LATS1 tumor suppressor gene and therefore most likely is dependent on nuclear YAP.

3.4.3.8 SNU-398

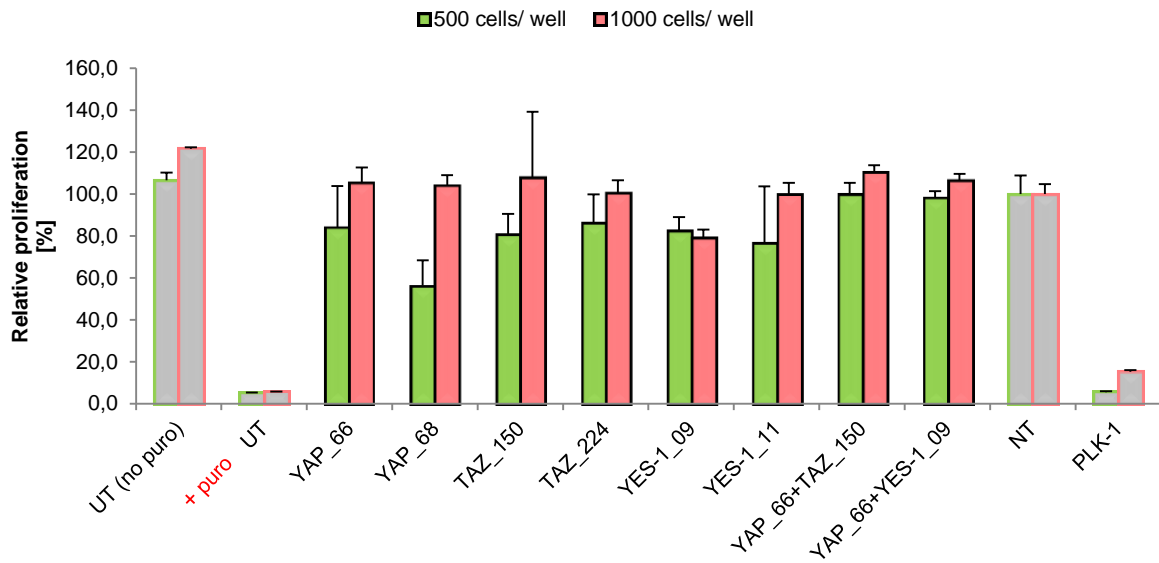


Figure 48: SNU-398 proliferation data

A) 500 cells/ well (green) B) 1000 cells/ well (red); readout: Alamar blue

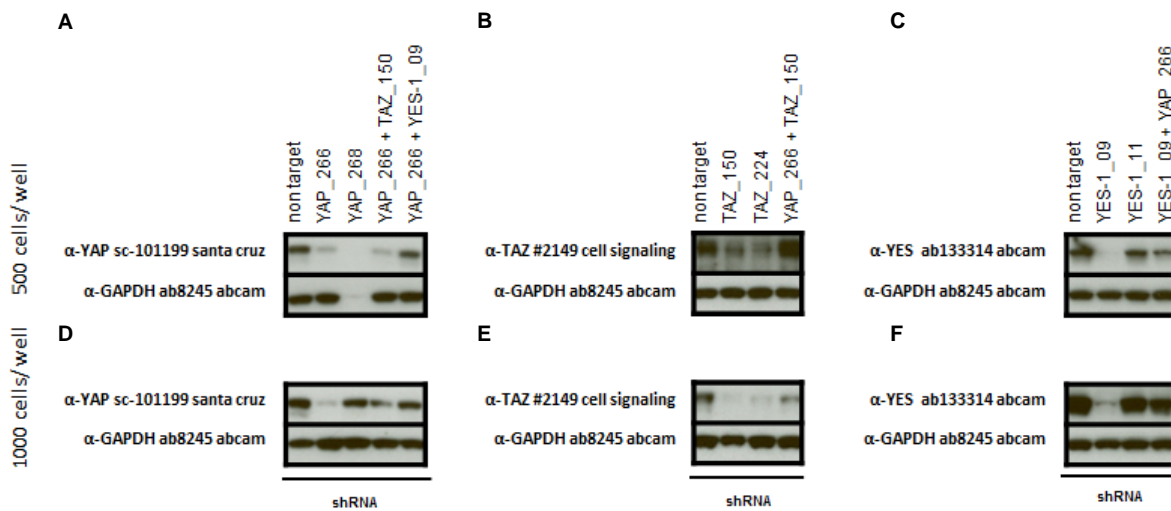


Figure 49: SNU-398 Western blot data

Protein levels of YAP, TAZ and YES-1 after shRNA- mediated knockdown **A-C)** 500 and **D-F)** 1000 cells/ well

Previously performed experiments including whole cell protein analysis and cytoplasmic as well as nuclear extraction already suggested cell line SNU-398 as independent on the Hippo pathway (Fig. 18). This assumption was verified by lentiviral shRNA mediated kd of YAP, TAZ and YES-1. For instance, the kd for YAP worked quite efficiently for shRNA_YAP_66 as well as in combination with TAZ for 500 cells/ well. No conclusion could be drawn for the treatment with shRNA_YAP_68 due to an invalid loading control (Fig. 49A). However, there was no effect detectable on proliferation after YAP kd (Fig. 48A+B). Despite that the TAZ kd could be confirmed on Western blot, the combined treatment with YAP only showed a pronounced reduction at a higher cell density (1000 cells/ well). Although the kd could be confirmed on Western blot, no effect on proliferation (Fig. 48) was detectable. SNU-398 was suggested to be partially sensitive towards kd of YES-1 (Fig. 18). However, only a minor effect on the proliferation was detectable at a lower cell density (Fig. 48A and Fig. 49C; shRNA_YES-1_09). The kd with shRNA_YES-11 did not work.

Kd of PLK-1 lead to a complete inhibition of proliferation and based on previous studies and the current shRNA data set, HCC cell line SNU-398 is neither dependent on the Hippo pathway proteins YAP and TAZ nor on YES-1.

3.4.3.9 SNU-423

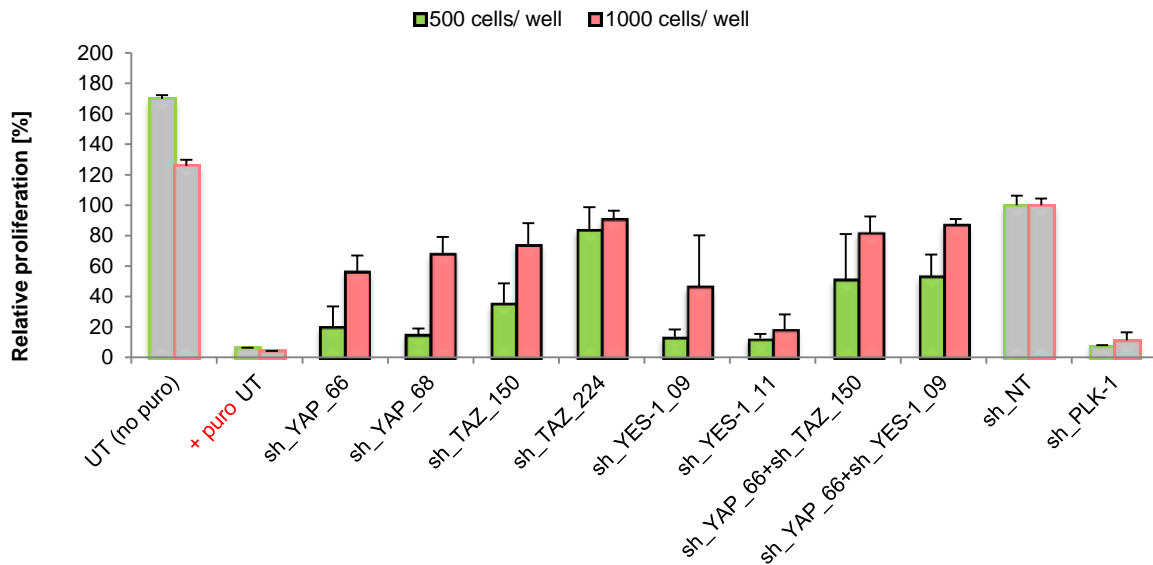


Figure 50: SNU-423 proliferation data

A) 500 cells/ well (green) B) 1000 cells/ well (red); readout: Alamar blue

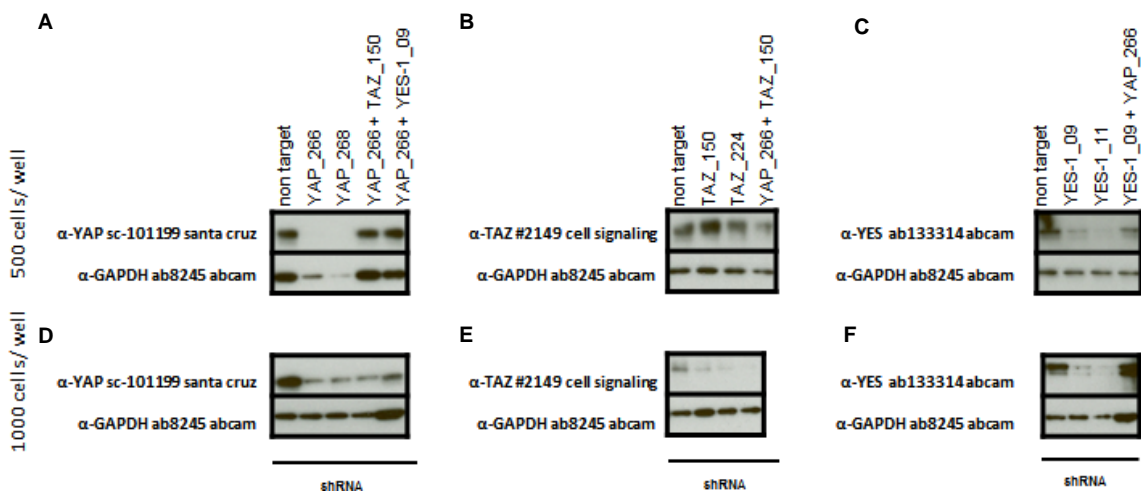


Figure 51: SNU-423 Western blot data

Protein levels of YAP, TAZ and YES-1 after shRNA- mediated knockdown A-C) 500 and D-F) 1000 cells/ well

In general, cell line SNU-423 exhibited sensitivity towards the transduction method itself (reduction in proliferation UT (no puromycin) vs. sh_NT; Fig.50). As a consequence the assay window was smaller with regard to other HCC cell lines

tested. Nevertheless, kd of YES-1 massively reduced the proliferation rate. SNU-423 could be characterized as dependent on YES-1 (Fig. 50A+B). The efficient kd was verified on Western blot (Fig. 51C+F). YAP dependency was mainly observed at a lower cell density where a pronounced kd on the protein level could be detected (Fig. 50A and Fig. 51A). At a higher cell density there was less effect on the proliferation. However, kd of YAP was also less efficient than at a lower cell density (Fig. 51D). Altogether, SNU-423 can be regarded as YAP-dependent which correlates well with our distribution (N/C) data (Fig. 18). In contrast, kd of TAZ did not lead to a pronounced reduction in the proliferation rate. In particular, at higher cell densities a more or less complete kd was shown on Western blot (Fig. 51E).

As observed for other HCC cell lines, combined kd (e.g. YAP+TAZ or YAP+YES-1; Fig. 50 and Fig. 51A) was neither significantly decreasing the proliferation rate nor the respective protein levels. In summary, SNU-423 can be regarded as dependent on YES-1 and YAP.

3.4.3.10 SNU-475

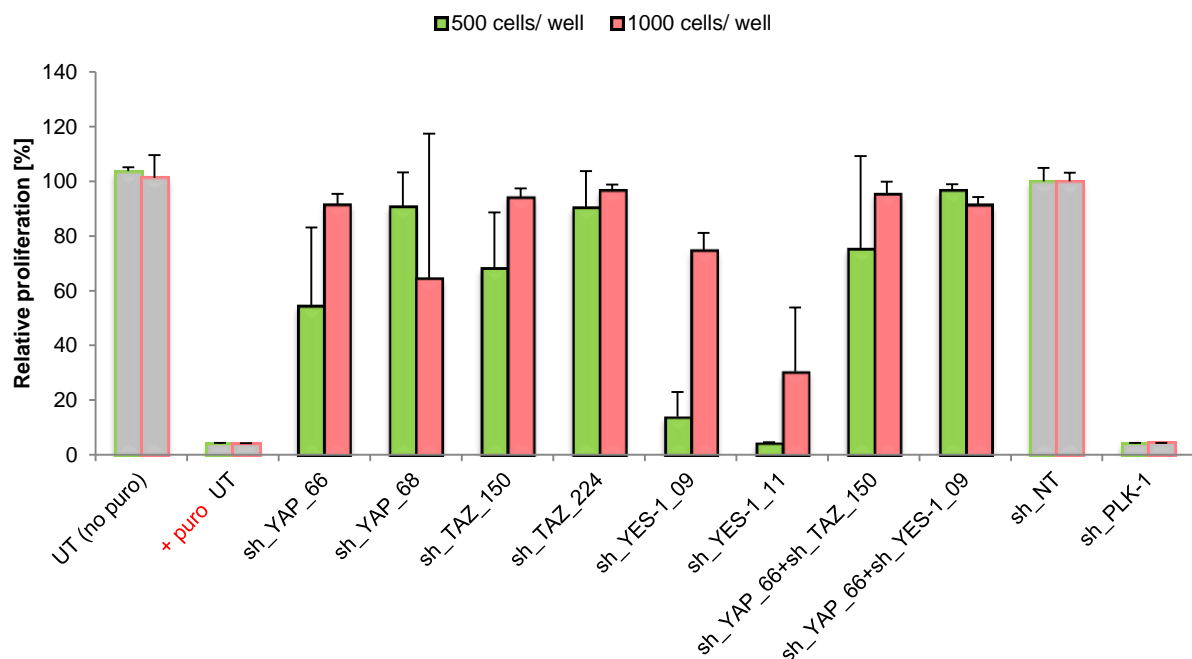


Figure 52: SNU-475 proliferation data

A) 500 cells/ well (green) B) 1000 cells/ well (red); readout: Alamar blue

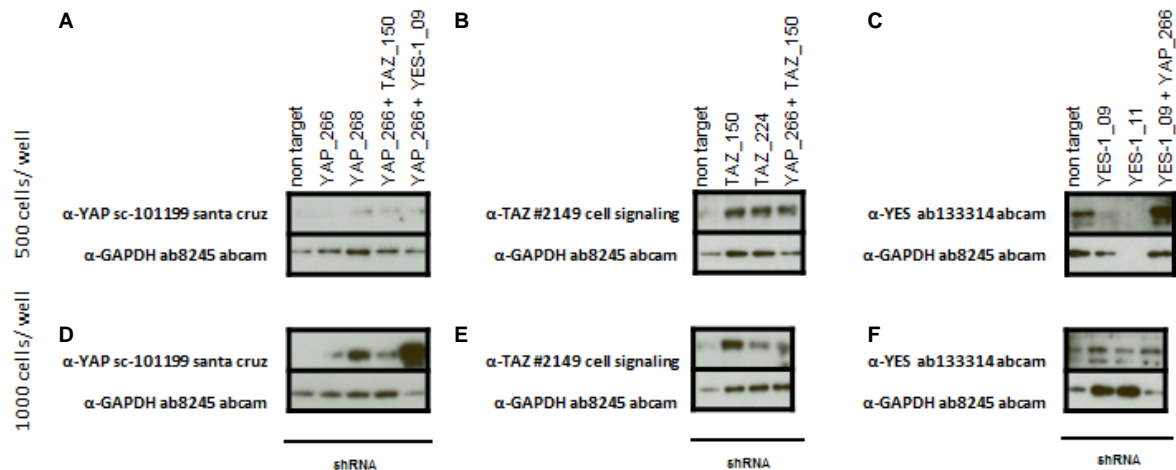


Figure 53: SNU-475 Western blot data

Protein levels of YAP, TAZ and YES-1 after shRNA-mediated knockdown A-C) 500 and D-F) 1000 cells/well

For SNU-475 no specific mutations were identified in Hippo-relevant genes (Table 30). In addition, Western blot analyses of cytoplasmic and nuclear extracts also suggested that this cell line seems to be independent on YAP and only to be partially addicted to TAZ (Fig. 17). Due to a repetitively invalid loading control of cells treated with non-targeting shRNA, no statement about kd efficiency of YAP or TAZ could be made. Only kd of YES-1 could be confirmed on Western blot at the lower cell density setting (Fig. 53C) exhibiting a massive reduction in the proliferation rate (Fig. 52A). SNU-475 can therefore be regarded as YES-1 dependent. The dependency on the two Hippo pathway proteins YAP and TAZ remains to be determined using alternative methods.

3.4.3.11 SUMMARY OF YAP KNOCKDOWN DATA

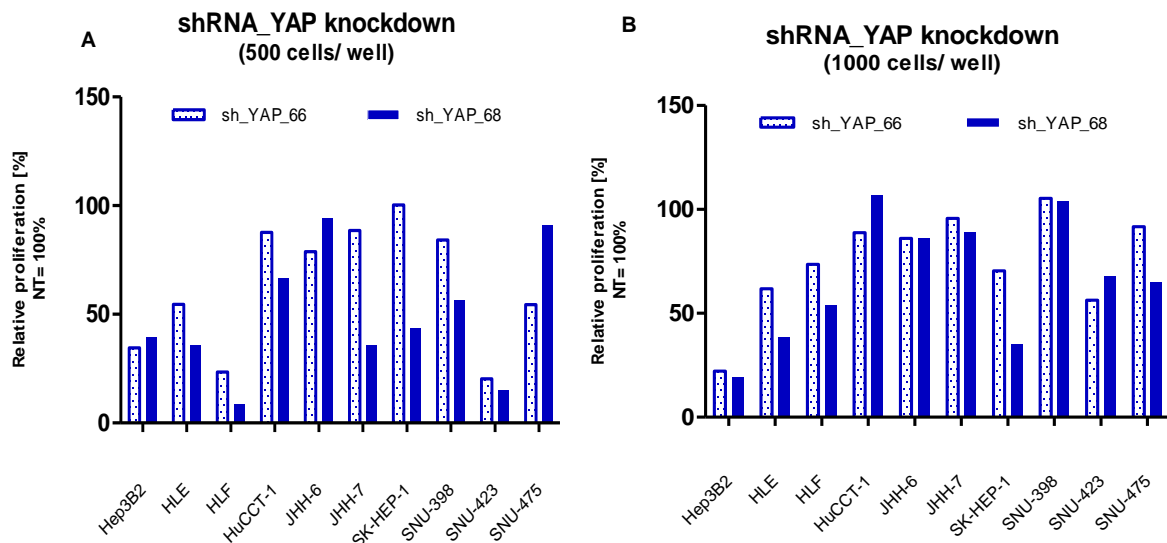


Figure 54: Sensitivity towards YAP knockdown

YAP knockdown was performed in 10 hepatocellular carcinoma cell lines by using two different shRNAs. Sensitivity of those cell lines was determined according to a decrease in proliferation **A)** 500 cells per well **B)** 1000 cells per well. Proliferation rate was normalized to NT. For experimental details see 3.4.3 Lentiviral Transduction.

Out of ten HCC cell lines analyzed, **Hep3B2.1-7**, **HLE**, **HLF** and **SNU-423** were shown to be sensitive towards YAP kd independent of the cell number or the construct used.

JHH-7 and **SK-HEP-1** were only sensitive towards shRNA_YAP_68 at a cell density of 500 cells/ well but were insensitive to kd mediated by shRNA_YAP_66. Interestingly, SK-HEP-1 exhibited an influence on proliferation after sh_YAP_68 but not after sh_YAP_66-mediated kd. This cell line was therefore categorized as partial sensitive. Due to variation of kd efficiency in the two different set ups (500 or 1000 cells/well) it is also very likely that cell density and/or cultivation parameters might play an important role.

In contrast, cell lines **HuCCCT-1**, **JHH-6** and **SNU-398** were completely insensitive towards kd of YAP. As the kd efficiency for **SNU-475** could not be confirmed on Western blot but a clear decrease in proliferation was observed, this cell line can only be regarded as putatively sensitive.

3.4.3.12 SUMMARY OF TAZ KNOCKDOWN DATA

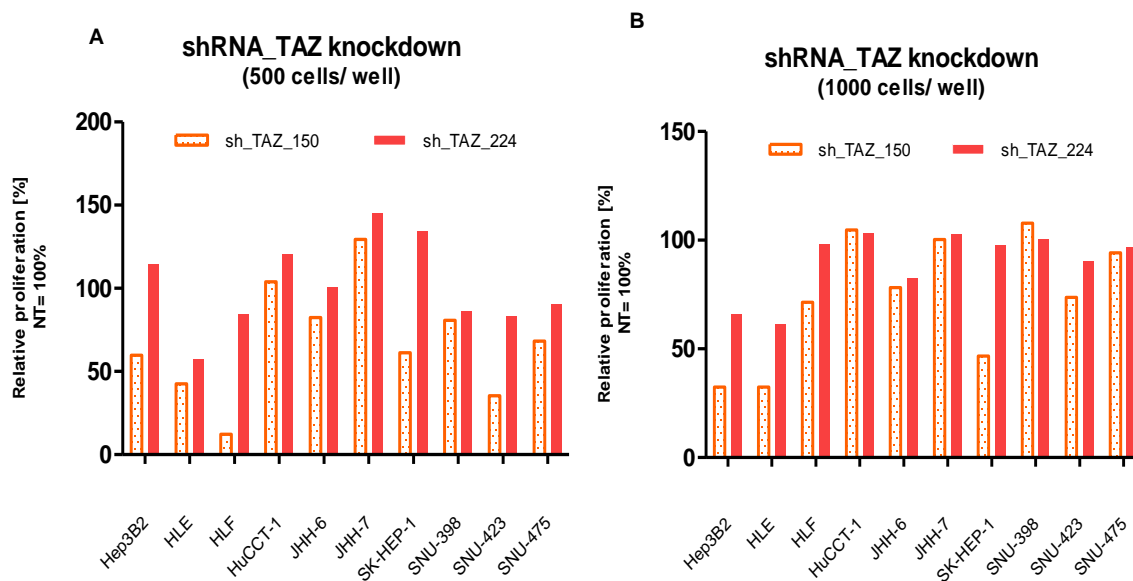


Figure 55: Sensitivity towards TAZ knockdown

TAZ knockdown was performed in 10 hepatocellular carcinoma cell lines by using two different shRNAs. Sensitivity of those cell lines was determined according to a decrease in proliferation **A)** 500 cells per well **B)** 1000 cells per well. Proliferation rate was normalized to NT. For experimental details see 3.4.3 Lentiviral Transduction.

In general, shRNA_TAZ-mediated kd revealed only a minor impact on proliferation as compared to the kd of YAP or YES-1. The effect is more pronounced at a lower cell density arguing again for a cell density dependent regulation [73]. In addition, sh_TAZ_150 exhibited a higher kd efficiency than sh_TAZ_224 (Fig. 55).

Hep3B2.1-7, HLE also **HLF** were **sensitive** towards shRNA_TAZ_150 knockdown and partially sensitive to the sh_TAZ_224-mediated knockdown at a lower cell density. Cell line **SK-HEP-1** only responds to shRNA_TAZ_150 knockdown for which a great reduction of proliferation could be shown in contrast to shRNA_TAZ_224. A complete insensitivity was shown for **HuCCT-1** and **JHH-7** and only a marginal effect was detected in **JHH-6, SNU-398, SNU-423** and **SNU-475**.

3.4.3.13 SUMMARY OF YES-1 KNOCKDOWN DATA

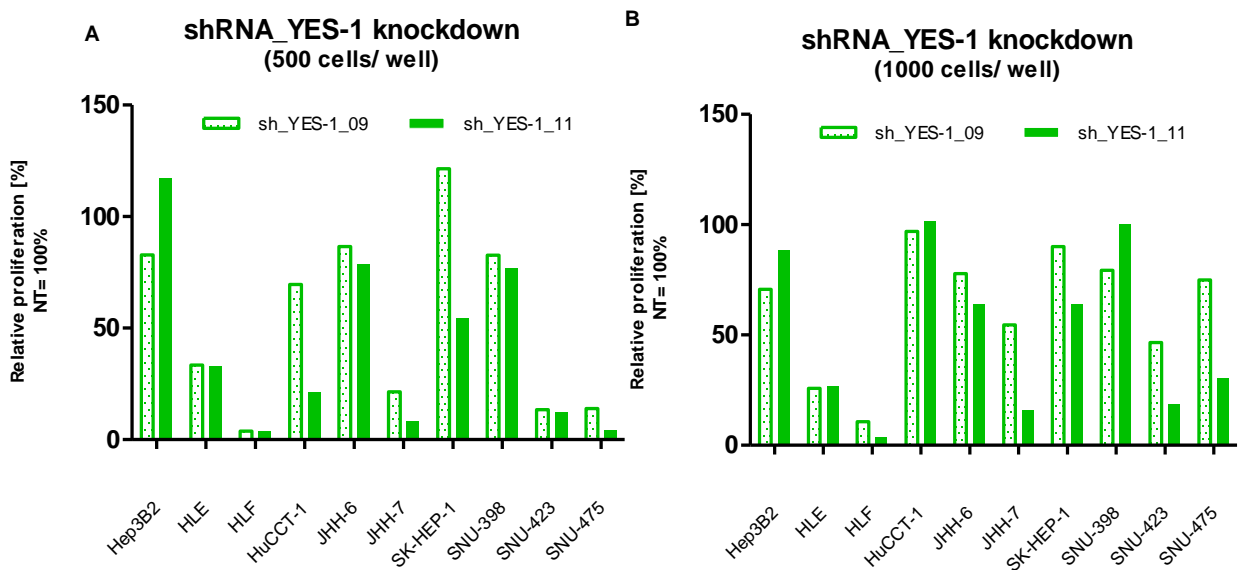


Figure 56: Sensitivity towards YES-1 knockdown

YES-1 knockdown was performed in 10 hepatocellular carcinoma cell lines by using two different shRNAs. Sensitivity of cell lines was determined according to a decrease in proliferation **A)** 500 cells per well **B)** 1000 cells per well. Proliferation rate was normalized to NT. For experimental details see 3.4.3 Lentiviral Transduction.

In contrast to knockdown of YAP or TAZ proteins, HCC cell lines generally are more sensitive to the knockdown of YES-1. The effect on the proliferation is also not dependent on the cell number (Fig. 56).

Cell lines characterized as **sensitive** towards YES-1 knockdown are: **HLE**, **HLF**, **JHH-7**, **SNU-423** and **SNU-475** whereas cell lines **Hep3B2.1-7**, **HuCCT-1**, **JHH-6**, and **SNU-398** were characterized as insensitive. **SK-HEP-1** exhibited only a partial sensitivity towards YES-1 knockdown.

Table 28: Summary of cell lines

Sensitive cell lines are illustrated in green, partial sensitive ones in orange and insensitive cell lines in red in regard to YAP, TAZ or YES-1 knockdown.

	HLE	HLF	SNU-423	SNU-475	JHH-7	Hep3B 2.1-7	SK-HEP-1	HuCCT-1	SNU-398	JHH-6	Cells/ well
YAP	Green	Green	Green	Orange	Orange	Green	Orange	Red	Orange	Red	500
	Green	Green	Green	Orange	Red	Green	Orange	Red	Red	Red	1000
TAZ	Green	Green	Green	Red	Red	Green	Orange	Red	Red	Red	500
	Green	Orange	Red	Red	Red	Green	Orange	Red	Red	Red	1000
YES-1	Green	Green	Green	Green	Green	Red	Orange	Green	Red	Red	500
	Green	Green	Green	Green	Green	Red	Orange	Red	Red	Red	1000

In summary, HCC cell lines can be categorized as follows: **i) HLE, HLF and SNU-423** are dependent on YAP, TAZ and YES-1, **ii) SNU-475 and JHH7** are dependent on YES-1 but not on YAP and TAZ, **iii) Hep3B 2.1-7** is dependent on YAP and TAZ but not on YES-1 and **iv) HuCCT-1, SNU-398 and JHH-6** are insensitive to knockdown of all three genes. **SK-HEP-1** is only partially dependent on the three genes (Table 28).

3.5 Rescue Experiment for YES-1

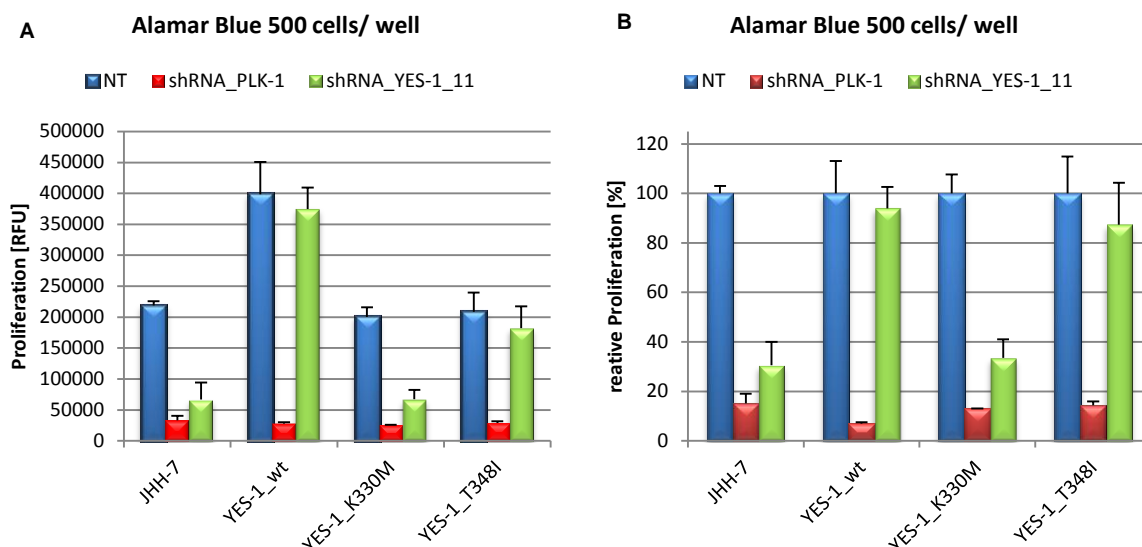


Figure 57: Rescue of YES-1 knockdown in JHH-7

Cells were transfected with YES-1_wt-, kinase dead- (K330M) or Dasatinib resistant- (T348I) plasmid, all of which were codon optimized and for that reason resistant to shRNA_YES-1. JHH-7 had been originally characterized as a YES-1 dependent cell line and therefore was used for a rescue experiment.

A) Proliferation after 13 days of shRNA knockdown

B) Relative Proliferation to non-targeting control; PLK-1 serves as the positive- and non-targeting as the negative control

Previously JHH-7 had been characterized as a YES-1 kd sensitive cell line. To gain more information on the contribution of YES-1 activity to survival and/or proliferation cell line JHH-7 was transfected with one of the three constructs YES-1_wt, kinase dead enzyme (YES-1_K330M) or a Dasatinib-resistant (YES-1_T348I) variant. Prior to the knockdown studies JHH-7 cell pools had been established stably over-expressing the rescue constructs YES-1_wt, YES-1_K330M or YES-1_T348I, respectively. Selection was started with Geneticin (500µg/ml) for 9 weeks prior to the shRNA-mediated kd of YES-1. Under non-rescue conditions, proliferation decreases similarly to previous experiments (3.4.3.6) upon shRNA_YES-1_11 treatment [57]. Overall, the knockdown of YES-1 caused a decrease in proliferation of approximately 70% (Fig. 57 B) and was verified on Western blot (Fig. 58A). JHH-7 cells which had been stably transfected with the YES-1_wt codon optimized plasmid could be rescued from the endogenous YES-1 kd using shRNA_YES-11 (Fig. 57A+B). The same held true for the Dasatinib-resistant variant of YES-1_T348I (Fig. 57B). Again expression of that recombinant mutated variant was demonstrated on Western blot

(Fig. 58). In contrast, the attempt to rescue proliferation and protein levels using the kinase dead version of YES-1_K330M failed. Rescue of proliferation/survival could not be achieved with mutated YES-1_K330M. However, the rescue data utilizing mutant YES-1_K330M have to be treated with caution as repetitively only a low expression level of the mutated variant could be achieved (Fig. 58C). A major aim of this rescue experiment was to show whether the kinase activity of YES-1 is important to sustain proliferation/survival or whether a mere protein interaction of YES-1 with components of the Hippo pathway is sufficient to trigger the activation of the Hippo pathway. It is very likely that the mutation K330M in the YES-1 kinase dead variant leads to an instability being responsible for the low or even undetectable protein amounts in the transfected cell pool (Fig. 58) as it had been described for other kinase dead enzymes [87-89]. To circumvent the problem of the putative destabilization of YES-1 kinase dead other experimental settings will have to be applied in future experiments.

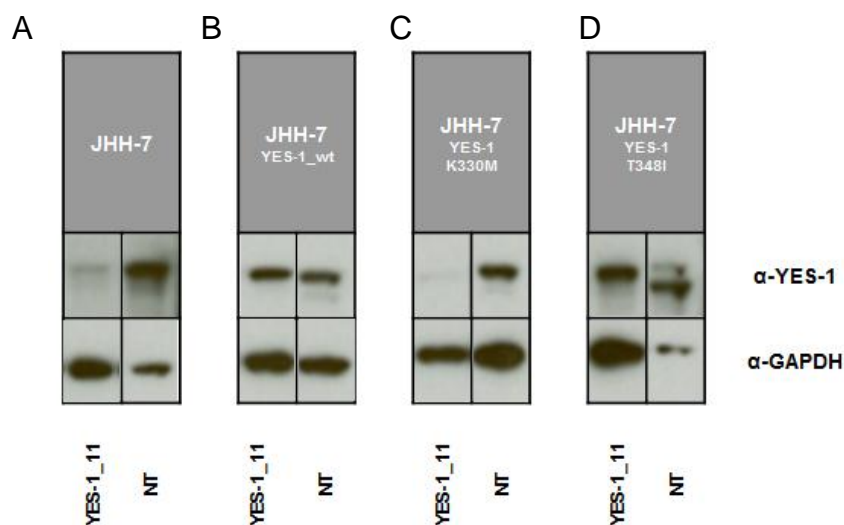


Figure 58: Western blot analysis of JHH-7 cell lysates after 13 days of shRNA-mediated YES-1 knockdown.

A) JHH-7 untreated cell line B) JHH-7 expressing shRNA-resistant YES-1_wt C) JHH-7 expressing shRNA-resistant YES-1_K330M (kinase dead variant) D) JHH-7 expressing shRNA-resistant YES-1_T348I (Dasatinib resistant kinase)

Protein levels of YES-1 (endogenous) in non-targeting (NT) cell lysates served as control for the knockdown efficiency in cells over-expressing the respective YES-1 rescue constructs.

3.6 Compound Treatment

3.6.1 DETERMINATION OF IC₅₀ VALUES

Dasatinib is an oral multi- BCR/ABL and SRC family tyrosine kinase inhibitor approved for first line use in patients with chronic myelogenous leukemia (CML) and Philadelphia chromosome-positive acute lymphoblastic leukemia (PH+ALL). It is being evaluated for use in numerous other cancers, including advanced prostate cancer [89]. Although originally designed as a BCR/ABL and SRC family tyrosine kinase inhibitor including YES-1, Dasatinib is a quite promiscuous inhibitor. Out of 317 tested kinases approximately one third were shown to be inhibited by Dasatinib; for YES-1 a K_D of 0.3nM was determined [90]. However, Dasatinib is a Src kinase inhibitor preferentially inhibiting YES-1 kinase [79].

Table 29: IC₅₀ values for 23 HCC cell lines treated with Dasatinib or Verteporfin.

Cells have been incubated with the respective cpds at different concentrations. After three days of incubation the proliferation was measured in an Alamar Blue Assay and the IC₅₀ values [μM] were calculated utilizing GraphPad Prism. Cell culture conditions for each HCC cell line see (2.1 Cell Lines and Culture Conditions).

Cell line	Dasatinib	Verteporfin	Cell line	Dasatinib	Verteporfin
	IC ₅₀ [μM]			IC ₅₀ [μM]	
C3A	71850.30	1.69	SNU-398	n.a.	23.56
HepG2	6.48	0.35	SNU-423	0.22	5.66
Hep3B2.1-7	27.44	5.25	SNU-475	1.49	7.44
HLE	n.a.	12.86	SNU-449	0.22	2.00
HLF	0.59	5.21	JHH-1	0.30	12.40
HuCCT-1	0.14	4.76	JHH-2	0.08	0.60
huH-1	4248.00	24.48	JHH-4	0.14	16.15
HuH-6 Clone 5	>50	19.34	JHH-5	154600	1.17
HuH-7	0.22	5.40	JHH-6	0.01	0.07
SK-HEP-1	12.74	9.50	JHH-7	3.18	1.06
SNU-387	0.03	8.51			

The IC₅₀ values for Dasatinib treatment varied from 0.03μM to 71mM. A sensitivity of an IC₅₀ below 1μM was detected for **HLF, HuCCT-1, HuH-7, SNU-387, SNU-423, SNU-449, JHH-1, JHH-2, JHH-4** and **JHH-6**. A medium sensitivity (IC₅₀ values in the low μM range) was identified for **HepG2, SNU-475** and **JHH-7**, respectively (Table 29). The Dasatinib inhibitory potential on YES-1 is in good agreement with our YES-1

knockdown studies (Table 28). Out of 10 HCC cell lines subjected to YES-1 shRNA-mediated kd HLF, SNU-423, SNU-475 and JHH-7 were shown to be sensitive. Partial sensitivity was detected for SK-HEP-1 and HuCCT-1 (Table 28).

Verteporfin (VP), a benzoporphyrin derivative, was originally developed as a photosensitizer for photodynamic therapy to eliminate the abnormal blood vessels in the eye associated with macular degeneration. After accumulation in the abnormal blood vessels VP is stimulated by non-thermal red light (693 nm) and in the presence of oxygen it produces highly reactive oxygen radicals such as singlet oxygen. This results in local damage of the blood vessels [91,92]. Interestingly, VP was also shown to be an inhibitor of YAP::TEAD protein interaction. VP appeared to bind YAP and repression of YAP::TEAD interaction by VP in HEK293 cells resulted in inhibition of a YAP/TEAD-Gal4/UAS-driven luciferase reporter gene assay [81]. Recombinant expressed YAP and TEAD2 protein was incubated with VP, and VP was shown to coelute with YAP demonstrating that VP selectively binds YAP. Importantly, VP was also able to inhibit the oncogenic activity of YAP *in vivo* [81]. As this pharmacological intervention interferes with HCC tumorigenesis and obviously being devoid of any effect on normal liver homeostasis, it supports the idea to perturb the YAP::TEAD interaction as a novel therapeutic strategy against HCC [30]. In order to learn more about the potency of VP to interfere with proliferation/survival of HCC cells we tested this compound in our HCC cell line panel. 15 out of 21 HCC cell lines responded to VP with an IC₅₀ value of less than 10 μM. Highest sensitivity was seen in **C3A**, **HepG2**, **SNU-449**, **JHH-2**, **JHH-5**, **JHH-6** and **JHH-7** in the low or sub-μM range (Table 29). Compared to our YAP-shRNA-mediated knockdown studies, a good correlation is seen for **HLF**, **SNU-423**, and **Hep3B2.1.-7**; to a lesser extend for **HLE**, **SNU-475**, **JHH-7** and **SK-HEP-1** and no correlation was seen for **HuCCT-1** and **JHH-6** (Table 28,29). As there are many parameters influencing these data sets such as transduction efficiency (in the case of kd studies), PD and PK properties of VP and time of exposure to the VP to name but a few, clearly more experiments are needed to finally decide on the dependency of these HCC cell lines on components of the Hippo pathway. One possibility to gain further information is the utilization of a YAP/TEAD-driven reporter assay (see 3.7.).

3.6.2 THE ANTI-PROLIFERATIVE EFFECT OF DASATINIB TREATMENT CAN BE REVERSED BY ECTOPIC EXPRESSION OF THE DASATINIB-RESISTANT YES-1 MUTANT (T348I)

For technical reasons such as reproducibility the HCC cell line SK-HEP-1 was chosen for conducting rescue experiments. SK-HEP-1 was previously shown to be sensitive to YES-1 kd (Fig. 19 and 46). The cellular Dasatinib IC₅₀ value in SK-HEP-1 was determined at 12.74µM. For rescue studies from Dasatinib inhibition the following eukaryotic expression vectors (pLX303- based; see also [79]) were used to revert the anti-proliferative effect of YES-1 inhibition: i) YES-1_wt) and ii) the mutant variant YES-1_T348I. The mutant variant was originally designed by Rosenbluh *et al.* [79] to generate a Dasatinib-resistant YES-1 protein. This mutant allowed us to demonstrate that Dasatinib exhibits no off-target effects but executes its anti-proliferative effect exclusively via YES-1 activity.

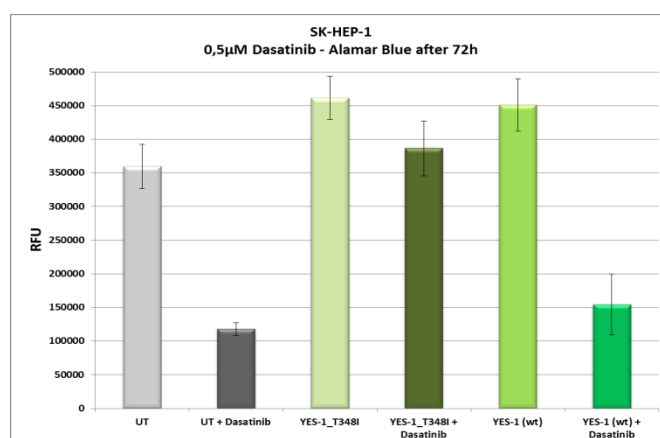


Figure 59: Proliferation rates [relative fluorescence units; RFU] of differently treated SK-HEP-1 cells.

- UT: Untreated/non-transfected (= wt cell line)
- UT + Dasatinib: Incubation of non-transfected cells with 0.5 µM Dasatinib for 72h
- YES-1_T348I: Cells transfected with the expression vector for the Dasatinib-resistant YES-1
- YES-1_T348I + Dasatinib: Cells transfected with the expression vector for the Dasatinib-resistant YES-1 and treated with Dasatinib (0.5 µM for 72h)
- YES-1 (wt): Cells transfected with expression vector for wt YES-1
- YES-1 (wt) + Dasatinib: Cells transfected with expression vector for wt YES-1 and treated with Dasatinib (0.5 µM for 72h)

YES-1_T348I expression lead to a complete rescue of the Dasatinib inhibitory effect. In contrast, no rescue was observed when YES-1_wt was transiently over-expressed (Fig. 59). Interestingly, transient over-expression of both YES-1_wt or YES-1_T348I lead to an increase in proliferation, an effect which also had been shown for other kinases [110,111]

3.7 Reporter Gene Assay

In order to allow monitoring of a YAP/TEAD-controlled induction of expression a reporter gene assay was developed. For this we made use of the published promoter region of one of the YAP/TEAD-driven genes, the connective tissue growth factor (*CTGF*).

3.7.1 TRANSFECTION EFFICIENCY

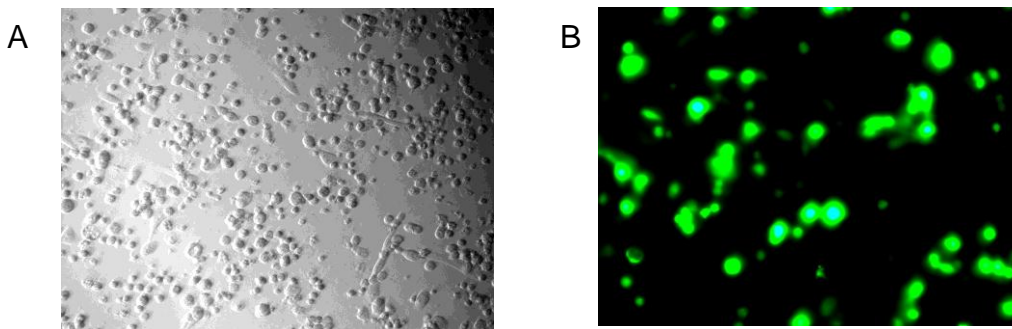


Figure 60: Evaluation of transfection efficiency using AMAXA Electroporation and Fluorescence microscopy

A) Bright-field microscopy of SK-HEP-1 cell line after transfection **B)** Fluorescence microscopy of SK-HEP-1 cell line after 48 hours of transfection with a GFP expressing plasmid

A prerequisite for the utilization of a reporter gene assay in a transient experimental setting is a reproducible transfection efficiency of at least 25%. Analysis of SK-HEP-1 transfected cells via bright-field and fluorescence microscopy revealed a transfection efficacy of approximately 40%.

3.7.2 CONSTRUCTION OF TEAD-DRIVEN REPORTER GENE PLASMIDS

In order to establish various TEAD-driven luciferase reporter gene plasmids we made use of two basic vectors from Promega: pGL4_16 and pGL4_28 (Fig.61 and 62; Manual #TM259 available online at: www.promega.com/protocols). Both plasmids give rise to expression of luciferase (luc2CP) under the respective promoter cloned upstream. Luc2CP is a synthetically derived luciferase sequence with humanized

codon optimization. The luc2CP gene also contains hCL1 and hPEST, both of which are protein destabilization sequences. In addition, pGL4_28 contains a minimal SV40 promoter allowing a baseline expression of the reporter gene. The minimal SV40 promoter is absent in pGL4_16.

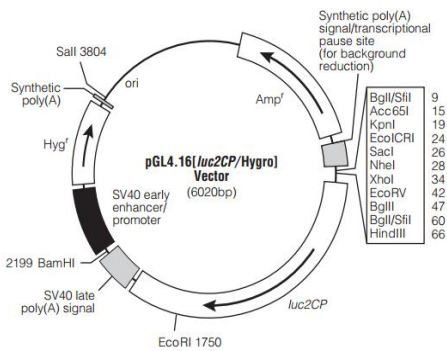


Figure 61: pGL4.16 Vector map

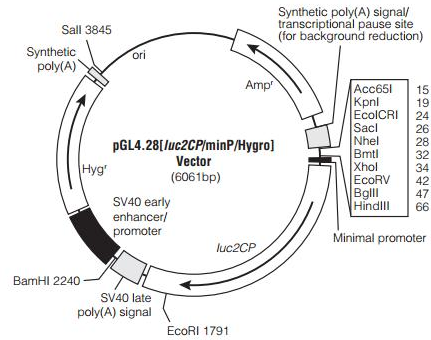


Figure 62: pGL4.28 [luc2CP/minP/Hygro] Vector map

Three TEAD-binding motifs were identified in the promoter sequence of *CTGF* [93] (Fig.63). This sequence was used to construct wt and modified *CTGF* variants as shown in Fig. 64.

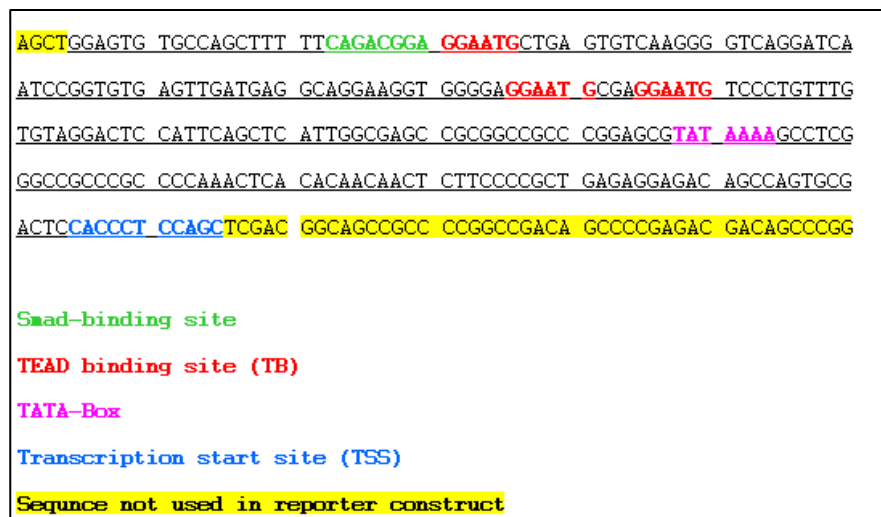


Figure 63: Human promoter region of the connective tissue growth factor (*CTGF*) [93]

The three TEAD-binding sites (TB) are depicted in red. Other regulatory sequence motifs such as a Smad-binding site, the TATA-box and the transcription start site (TSS) are also indicated. Based on this sequence various reporter gene plasmids were constructed (see Fig. 64).

Designed Promoter Constructs	
CTGF-wt:	CTGF-wt(-Smad):
GGAGTG TGCCAGCTTT TTCAGACCGGA GGAATGCTGA GTGTCAAGGG GTCAGGATCA ATCOGGTGTG AGTTGATGAG GCAGGAAGGT GGGGAGGAAT CGAGGAATG TCCCTGTTTG TGTAGGACTC CATTGAGCTC ATTGGCGAGC CGCGGCCGCC CGGAGCGTAT AAAAGCCTCG GGCGCCCGC CCCAAACCTCA CACAACAACCT CTTCOCOCCT GAGAGGAGAC AGCCAGTGGC ACTCCACCCCT CCAGC	GGAGTG TGCCAGCTTT TTGGAATGCTGA GTGTCAAGGG GTCAGGATCA ATCOGGTGTG AGTTGATGAG GCAGGAAGGT GGGGAGGAAT CGAGGAATG TCCCTGTTTG TGTAGGACTC CATTGAGCTC ATTGGCGAGC CGCGGCCGCC CGGAGCGTAT AAAAGCCTCG GGCGCCCGC CCCAAACCTCA CACAACAACCT CTTCOCOCCT GAGAGGAGAC AGCCAGTGGC ACTCCACCCCT CCAGC
CTGF-mut:	CTGF-6x:
GGAGTG TGCCAGCTTT TTCAGACCGGA GGAATGCTGA GTGTCAAGGG GTCAGGATCA ATCOGGTGTG AGTTGATGAG GCAGGAAGGT GGGGAGGACT CGAGGACTG TCCCTGTTTG TGTAGGACTC CATTGAGCTC ATTGGCGAGC CGCGGCCGCC CGGAGCGTAT AAAAGCCTCG GGCGCCCGC CCCAAACCTCA CACAACAACCT CTTCOCOCCT GAGAGGAGAC AGCCAGTGGC ACTCCACCCCT CCAGC	GGAGTG TGCCAGCTTT TTCAGACCGGA GGAATGCTGA GTGTCAAGGG GTCAGGATCA ATCOGGTGTG AGTTGATGAG GCAGGAAGGT GGGGAGGAAT CGAGGAATG TCCCTGTTTG TGTAGGAGGAATGCTC CATTGAGCTC AGGAATGTTGGGAGGAATGCG CGCGGCCGCC CGGAGCGTAT AAAAGCCTCGGGCGCCGCC CCCAAACCTCA CACAACAACCT CTTCOCOCCT GAGAGGAGAC AGCCAGTGGC ACTCCACCCCT CCAGC
	CTGF-del (TB1-3):
	GGAGTG TGCCAGCTTT TTCAGACCGGA CTGA GTGTCAAGGG GTCAGGATCA ATCOGGTGTG AGTTGATGAG GCAGGAAGGT GGGGACGA TCCCTGTTTG TGTAGGACTC CATTGAGCTC ATTGGCGAGC CGCGGCCGCC CGGAGCGTAT AAAAGCCTCG GGCGCCCGC CCCAAACCTCA CACAACAACCT CTTCOCOCCT GAGAGGAGAC AGCCAGTGGC ACTCCACCCCT CCAGC

Figure 64: Promoter sequences of various CTGF promoter-driven luciferase reporter vectors

Each synthetically generated promoter cDNA fragment was cloned into the HindIII/ XhoI sites of pGL4_16 and pGL4_28, respectively.

CTGF-wt: unmodified wild-type CTGF promoter sequence

CTGF-mut: single point mutations in all three TEAD binding motifs (indicated by black and bolt letter)

CTGF-wt(-Smad): unmodified wild-type CTGF promoter sequence lacking the Smad-binding motif

CTGF-6x: as the wild type CTGF promoter but instead of the original three TEAD binding motifs are six binding motifs present

CTGF-del (TB1-3): all three TEAD-binding motifs are deleted

3.7.3 CHARACTERIZATION OF TEAD-DRIVEN REPORTER GENE CONSTRUCTS

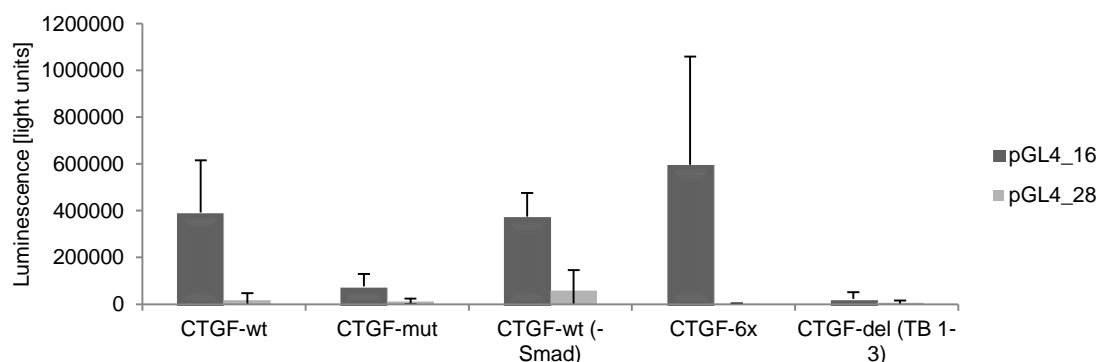


Figure 65: Characterization of TEAD-driven reporter gene plasmids in SK-HEP-1

Luciferase reporter gene activity in cell line SK-HEP-1 was measured after 48 hours past transfection. The black bars refer to constructs based on the pGL4_16 basis – a vector lacking the SV40 minimal promoter, grey bars to pGL4_28 a similar but SV40 minimal promoter containing vector. For a detailed description of vectors see (3.7.2).

Vectors harboring the minimal SV40 promoter did not lead to the generation of a suitable luciferase signal whereas vectors with only the *CTGF* promoter led to a pronounced luminescence (Fig. 65). For that reason the pGL4_16 series was chosen for further experiments including kd experiments in SK-HEP-1 and JHH-7 cell line as well as compound experiments.

To summarize, luminescence signals of pGL4_16 *CTGF*-wt and *CTGF*-wt (-Smad) are in the same range (400 000 light units). Therefore, the presence or absence of the Smad site has no influence on the *CTGF* promoter in this setting. As expected, an even more pronounced signal was observed with the vector containing six TEAD recognition sites (pGL4_16 *CTGF*-6x; Fig. 65). In contrast, the introduction of a single point mutation in each of the TEAD recognition motifs (pGL4_16 *CTGF*-mut) or the deletion of these motifs (pGL4_16 *CTGF*-del(TB 1-3)) had a dramatic influence on the activation of the promoter, as there is almost no signal detectable.

3.7.4 INFLUENCE OF KNOCKING DOWN PROTEINS OF THE HIPPO PATHWAY AND YES-1 ON THE TEAD-DRIVEN REPORTER GENE ACTIVITY

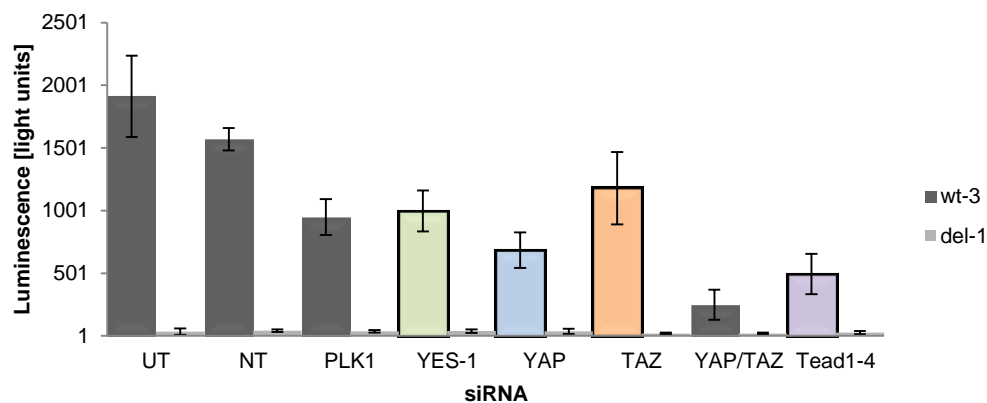


Figure 66: Reporter gene activity in SK-HEP-1 Clone-wt3 (wt-3) and SK-HEP-1 Clone-del1 (del-1)

Cells harbor either pGL4_16 *CTGF*-wt or pGL4_16 *CTGF*-del(TB1-3) vector. Luminescence was measured after 48h of siRNA-mediated kd of the indicated protein(s). **UT**: Untreated, **NT**: Non-targeting control

In order to investigate the role of “Hippo proteins” and YES-1 kinase on the TEAD-promoter-driven luciferase expression, a single cell clone was generated either harboring reporter gene vector pGL4_16 *CTGF*-wt or pGL4-16 *CTGF*-del(TB1-3). Knocking down YES-1, YAP, TAZ, TEAD1-4 or both YAP/ TAZ the luciferase signal was significantly reduced. The most efficient reduction in the luciferase signal was detected via the double kd of YAP/ TAZ or via kd of all four TEAD transcription factors (TEAD1-4), respectively. PLK-1 kd also causes a reduction after 48 hours in luminescence but this is most likely due to the fact that kd of PLK-1 at that time point caused already apoptosis of cells leading to a reduction in the luciferase signal. For further studies earlier time points were chosen where kd of PLK-1 had only a neglectable effect on the TEAD-driven reporter gene activity.

3.7.5 INFLUENCE OF YES-1 ON REPORTER GENE ACTIVITY

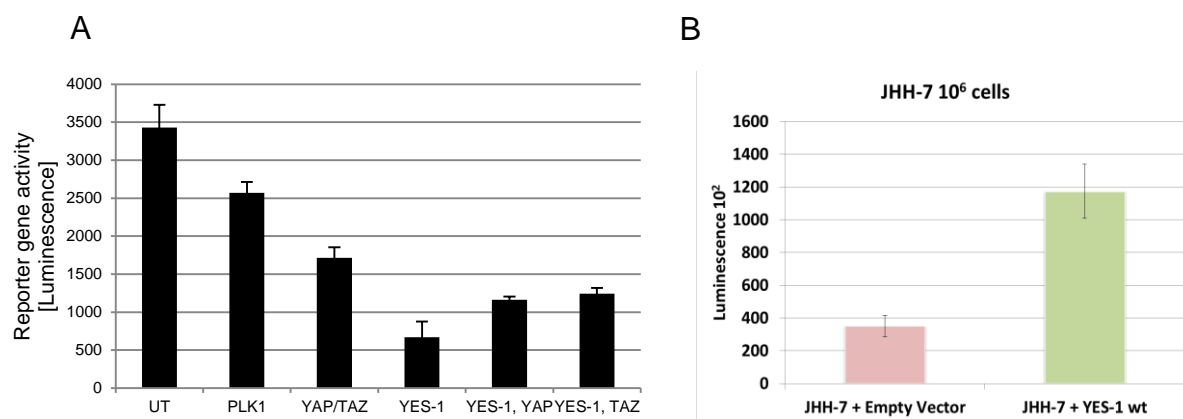


Figure 67: TEAD-driven reporter gene activity after 24 hours of kd or over-expression of YES-1

- A) SK-HEP-1 Clone-wt-3; 3000 cells; 24h of siRNA treatment of the indicated gene or combined kd of genes
B) Transient overexpression of YES-1 increase reporter gene activity after 24 hours in HCC cell line JHH-7

To test whether YES-1 influences YAP/TEAD dependent expression of genes like *CTGF*, we made use of our TEAD-driven reporter gene assay. SK-HEP-1 and JHH-7 were shown in previous experiments to be sensitive to YES-1 kd and were therefore chosen for this experiment. Regarding results obtained from siRNA-mediated kd suppression of single kd of YES-1 dramatically impairs reporter gene activity indicating that it plays an essential role in YAP/TEAD-dependent gene activation (Fig. 67). Combined kd of YES-1 with either YAP or TAZ had a similar inhibitory effect on the reporter gene activity. In addition, transient transfection of JHH-7_pGL16_*CTGF*_wt cell line with a wt YES-1 plasmid, the reporter gene activity increased dramatically compared to the non-transfected cells (Fig. 67). Altogether these data support our previous findings that SK-HEP-1 is a Hippo- and YES-1-dependent cell line and JHH-7 exhibits a pronounced basic YES-1 activity. This data set also suggests that at least in these two cell lines YES-1 activity contributes essentially to the *CTGF*-promoter driven induction of luciferase.

3.7.6 UTILIZATION OF THE *CTGF*-PROMOTER DRIVEN REPORTER GENE ASSAY FOR COMPOUND PROFILING

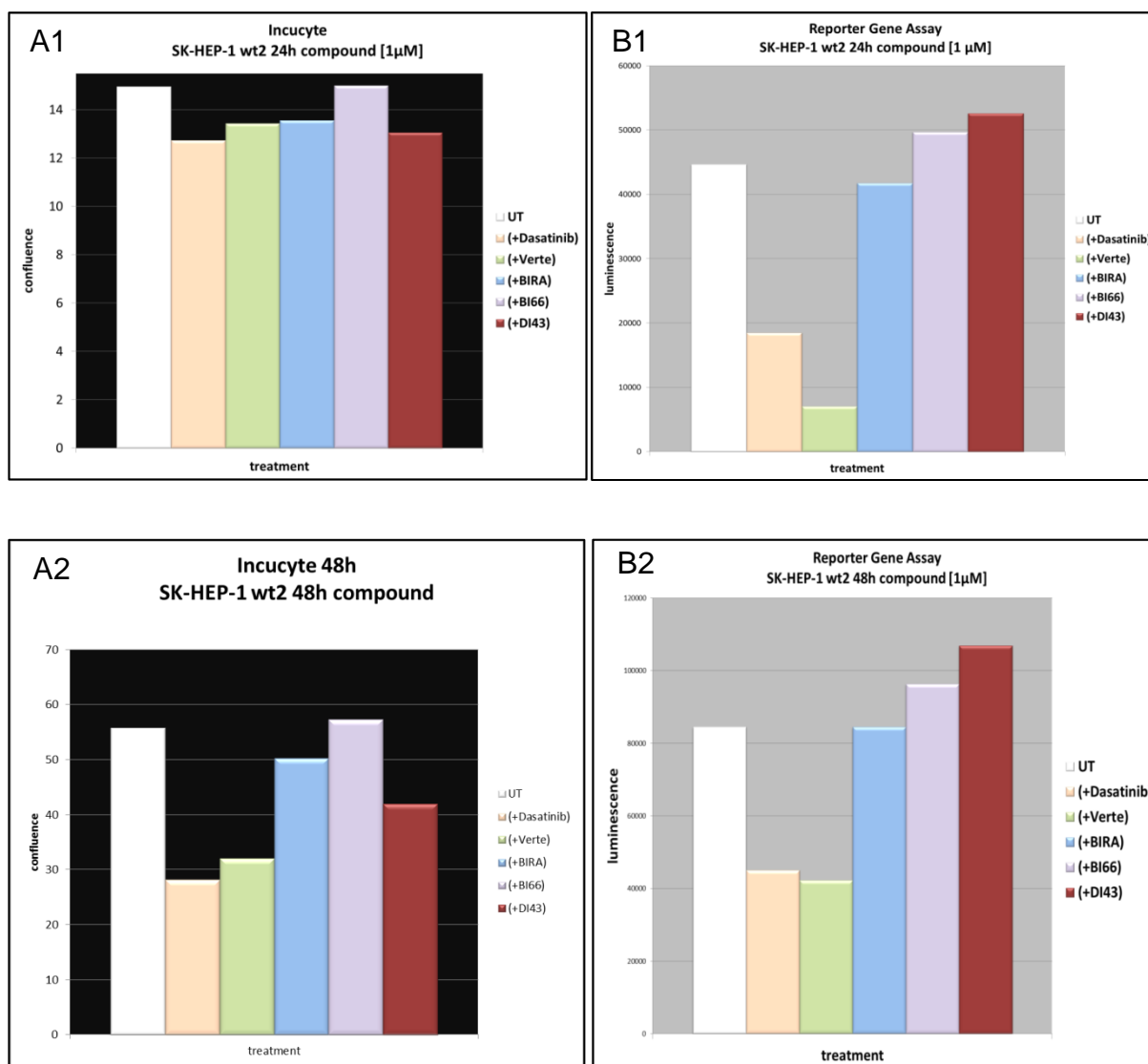


Figure 68: Cell density and Reporter gene assay in SK-HEP-1 harboring *CTGF*-promoter driven luciferase reporter gene plasmid pGL4_16 *CTGF*-wt

Cell density (Incucyte) was determined after treatment for 24h (A1) or 48h (A2) with the indicated compounds (all at 1 μ M). Corresponding reporter gene assays were performed at 24h (B1) and 48h (B2), respectively.

UT: Untreated; Dasatinib: YES1 inhibitor; Verteporfin (Verte): YAP/TEAD PPI; BI00404566 (BI66): BDE9 inhibitor; DI00026043 (DI43): TGF- β inhibitor; BIRA0766BS (BIRA): p56 lck kinase inhibitor.

To test whether similar results obtained from suppression of Hippo genes and YES-1 can also be achieved by inactivating those components by small molecule inhibitors, five different compounds were applied to SK-HEP-1 cells harboring the *CTGF* reporter system (Fig. 68). Cell confluence was measured using Incucyte to exclude that effects of impaired reporter gene activity are only due to anti-proliferative effects in general. Therefore, to distinguish between unspecific and specific effects different inhibitors were used including a small molecule tyrosine kinase (YES-1) inhibitor (Dasatinib), a YAP/TEAD protein-protein interaction inhibitor (Verteporfin), a BDE9 inhibitor (BI00404566), a TGF- β inhibitor (DI00026043) and a p56 lck kinase inhibitor (BIRA0766BS). The first two inhibitors are specific for the reporter gene assay whereas the latter three are expected not to interfere with the *CTGF*-driven reporter. Indeed, Fig. 68A1 shows that the proliferation was not influenced by compounds after 24h whereas on the reporter gene activity a significant difference between untreated control and Dasatinib or Verteporfin could be observed. In contrast, the other three compounds exhibited no influence at all. Verteporfin had been described to inhibit the interaction of YAP/TEAD in the nucleus [81] which could be confirmed (Fig. 68A1/2) in our experiment. Dasatinib treatment lead also to a massive reduction of *CTGF* reporter gene activity which strengthens the hypothesis that the activated form of p-YAP-Y-357 mediated through YES-1 kinase [79] is essential for gene expression. The same effect was observed after 48 hours treatment. In contrast to the other compounds treatment with Dasatinib [1 μ M] or Verteporfin [1 μ M] already had an influence on the proliferation supporting our previous findings that these cells are dependent on the activity of YAP/TEAD and YES-1. An increase of Dasatinib up to 20 μ M did not further reduce the already weak luciferase signal after incubation for 24h. Perhaps the remaining signal level represents the basal background activity of the reporter gene system in these cells (Fig. 69).

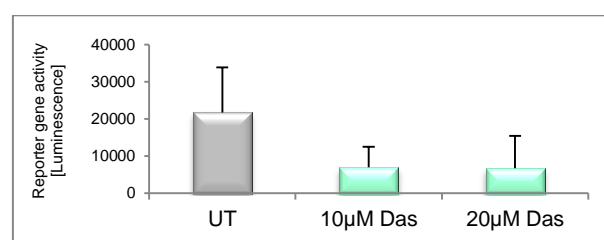


Figure 69: *CTGF*-promoter-driven luminescence after 24h Dasatinib treatment in SK-HEP-1 Clone wt3

UT: Untreated; Das: Dasatinib

3.7.7 AAV PARTICLE-MEDIATED EXPRESSION OF A PEPTIDE DERIVED FROM THE YAP/TEAD INTERPHASE INHIBITS THE *CTGF*-DRIVEN REPORTER GENE ASSAY

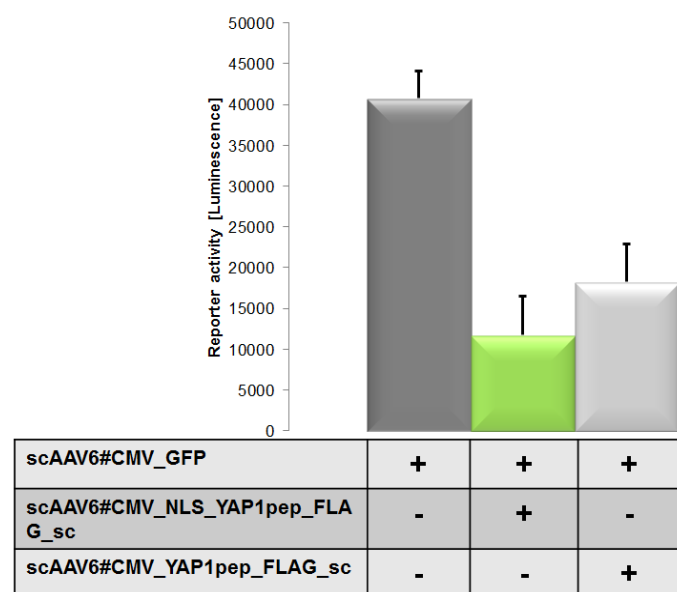


Figure 70: SK-HEP-1 Clone-wt3 transduced with AAV particles expressing the YAP/TEAD interphase peptide

For this assay 1×10^4 cells/ well in a 96-well plate and a MOI of 100000 was used.

Cells which have been stably transfected with Reporter gene *CTGF*_wt plasmids (SK-HEP-1 Clone-wt3) were used for this assay and treated with AAV particles which express a YAP/TEAD interphase peptide [82]. Two differently designed particles were used, one w/o a nuclear targeting sequence (NLS) the other construct containing a NLS motif (scAAV6#CMV-NLS_YAP1pep_FLAG-sc). scAAV#CMV_GFP was taken as a negative control.

YAP and TEAD interaction is crucial for target gene expression. The transcriptional co-activator interacts with its counterpart through three interfaces. Interface three seemed to be the most important one, shown by co-IP after introduction of mutations at respective areas [82]. To validate specificity of our reporter system we designed a small peptide (Fig. 71) carrying exactly those sequences necessary for YAP/TEAD interaction.

NLS-YAP1-FLAG:
 MPKKRKRK^{red}VAGHQIVHVRGDSETDLEALFNAV MNPKTANVPQTVPMRLRKL^{green}PDSFFKPPEDYK^{green}DDDDK^{green}*

YAP1-FLAG:
 MAGHQIVHVRGDSETDLEALFNAV MNPKTANVPQTVPMRLRKL^{green}PDSFFKPPEDYK^{green}DDDDK^{green}*

Figure 71: AA sequences of the inhibitory peptide of the YAP/ TEAD interaction as published by Li, 2010 [82]

The red marked sequence refers to the artificially introduced nuclear target signal, the green one to a synthetic FLAG motif.

The recombinant AAV particles had been established in Dr. D. Mennerich's lab at BI/Biberach. Out of different GFP-expressing AAV strains tested (AAV1, 2, 5, 6 and 8), AAV6 exhibited the most appropriate transduction efficacy in HCC cells (data not shown). The respective recombinant AAV6 particles were applied to our cellular reporter gene assay system to interfere with the YAP/TEAD interaction and thereby reducing the luciferase reporter signal. The nuclear targeting signal (NLS) was introduced to allow an efficient nuclear import of the inhibitory peptide as the YAP/TEAD complex is expected to be formed most preferentially in the nucleus. The AAV transduction was done essentially as described in Material and Methods (see 2.2.22). Transduction of cells with a GFP control AAV6 particle allowed the generation of a pronounced luminescence signal (Fig. 70). However, when cells were treated with AAV6 particles expressing the inhibitory peptides a massive decrease in the reporter gene signal was detectable. In addition, the AAV6 construct with the nuclear translocation tag (CMV_NLS_YAP1pep_FLAG_sc) gave rise to a more pronounced decrease in the reporter signal than that of AAV6 particle lacking the nuclear targeting sequence (CMV_YAP1pep_FLAG_sc). In summary, both AAV6 particles were able to reduce the signal, most likely by interrupting the YAP::TEAD interaction in the nucleus supporting the data from Li, 2010 [82].

3.8 Co-Immunoprecipitation Studies to analyze the putative Interaction of YAP, TAZ, TEAD and YES-1

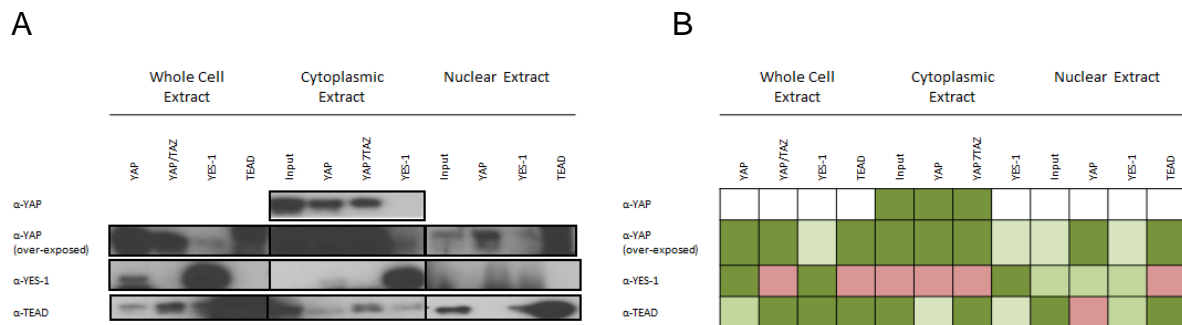


Figure 72: Co-Immunoprecipitation of YAP, YAP/TAZ, YES-1 and TEAD in JHH-7

A) Western blot of whole cell, cytoplasmic and nuclear extracts. Detection antibodies are indicated at the left of each figure (α -YAP, α -YES-1 and α -TEAD1). Pull-down antibodies are depicted at the top of each figure (YAP, YAP/TAZ, YES-1 and TEAD) **B)** Schematic overview of interaction (green) or no interaction (red) among the proteins tested.

In order to identify possible interaction partners of YAP (in particular YES-1) a co-immunoprecipitation was performed. Utilizing a YAP antibody for pull-down experiment, YAP protein itself could be detected with YAP antibody in all cellular extracts (Fig. 72; α -YAP, left column). In addition, YES-1 could be co-immunoprecipitated in whole cell- as well as in nuclear-extracts. The interaction of YAP and TEAD was confirmed by using YAP/TAZ antibody for precipitation in whole cell and cytoplasmic extracts. After pull-down of YES-1, the kinase itself could be detected in all 3 cell fractions. An interaction with YAP was shown in whole cell lysate as well as in nuclear extracts. The question whether TEAD interacts with YES-1 remains to be answered as the TEAD band outshined the YES-1 protein band on Western blot. However, TEAD1 was found to be immunoprecipitated as it could be detected in the nucleus as well as in whole cell lysate. An interaction with YAP could be observed in the whole cell- as well as in the nuclear-extract.

Our preliminary data support the idea that YES-1 most likely interacts with YAP and TEAD1. Further detailed studies will be necessary to learn more about the molar ratio of all these interacting proteins as well as about the YES-1 interaction specificity towards the members of the TEAD protein family.

4 DISCUSSION

The Hippo pathway was first characterized in *Drosophila melanogaster* [24] and was shown to play a fundamental role in the control of organ growth, tumor suppression, stem cell function and regeneration [31]. In mammals, the Hippo pathway is activated by many factors including Kibra, NF2, FRMD6 and cadherins in mammals [38]. Once started, a series of phosphorylation steps is triggered with the ultimate aim to phosphorylate YAP, a co-transcription factor, at serine 127 providing a repressive mark [32]. This leads to the retention of YAP in the cytoplasm and pro-survival and anti-apoptotic genes, like *CTGF* and *BCL-2* are no longer expressed. This in turn results in an inhibition of cell proliferation [66]. The Hippo pathway is important during embryogenesis, where the pathway has to be turned off in order to allow tissue growth. Conversely, the pathway is activated in adult tissue through contact inhibition in order to inhibit tissue over-growth [38]. Due to a malfunction of the Hippo pathway, which is often observed in cancer cells, the co-transcription factor YAP is able to move into the nucleus and interacts with DNA-binding proteins like TEAD1-4. This protein complex binds to the promoter sequence of target genes [71]. The expression of pro-survival and anti-apoptotic genes leads to an increase in proliferation which contributes to tissue over-growth and malignancy [33]. Based on *in vitro*, *in vivo* and IHC studies of tumor patient samples, it is evident that the YAP oncogene is linked to tumorigenicity of several solid cancer types such as prostate, colon and liver [80]. Therapeutically, interfering with a protein::protein interaction such as of YAP and TEADs is a major challenge. Unfortunately efforts thus far have not resulted in an efficacious NCE [94]. Exceptions include the clinically used photosensitizer Verteporfin [95] and a peptide construct based upon the work presented by Zhou Z. *et al.* [96]. To learn more about the contribution of upstream kinases possibly involved in the activation of the YAP/TEAD complex or of YAP itself, we investigated the role of YES-1 kinase and its contribution to Hippo-pathway dependent gene expression. YES-1 was shown to activate YAP by phosphorylation of tyrosine 357 [79], therefore we hypothesized that it contributes to deregulation of the Hippo pathway. Inhibition of an upstream kinase target would allow specific and efficient inhibition of either the activation of YES-1 or the formation of the transcriptional complex. Furthermore, it might prevent the entrance of YAP into the nucleus or might

influence all of these molecular events together. Based on published data HCC can be regarded as a tumor being dependent on the Hippo pathway. According to the ratio of incidence vs. mortality this aggressive tumor type has a high medical need for novel and efficacious treatment modalities. Currently the most efficient curative therapy is surgery but nevertheless many patients die because of tumor recurrence and spread [80].

Transiently expressed YES-1 increases LATS1 expression

Levels of proteins implicated in the Hippo- or WNT- pathway were tested in 19 hepatocellular carcinoma cells (HCC) and two YES-1 over-expressing cell lines. The protein patterns differed from one cell line to another (for a detailed description see 3.1). As cell density and mechanical stress had been described as parameter for YAP/TAZ inactivation [73], varying cell densities and different time points of cell lysis might be a possible explanation of these diverse patterns. Despite this, a correlation between YAP and TEAD1 was observed, whereby cells with a high amount of YAP1 also exhibit significant elevated levels of TEAD1 (Fig. 17). On closer examination of the changes in protein levels obtained from YES-1 over-expression several statements can be made: Firstly, YAP and TEAD1 protein levels significantly decreased after transiently expressing either YES-1_wt or kinase dead mutant YES-1_K330M. As also over-expression of a non-functional version of YES-1 induces changes in the protein levels of YAP and TEAD1, another inherent function different from the enzymatic kinase activity might contribute to this effect. Alternative functions of kinase dead mutants had been reported for instance for a novel splice variant of interleukin-1 receptor associated kinase 1 (IRAK1c). Although lacking kinase activity, IRAK1c was shown to play a negative regulatory role in Toll/IL-1R-induced inflammatory signaling [97].

A second observation was that the expression of *c-MYC*, a suggested target gene of the Hippo pathway increases. This finding is in agreement with our previous assumption that YES-1 might be a key driver of YAP/TEAD dependent transcription.

Thirdly, p-MOB1 was not detected after YES-1 over-expression. In addition, MST1 levels significantly decreased whereas p-YAP-S-127 (inactivating phosphorylation) as well as LATS1 protein levels increased after YES-1 over-expression. This particularly held true when the catalytically inactive mutant (K330M) was expressed. The exact

mechanism is not understood yet. One explanation could be that transient expression of YES-1 led to an increase of p-YAP-Y-357 (activating phosphorylation). Therefore cells might try to compensate active YAP levels by expressing LATS1, which has a negative regulatory effect on YAP (Fig. 17). Due to lack of a specific anti p-YAP-Y-375 antibody this remains to be determined. Another idea of how to more precisely describe the regulatory function of YES-1 on YAP would be the utilization of YAP alanine mutants YAP-Ser-127→Ala and YAP-Tyr-357→Ala, respectively in future experiments.

YES-1 kinase is located in the cytoplasm as well as in the nucleus

YAP1 (YES-1 associated kinase 1) was particularly found accumulated in the nucleus of 62% of 177 pairs of tumors investigated [80]. Furthermore, over-expression of YAP in HCC was also linked to poorer tumor differentiation. This suggests that YAP is an independent prognostic marker for overall survival and disease-free survival [80]. In our studies utilizing HCC cell lines YAP was found accumulated in the nucleus in 6 out of 21 and also present in notable amounts in additional 10 cell lines (see 3.2). Those 16 cell lines were therefore regarded as potentially Hippo-pathway driven.

YES-1 had been shown to contribute to gene expression by forming a complex with YAP, β -catenin and TBX5 in the nucleus of colon carcinoma cell lines [79]. We therefore addressed the question whether the reported YES-1 kinase distribution in colon cancer cell lines is similar in those HCC cell lines, supposed to be Hippo pathway driven. Our analysis revealed that YES-1 kinase is present in the cytoplasm as well as in the nucleus in most of the analyzed HCC cell lines. Again varying patterns of protein distribution (Fig. 18) were detected. Out of 21 cell lines 7 showed a significant increase in YES-1 in the nucleus (Fig. 18). Interestingly, YES-1 appeared as a two band pattern on the Western blot (see 3.2), most likely due to the suggested splice variants (<http://www.ensembl.org/>). It remains to be determined why some cell lines only show either the lower- or the higher molecular weight band in one of the two fractions and why YES-1 is present just in the cytoplasm or in the nucleus of individual HCC cell lines (see 3.2). Interestingly, cells with a nuclear increase of YAP exhibit significantly reduced amount of YES-1 in the nucleus (Fig.8). These results might support the hypothesis that YES-1 activates YAP in the cytoplasm. As a consequence YAP is then able to enter into the nucleus if it is not further phosphorylated by LATS1 (Fig. 10C).

siRNA-mediated knockdown (kd) of YES-1 decreases TAZ and TEAD1 protein levels

siRNA-mediated kd of TAZ, YAP, TEADs and YES-1 in HCC cell lines revealed a “wiring” between the respective proteins. Particularly, kd of YES-1 and/or TAZ were linked with a decrease in TEAD1. However, it is currently not clear whether this “wiring” takes place at the transcriptional or (post)-translational level. Based on the low siRNA transduction rate of HCC cell lines (see 3.3.) we next made use of a lentiviral-mediated shRNA transduction.

Half of HCC cell lines tested show sensitivity towards RNAi-mediated YES-1 knockdown

To investigate the role of YAP, TAZ, YES-1 and TEAD1-4 on the proliferation of HCC cell lines, lentiviral shRNA-mediated (kd) studies were performed. The distribution pattern of YAP and YES-1 in the nucleus and cytoplasm was used as a selection biomarker for HCC cell lines likely to be dependent on the Hippo pathway (Fig.17 and 18). Out of ten HCC cell lines, four were clearly dependent on YAP and two additional cell lines exhibited a partial sensitivity to YAP kd. In contrast, kd of TAZ had little influence on the proliferation. Only three out of the ten HCC cell lines exhibited sensitivity at lower cell densities. A similar effect for TAZ has been described in colon carcinoma cell lines [79]. On the contrary, the majority of the HCC cell lines were sensitive to kd of YES-1. Six out of ten exhibited a dependency on YES-1 independent of cell number and shRNA used. Interestingly, cell lines which we had previously been characterized as YES-1 dependent (3.4.3.13) also express YES-1 in high amounts (Fig. 17). Most of those cell lines also exhibited a significantly increased amount of LATS1 (Fig. 17) suggesting YES-1 or LATS1 amplification/over-expression as a predictive biomarker for YES-1 driven liver cancers.

Cell proliferation can be rescued by ectopic YES-1_wt protein

In order to exclude any off-target effect of an RNAi-mediated kd a rescue experiment is mandatory. For this we made use of shRNA-resistant cDNA constructs of YES-1_wt and YES-1_T348I. The T348I YES-1 mutant was described by Rosenbluh *et al.* as resistant to Dasatinib treatment [89]. For both constructs a codon optimized cDNA expression vector was generated. In both cases a clear rescue phenotype was achieved in cells with a kd of the endogenous YES-1. This strongly supports our hypothesis that YES-1 kinase activity essentially contributes to YAP activation/stabilization. In addition, a kinase dead YES-1 was used for rescue as well (K330M). In contrast to the enzymatically active constructs no rescue could be achieved with the kinase dead version of YES-1. However, it has to be noted that in the case of YES-1 mutant K330M only a low expression level was detected on Western blot and as a consequence this data set has to be cautiously interpreted. Several reasons might be adduced to explain the low expression level of mutant K330M: i) the mutation is leading to a protein instability as it was shown for several kinases such as PIM1 [98], ii) the mutation might interfere with an efficient recognition by the detection antibody and iii) the mutation might lead to an instability of the respective mRNA as it was shown e.g. for DDR2 [99]. As YES-1 was also described to bind YAP1 [80] and a function other than the kinase activity of YES-1 might also play an essential role. For instance the ability to interact with other proteins such as YAP, TBX5 as shown in colon cancer cells [79]. Additionally, a mutation might also lead to a change in the subcellular localization as described for the transcription factor GLI3 of the Hedgehog pathway [100].

Knockdown of YES-1 inhibits expression of a TEAD-driven reporter gene in SK-HEP-1 cells

The native promoter region of the connective tissue growth factor (*CTGF*) contains three TEAD binding motifs [93]. Based on this promoter region a reporter gene assay was established driving luciferase expression. In order to identify the most appropriate reporter gene construct the cell line SK-HEP-1 was transfected with plasmids bearing variants of the *CTGF* promoter sequence. Five different constructs were cloned either containing an SV40 minimal promoter or lacking. The promoter regions were as follows: i) unmodified wild-type *CTGF* promoter sequence (*CTGF*-wt), ii) single point mutations in all three TEAD binding motifs (*CTGF*-mut), iii) unmodified

wild-type *CTGF* promoter sequence lacking the Smad-binding motif (*CTGF*-wt(-Smad)), iv) wild type *CTGF* promoter but instead of the original three containing six TEAD binding motifs (*CTGF*-6x) and v) promoter where all three TEAD-binding motifs had been deleted (*CTGF*-del (TB1-3)) (Fig. 65). In summary, the presence of the minimal SV40 promoter led only to the generation of a marginal reporter gene signal. The most pronounced signals were obtained by using *CTGF*-6x followed by the *CTGF*-wt and the *CTGF*-wt (-Smad) construct indicating that the absence of the Smad binding motif has no converse effect on the reporter gene expression. In contrast, both reporter gene vectors either containing the mutated TEAD motifs or lacking them were found to be inactive (Fig. 65). For further studies the pGL4_16 *CTGF*-wt reporter gene vector was chosen. Upon kd of TEAD1-4 a great drop in luminescence was observed (Fig. 66). Knocking down both YAP and TAZ led even to an almost complete eradication of the reporter signal. As TAZ, the paralog of YAP1, had been shown to substitute YAP1 for the TEAD binding [32] it was to be expected that a double knockdown seemed to be more efficient (Fig. 66). Utilizing PLK-1 kd as a negative control, there was also a slight decrease in luminescence detectable which might be caused by apoptotic cells. Therefore, for following experiments a time point was chosen when only the kd of YAP, TEAD or TAZ inhibited the reporter gene assay but not that of PLK-1.

Interestingly, a kd of YES-1 also strongly interfered with the reporter gene activity (Fig. 67) whereas transiently expressed YES-1 in JHH-7 containing the reporter gene construct *CTGF*-wt increased the reporter gene activity massively (Fig. 68B). Based on these data sets, YES-1 can be regarded as an essential activator of the YAP/TEAD-driven Hippo pathway. This confirms the hypothesis that YES-1 acts in a Hippo dependent manner. Direct evidence for YES-1 being essentially involved in the induction of a TEAD-motif containing promoter has not previously been shown in human cells. Interestingly, it had been reported that colon cancer cells escape 5FU chemotherapy-induced cell death by entering stemness and quiescence associated with the YES-1/YAP axis [101] supporting our hypothesis that YES-1 might be a master regulator of the YAP/TEAD-driven transcription.

Adeno-Associated Virus (AAV) particles recombinantly designed to express YAP::TEAD interfering peptides significantly impairs the CTGF promoter-driven reporter activity.

Originally Li and colleagues have shown that the YAP::TEAD complex can be disrupted by peptides derived from the proposed YAP interaction sites on TEAD [82]. In order to disrupt this interaction in the cell we made use of two recombinant AAV particles expressing either the YAP::TEAD blocking peptide without a nuclear targeting sequence (NLS) or with an NLS motif. The expression cassette was designed for the full length YAP blocking peptide (covering all three interaction sites between amino acid position 50-100 of YAP; for details see Li *et al.*, 2010 [82]). The recombinant AAV particles were generated and provided by D. Mennerich and T. Lamla (Boehringer Ingelheim Pharma GmbH & Co. KG). Among eight serotypes, AAV6 was shown to be the best transducing AAV serotype for HCC cell lines. AAV particles expressing GFP were used as a control. Transduction of cells with a GFP control AAV6 particle allowed the generation of a pronounced reporter luminescence signal (Fig. 71). However, when cells were treated with AAV6 particles expressing the inhibitory peptides a massive decrease in the reporter gene signal was detectable. Interestingly, the AAV6 construct with the nuclear translocation tag gave rise to a more pronounced decrease in the reporter signal than that of AAV6 particle lacking the nuclear targeting sequence (Fig. 71). In summary, our data set supports the idea of a YAP::TEAD interaction in the nucleus as suggested by Li *et al.* [82]. For future experiments it will be of relevance to further reduce the length of the blocking peptides to allow the identification of the core motif essentially contributing to the YAP::TEAD interaction. Once the minimal sequence has been identified alanine-scanning could lead to the identification of the critical amino acids responsible for the specific YAP::TEAD interaction. The identification of such residues is a prerequisite for the design of protein interaction inhibitors. Recently, such an approach had been successfully applied for the identification of the roles of conserved charged residues in the extracellular domain of an epithelial sodium channel subunit [102].

HCC cell lines exhibit sensitivity to Dasatinib treatment in proliferation as well as in reporter gene activity assays.

Dasatinib, a tyrosine kinase inhibitor, is also known to inhibit YES-1 kinase activity [79]. For that reason Dasatinib was tested on our HCC cell line panel (Tab. 29). The results are in good agreement with our genetic approaches to YES-1 kd (Tab. 28). Most interestingly, Dasatinib also decreased the *CTGF* promoter-driven reporter gene activity (Figs. 69 and 70) clearly demonstrating that indeed the enzymatic activity of YES-1 is required for the induction of the reporter construct. In addition, Verteporfin an inhibitor of YAP::TEAD interaction [33] was tested in 23 different HCC cell lines. This compound was also shown to greatly reduce activity of reporter signal. Originally this compound was designed as a photosensitizer for photodynamic therapy to eliminate the abnormal blood vessels in the eye associated with conditions such as the wet form of macular degeneration [91]. It has been recently shown that it also interferes with YAP::TEAD interaction [81]. In summary, recombinant AAV-based expression of YAP::TEAD interfering peptides or treatment with Dasatinib led to a strong reduction in expression of a TEAD-driven reporter gene. Additionally, the application of Dasatinib led to a dose dependent inhibition of proliferation with a half maximum inhibitory concentration values (IC_{50}) of 0.03 to 72 μ M in the HCC cell lines tested (Table 29). Treatment with Verteporfin resulted in IC_{50} values between 0.07 and 23.56 μ M (Table 29). Cells responsive to Dasatinib and Verteporfin were identified (SNU-449, JHH-2, JHH-6 and JHH-7). Adequate IC_{50} values for Dasatinib treatment were also observed in HLF, HuCCT-1, HuH-7, SNU-387, JHH-1, JHH-2 and JHH-4. Combining our data sets from kd studies with those from the peptide and compound treatment approaches the following HCC cell lines are regarded as YAP/TEAD/YES-1 driven: HLE, HLF and SNU-423.

The anti-proliferative effect of Dasatinib treatment can be reversed by ectopic expression of the Dasatinib-resistant YES-1 mutant (T348I).

The YES-1 mutant (YES-1_T348I) has been reported to be resistant to Dasatinib [79]. Therefore we made use of this mutant to verify that the enzymatic activity is essential for the proliferation of HCC cells. Indeed, expression of this resistant mutant in the presence of Dasatinib led to a complete rescue of the Dasatinib inhibitory effect (Fig. 59). In contrast, no rescue could be demonstrated when wt YES-1 was over-expressed. Interestingly, transient over-expression of both YES-1_wt and YES-1

mutant T348I led to an increase in proliferation, an effect which also had been shown for other kinases [103-106]. Most importantly, this result supports the therapeutic concept of inhibiting the proliferation of HCC cells by inhibition of YES1 kinase activity.

YES-1 interacts with YAP and TEAD-1

During this study the interaction of YAP with TEAD1 that has been previously described [31], was confirmed. Particularly, the usage of a YAP/TAZ recognizing antibody worked most efficiently for the co-immune precipitation experiments. Originally, YAP was identified as a binding partner of YES-1 [66]. Our study demonstrated an interaction of YES-1 with YAP and with TEAD1 as well. *Vice versa*, after precipitating YAP1, the interaction with YES-1 could also be confirmed. This data set supports the idea that YES-1 interacts with YAP and most likely with TEAD1 as well. In future experiments it will be of interest to see whether the complex of YAP::TEAD is required for an efficient interaction with YES-1 or whether YES-1 can already bind to them individually. Another important aspect is the cellular location where these interactions take place. YES-1 may be binding to YAP in the cytoplasm and subsequently transported into the nucleus. Once there, YES-1 is then involved in the interaction between YAP and TEAD. On the other hand, YES-1 may only be interacting with YAP in the cytoplasm. As an interaction was demonstrated in whole cell lysates as well as in the nuclear extracts it seems more likely that YES-1 is interacting with both proteins in the nucleus. Perhaps the first interaction between YES-1 and YAP or TEAD1 is required for the transfer into the nucleus. In β -catenin-driven colon cancer cells phosphorylation of YAP1 by YES-1 has been shown to lead to localization of this complex to the promoters of anti-apoptotic genes including *BCL2L1* and *BIRC5* [79]. So far we do not know whether YES-1 in HCC cells is phosphorylating YAP at the proposed activating position on Y-375 [79] or other residues. However, it is clear that the kinase activity of YES-1 is essential for the activation of a YAP/TEAD driven reporter construct in HCC cells. Whether YES-1 is also phosphorylating TEAD or acts as a kind of “molecular glue” for the YAP::TEAD interaction in the nucleus remains to be determined.

5 ABSTRACT

The project aimed at the elucidation of the contribution of the SRC-like kinase YES-1 to the tumorigenesis of hepatocellular carcinoma (HCC). The working hypothesis implied that YES-1 plays an essential role in the activation of the YAP/TEAD-driven expression. RNAi-mediated knockdown of genes of the Hippo pathway and YES-1 was correlated with sensitivity. Half of HCC lines tested were shown to be sensitive towards YES-1 knockdown including a rescue from the anti-proliferative effect by over-expression of RNAi-resistant wt-YES-1 but not by the kinase dead YES-1. The kinase was found to be located in the cytoplasm as well as in the nucleus. No prediction about dependency on YES-1 could be made based on the intracellular distribution pattern of YES-1 and other Hippo proteins. Interestingly, LATS1, a core kinase of the Hippo pathway, was found to be up-regulated in cells which were dependent on YES-1. An interaction between YES-1, YAP and TEADs could be demonstrated *via* co-immunoprecipitation. By using a YAP/TEAD dependent reporter gene assay based on the *CTGF* promoter (“connective tissue growth factor”; target gene of YAP/TEAD), activation of the reporter gene could be shown after transiently expressing YES-1 or deactivation after YES-1 knockdown, respectively. The application of small-molecule inhibitors like Dasatinib (inhibitor of YES-1) and Verteporfin (inhibitor of YAP::TEAD) as well as YAP::TEAD interaction inhibiting peptides exhibited an impaired reporter gene activity. IC₅₀ values of these compounds were determined and correlated with genomic analyses. In conclusion, YES-1 kinase plays an essential role in YAP/TEAD-dependent activation of transcription.

6 ZUSAMMENFASSUNG

Ziel des Projektes war, die Rolle der Kinase YES-1 im Hippo Signaltransduktionsweg in Leberkarzinomzelllinien zu charakterisieren. Die Hypothese beruhte auf der Annahme, dass YES-1 eine essentielle Rolle bei der Aktivierung der YAP/TEAD (Transkriptionsfaktoren des Hippo-Signaltransduktionsweges) abhängigen Expression im Leberkarzinom spielt. Um dies zu testen, wurde ein RNAi-vermittelter „Knockdown“ der Gene des Hippo Signalweges als auch von YES-1 selbst durchgeführt und der Effekt auf die Proliferation analysiert. Die Hälfte der behandelten Zelllinien zeigte Sensitivität gegenüber RNAi-vermittelter YES-1 Runterregulierung. Der anti-proliferative Effekt konnte durch Überexpression einer RNAi-resistenten Variante von wt-YES-1 aufgehoben werden. YES-1 wurde sowohl im Zytoplasma als auch im Nukleus detektiert, wobei zunächst kein Zusammenhang zwischen der sub-zellulären Lokalisation von Proteinen des Hippo Signalweges und der direkten Aktivierung durch YES-1 hergestellt werden konnte. Interessanterweise wiesen alle YES-1 überexprimierenden Zellen eine Hochregulierung von LATS1, einer zentralen Kinase im Hippo Signalweg, auf. Mit Hilfe von Ko-Immünpräzipitation wurde eindeutig eine Interaktion zwischen YES-1 einerseits und YAP und TEAD andererseits nachgewiesen. Mittels eines YAP/TEAD abhängigen Reportergensystems, das auf der Promotorsequenz des *CTGF* („connective tissue growth factor“; Zielgen von YAP/TEAD) basierte, konnte die Aktivierung nach transienter YES-1 Expression bzw. Deaktivierung nach YES-1 „Knockdown“ beobachtet werden. Der Einsatz niedermolekularer Verbindungen wie Dasatinib (Inhibitor von YES-1) und Verteporfin (Inhibitor der YAP::TEAD Interaktion) als auch die Verwendung YAP::TEAD Interaktion inhibierender Peptide, zeigte erfolgreiche Deaktivierung des Reporters. Für diese Verbindungen wurden die EC_{50} Werte bestimmt. Die im Zuge der Arbeit generierten Daten lassen die Schlussfolgerung zu, dass YES-1 eine essentielle Rolle in der YAP/TEAD-abhängigen Aktivierung der Transkription spielt.

7 REFERENCES

1. **Hanahan D., Weinberg R.** 2000. The Hallmarks of Cancer. *Cell* **100**: 57-70
2. **Slamon D.J., Clark G.M., Wong S.G., Levin W.J., Ullrich A., McGuire W.L.** 1987. Human breast cancer: correlation of relapse and survival with amplification of the HER-2/neu oncogene. *Science* **235**: 177-182
3. **Pao W., et al.** 2004. EGF receptor gene mutations are common in lung cancers from “never smokers“ and are associated with sensitivity of tumors to gefitinib and erlotinib. *PNAS* **101**: 13306-13311
4. **Paez J.G., et al.** 2004. EGFR Mutations in Lung Cancer: Correlation with Clinical Response to Gefitinib Therapy. *Science* **304**: 1497-1500
5. **Lukashev M.E., Werb Z.** 1998. ECM signaling: orchestrating cell behaviour and misbehaviour. *Trends Cell Biol* **8**: 437-441
6. **Giancotti F.G., Ruoslahti E.** 1999. Integrin signaling. *Science* **285**: 1028-1032
7. **Alpin A.E., Howe A., Alahari S.K. and Juliano R.L.** 1998. Signal transduction and signal modulation by cell adhesion receptors: the role of integrins, cadherins, immunoglobulin-cell adhesion molecules and selectins. *Pharmacol. Rev.* **50**: 197-263
8. **Hannon G.J. and Beach D.** 1994. P15^{INK4B} is a potential effector of TGF-beta-induced cell cycle arrest. *Nature* **371**: 257-261
9. **Nguyen HP., Ramírez-Fort MK, Rady PL.** 2014. The biology of human papillomaviruses. *Current Probl Dermatol* **45**: 19-32
10. **Butt A.J., Firth S.M. and Baxter R.C.** 1999. The IGF axis and programmed cell death. *Immunol. Cell. Biol.* **77**: 256-262
11. **Merino D., Malkin D.** 2014. p53 and Hereditary Cancer. *Subcell Biochem* **85**: 1-16
12. **Hayflick L.** 1997. Mortality and immortality at the cellular level. *Biochemistry* **62**: 1189-1190
13. **Veikkola T. and Alitalo K.** 1999. VEGFs, receptors and angiogenesis. *Semin. Cancer Biol.* **9**: 211-220
14. **Sporn M.B.** 1996. The war on cancer. *Lancet* **347**: 1377-1381
15. **Yilmaz M., Christofori G.** 2009. EMT, the cytoskeleton, and cancer cell invasion. *Cancer Metastasis Rev.* **28**: 15-33

16. **Liu. M., Jiang L. and Guan X.Y.** 2014. The genetic and epigenetic alterations in human hepatocellular carcinoma: a recent update. *Protein Cell* **5**: 673-691
17. **Pan D.** 2007. Hippo signaling in organ size control. *Genes Dev.* **21**: 886-897
18. **Chen L., Loh P.G. and Song H.** 2010. Structural and functional insights into the TEAD-YAP complex in the Hippo signaling pathway. *Protein Cell* **1**: 1073-1083
19. **Chan S.** et al. 2010. The Hippo Pathway in Biological Control and Cancer Development. *Journal of Cellular Physiology* **226**: 928-939
20. **Barolo S. and Posakony J.W.** Three habits of highly effective signaling pathways: principles of transcriptional control by developmental cell signaling. *Genes Dev.* **16**: 1167-1181
21. **Bao Y., et al.** 2011. Mammalian Hippo pathway: from development to cancer and beyond. *The Journal of Biochemistry* **149**: 361-37
22. **Zeng Q. and Hong W.** 2008. The emerging role of the hippo pathway in cell contact inhibition, organ size control, and cancer development in mammals. *Cancer Cell* **13**: 188-192
23. **Xu T.** et al. 1995. Identifying tumor suppressors in genetic mosaics: The *Drosophila* lats gene encodes a putative protein kinase. *Development* **121**: 1053-1063
24. **Mo J.** et al. 2014. The Hippo signaling pathway in stem cell biology and cancer. *EMBO reports* **15**: 1-15
25. **Lai Z.** et al. 2005. Control of Cell Proliferation and Apoptosis by Mob as Tumor Suppressor, Mats. *Cell* **120**: 675-685
26. **Huang J.** et al. 2005. The Hippo Signaling Pathway Coordinately Regulates Cell Proliferation and Apoptosis by Inactivating Yorkie, the *Drosophila* Homolog of YAP. *Cell* **122**: 421-434
27. **Oh H. and Irvine K.D.** 2008. In vivo regulation of Yorkie phosphorylation and localization. *Development* **135**: 1081-1088
28. **Ren F., Zhang L. and Jiang J.** 2010. Hippo signalling regulates Yorkie nuclear localization and activity through 14-3-3 dependent and independent mechanisms
29. **Bao Y., et al.** 2011. Mammalian Hippo pathway: from development to cancer and beyond. *The Journal of Biochemistry* **149**: 361-379
30. **Stanger B.** 2012. Quit your YAP:ing: a new target for cancer therapy. *Genes & Development* **26**: 1263-1267

31. **Johnson R.** and **Halder G.** 2014. The two faces of Hippo: targeting the Hippo pathway for regenerative medicine and cancer treatment. *Nature Reviews* **13**: 63-79
32. **Avruch J., Zhou D.,** et al. 2012. Protein kinases of the Hippo pathway: regulation and substrates. *Cell Dev. Biol*, **23**: 770-784
33. **Hiemer S. E.** and **Varelas X.** 2012. Stem cell regulation by the Hippo pathway. *Biochimica et Biophysica Acta* **1830**: 2323-2334
34. **Pan D.** 2010. The Hippo Signaling Pathway in Development and Cancer. *Dev. Cell*. **19**: 491-505
35. **Yagi R.,** et al. 1999. A WW domain-containing Yes-associated protein (YAP) is a novel transcriptional co-activator. *The EMBO Journal* **18**: 2551-2562
36. **Yu F.X.** et al. 2013. Regulation of the Hippo-YAP pathway by G-protein coupled receptor signaling. *Cell* **150**: 780-791
37. **O'Hayre M, Degese MS, Gutkind JS.** et al. 2014. Novel insights into G protein and G protein-coupled receptor signaling in cancer. *Curr. Opin. Cell Biol.* **27**: 126-135
38. **Harvey K. F., Zhangl X.** and **Thomas D.M.** 2013. The Hippo pathway and human cancer. *Nature* **13**: 246-257
39. **Grusche F., Richardson H.** and **Harvey K.** 2010. Upstream Regulation of the Hippo Size Control Pathway. *Curr. Biol.* **20**: 574- 582
40. **Yu J.,** et al. 2010. Kibra functions as a tumor suppressor protein that regulates Hippo signaling in conjunction with Merlin and Expanded. *Dev. Cell.* **18**: 288-299
41. **Grzeschik N.** et al. 2010. Lgl, aPKC, and Crumbs regulate the Salvador/Warts/Hippo pathway through two distinct mechanisms. *Curr. Biol.* **20**: 573-581
42. **Zhou D.** et al. 2009. Mst1 and Mst2 Maintain Hepatocyte Quiescence and Suppress Hepatocellular Carcinoma Development through Inactivation of the Yap1 Oncogene. *Cancer Cell* **16**: 425-438
43. **Halder G., Dupont S.** and **Piccolo S.** 2012. Transduction of mechanical and cytoskeletal cues by YAP and TAZ. *Nature Reviews* **13**: 591-600

44. **Zhao B.**, et al. 2010. Angiomotin is a novel Hippo pathway component that inhibits YAP oncoprotein. *Genes & Development* **25**: 51-63
45. **Bazellieres E.**, et al. 2009. Crumbs proteins in epithelial morphogenesis. *Front. Biosci.* **14**: 2149-2169
46. **Ling C.** et al. The apical transmembrane protein Crumbs functions as a tumour suppressor that regulates Hippo signaling by binding to Expanded. *Proc. Natl Acad. Sci. USA* **107**: 10532-10537
47. **Yu F.X.** et al. 2013. Regulation of the Hippo-YAP pathway by G-protein coupled receptor signaling. *Cell* **150**: 780-791
48. **O'Hayre M, Degese MS, Gutkind JS.** et al. 2014. Novel insights into G protein and G protein-coupled receptor signaling in cancer. *Curr. Opin. Cell Biol.* **27**: 126-135
49. **Kim N. G.** et al. 2011. E-cadherin mediates contact inhibition of proliferation through Hippo signaling-pathway components. *Proc. Natl Acad. Sci. USA* **108**: 11930-11935
50. **Romano D, Matallanas D, Frederick DT, Flaherty KT and Kolch W.** 2014. One Hippo and many masters: differential regulation of the Hippo pathway in cancer. **42**: 816-821
51. **Wang W., Huang J. Wang X.** et al. 2012. PTPN14 is required for the density-dependent control of YAP1. *Genes Dev.* **26**: 1959-1971
52. **Huang J.** et al. 2013. YAP modifies cancer cell sensitivity to EGFR and surviving inhibitors and is negatively regulated by the non-receptor type protein tyrosine phosphatase 14. *Oncogene* **32**: 2220-2229
53. **Polesco C.** et al. 2006. The *Drosophila* RASSF homolog antagonizes the Hippo pathway. *Curr. Biol.* **16**: 2459-2465
54. **Ribeiro P.S.** et al. 2010. Combined functional genomic and proteomic approaches identify a PP2A complex as a negative regulator of Hippo signaling. *Mol. Cell* **39**: 521-534
55. **Wehr M.C.** et al. 2013. Salt-inducible kinases regulate growth through the Hippo signalling pathway in *Drosophila*. *Nature Cell Biol.* **15**: 61-71
56. **Hamaratoglu F.** et al. 2006. The tumour-suppressor genes NF2/ Merlin and Expanded act through Hippo signalling to regulate cell proliferation and apoptosis. *Nature Cell Biol.* **8**: 27-36

57. **Chen C.L.** et al. 2012. Tumor suppression by cell competition through regulation of the Hippo pathway. *Proc. Natl Acad. Sci. USA* **107**: 484-489
58. **Liu A. M., Poon RT and Luk JM.** 2010. MicroRNA-375 targets Hippo-signaling effector YAP in liver cancer and inhibits tumor properties. *Biochem Biophys Res Commun.* **394**: 623-627
59. **Liu A.M.** et al. 2010. Targeting YAP and Hippo signaling pathway in liver cancer. *Expert Opin. Ther. Targets* **14**: 855-868
60. **Zhao B., Wei X., Li W., et al.** 2007. Inactivation of YAP oncoprotein by the Hippo pathway is involved in cell contact inhibition and tissue growth control. *Genes Dev.* **21**: 2747-2761
61. **Badouel C.** et al. 2009. The FERM-domain protein Expanded regulates Hippo pathway activity via direct interactions with the transcriptional activator Yorkie. *Dev Cell.* **16**: 411-420
62. **Overholtzer M., Zhang J., Smolen G.A., et al.** 2007. Transforming properties of YAP, a candidate oncogene on the chromosome 11q22 amplicon. *Proc. Natl. Acad. Sci.* **103**: 12405-12410
63. **Steinhardt A. A.** et al. 2008. Expression of Yes-associated protein in common solid tumors. *Human Pathol* **39**: 1582-1589
64. **Kanai F.** et al. 2000. TAZ: A novel transcriptional co-activator regulated by interactions with 14-3-3 and PDZ domain proteins. *EMBO J* **19**: 6778-6791
65. **Chan S.W.** et al. 2008. A role for TAZ in migration, invasion and tumorigenesis of breast cancer cells. *Cancer Res* **68**: 2592-2598
66. **Liu X.** et al. 2012. PTPN14 interacts with and negatively regulates the oncogenic function of YAP. *Oncogene* **32**: 1-8
67. **Sawada A.** et al. 2008. Redundant roles of TEAD1 and TEAD2 in notochord development and the regulation of cell proliferation and survival. *Mol Cell Biol* **28**: 3177- 3189
68. **Chen Z., Friedrich G.A. and Soriano P.** 1994. Transcription enhancer factor I disruption by retroviral gene trap leads to heart defect and embryonic lethality in mice. *Genes Dev* **8**: 2293-2301
69. **Chen L.** et al. 2010. Structural basis of YAP recognition by TEAD4 in the Hippo pathway. *Genes Dev.* **24**: 290-300

70. **Tian W.** et al. 2010. Structural and functional analysis of the YAP- binding domain of human TEAD2. *Proc Natl Acad Sci USA* **107**: 7293-7298
71. **Harvey K. F., Zhangl X. and Thomas D.M.** 2013. The Hippo pathway and human cancer. *Nature* **13**: 246-257
72. **Li H.** et al. 2012. Deregulation of Hippo kinase signalling in Human hepatic malignancies. *Liver International* 1478-3223
73. **Aragona M.** et al. 2013. A Mechanical Checkpoint Controls Multicellular Growth through YAP/TAZ Regulation by Actin-Processing Factors. *Cell* **29**: 1047-1059
74. **Dong J.** et al. Elucidation of a universal size-control mechanism in *Drosophila* and mammals. *Cell* **130**: 1120-1133
75. **Clump D. A.** et al. 2005. c-YES response to growth factor activation. *Growth Factors* **23**: 263-272
76. **Ariki M.** et al. 1997. Identification of Autophosphorylation Sites in c-YES Purified from Rat Liver Plasma Membranes. *J.Biochem.* **121**: 104-111
77. **Azzolin L.** et al. 2012. Role of TAZ as Mediator of Wnt Signaling. *Cell* **151**: 1-14
78. **Bilial E.** et al. 2010. Identification of the YES-1 Kinase as a Therapeutic Target in Basal-Like Breast Cancers. *Genes & Cancer* **1**: 1063-1073
79. **Rosenbluh J.** et al. 2012. β -Catenin-Driven Cancers Require a YAP1 Transcriptional Complex for Survival and Tumorigenesis. *Cell* **151**: 1-17
80. **Xu M. Z,** et al. 2009. Yes-Associated Protein Is an Independent Prognostic Marker in Hepatocellular Carcinoma. *Cancer* **115**: 4576-85
81. **Yi Liu-Chittenden, Bo Huang, Joong Sup Shim,** et al. 2012. Genetic and pharmacological disrupton of the TEAD-YAP complex suppresses the oncogenic activity of YAP. *Genes Dev.* **26**: 1300-1305
82. **Li Z.** et al. 2010. Structural insights into the YAP and TEAD complex. *Genes & Development* **24**: 235-240
83. **Kwang-Pyo Lee,** et al. 2010. The Hippo-Salvador pathway restrains hepatic oval cell proliferation, liver size and liver tumorigenesis. *PNAS* **107**: 8248-8253

84. **Dawang Zhou**, et al. 2009. Mst1 and Mst2 Maintain Hepatocyte Quiescence and Suppress Hepatocellular Carcinoma Development through Inactivation of the Yap1 Oncogene. *Cell* **16**: 425-438
85. **Soeiro R., Vaughan M.H. and Darnell J.E.** 1968. The effect of puromycin on intranuclear steps in ribosome biosynthesis. *The Journal of Cell Biology* **36**: 91-101
86. **Jalili A.**, et al. 2011. Polo-Like Kinase 1 Is a Potential Therapeutic Target in Human Melanoma. *Journal of Investigative Dermatology* **131**: 1886-1895
87. **Beilina A.**, et al. 2005. Mutations in PTEN-induced putative kinase 1 associated with recessive parkinsonism have differential effects on protein stability. *PNAS* **102**: 5703-5708
88. **Nembrini J.**, et al. 2009. The Kinase Activity of Rip2 Determines Its Stability and Consequently Nod-1 and Nod2- mediated Immune Responses. *J. Biol Chem* **284**: 19183-19188
89. **Das J.**, et al. 2006. 2-aminothiazole as a novel kinase inhibitor template. Structure-activity relationship studies toward the discovery of N-(2-chloro-6-methylphenyl)-2-[[6-[4-(2-hydroxyethyl)-1-piperazinyl]-2-methyl-4-pyrimidinyl]amino]-1,3-thiazole-5-carboxamide (dasatinib, BMS-354825) as a potent pan-Src kinase inhibitor. *J. Med. Chem.* **49**: 6819-6832
90. **Karaman M.W.**, et al. 2008. A quantitative analysis of kinase inhibitor selectivity. *Nature Biotechnology* **26**: 127-132
91. **Scott L. J.**, et al. 2000. Verteporfin. *Drugs & Aging* **16**: 139-146
92. **Karim S.P.**, et al. 2013. Profile of verteporfin and its potential for the treatment of central serous chorioretinopathy. *Clinical Ophthalmology* **7**: 1867-1875
93. **Zhao B.**, et al. 2008. TEAD mediated YAP-dependent gene induction and growth control. *Genes & Development* **22**: 1962-1971
94. **Sudha G.** et al. 2014. An overview of recent advances in structural bioinformatics of protein-protein interactions and a guide to their principles. *Progress in Biophysics and Molecular Biology* **116**: 141-150
95. **Brodowska K.** et al. 2014. The clinically used photosensitizer Verteporfin (VP) inhibits YAP-TEAD and human retinoblastoma cell growth in vitro without light activation. *Exp Eye Res.* **124**: 67-73

96. **Zhou Z.** et al. 2015. Targeting Hippo pathway by specific interruption of YAP-TEAD interaction using cyclic YAP-like peptides. *The FASEB Journal*. **29**: 724-32
97. **Rao N.** et al. 2005. A Novel Splice Variant of Interleukin-1 Receptor (IL-1R)-Associated Kinase 1 Plays a Negative Regulatory Role in Toll/IL-1R-Induced Inflammatory Signaling. *Mol Cell Biol*. **25**: 6521-6532
98. **Lori C.** et al. 2013. Effect of Single Amino Acid Substitution Observed in Cancer on Pim-1 Kinase Thermodynamic Stability and Structure. *PLOS ONE* **8**: 1-11
99. **Duan J.** et al. 2002. Synonymous mutations in the human dopamine receptor D2 (DRD2) affect mRNA stability and synthesis of the receptor. *Human Molecular Genetics* **12**: 205-216
100. **Krauss S.** et al. 2009. Point Mutations in GLI3 Lead to Misregulation of its Subcellular Localization. *PLOS ONE* **4**: 1-13
101. **Touil Y.** et al. 2013. Colon Cancer Cells Escape 5FU Chemotherapy-Induced Cell Death by Entering Stemness and Quiescence Associated with the c-Yes/YAP Axis. *Clin Cancer Res*. **20**: 837-846
102. **Edelheit O.** et al. 2011. Identification of the roles of conserved charged residues in the extracellular domain of an epithelial sodium channel (ENaC) subunit by alanine mutagenesis. *Physiol. Renal Physiol*. **300 (4)**: F887–97
103. **Beith J.L.** et al. 2008. Insulin stimulates primary beta-cell proliferation via Raf-1 kinase. *Endocrinology*. **149(5)**: 2251-60
104. **Cruet-Hennequart S.** et al. 2003. alpha(v) integrins regulate cell proliferation through integrin-linked kinase (ILK) in ovarian cancer cells. *Oncogene* **20(11)**: 1688-702
105. **Tervonen T.A.** et al. 2006. Overexpression of a truncated TrkB isoform increases the proliferation of neural progenitors. *European Journal of Neuroscience* **24**: 1277-85
106. **Zender L.** et al. 2006. Identification and validation of oncogenes in liver cancer using an integrative oncogenomic approach. *Cell* **125**: 1253-1267
107. **Croce C.M.** et al. 2015. MicroRNA and cancer – A brief overview. *Elsevier* **57**: 1-9

108. **Yan M.** et al. 2012. microRNA-21 promotes tumor proliferation and invasion in gastric cancer by targeting PTEN. *Oncol Rep.* **27(4)**: 1019-26
109. **Kolenda T.** et al. 2014. The mystery of let-7d – a small RNA with great power. *Contemp Oncol (Pozn).* **18 (5)**: 293-301
110. **Chen L.** et al. 2014. Distinct roles of Akt1 in regulating proliferation, migration and invasion in HepG2 and HCT116 cells. *Oncol. Rep.* **31(2)**:737-44
111. **Chan J.** et al. 2011. Integrin-linked kinase overexpression and its oncogenic role in promoting tumorigenicity of hepatocellular carcinoma. *PLoS One* **6**:e16984
112. **Sehgal A.** et al. 2013. Liver as a target for oligonucleotide therapeutics. *J. Hepatol.* **56(6)**: 1354-9

8 ATTACHMENTS

8.1 List of Tables

Table 1: Core components of the Hippo pathway and its modulators [31]	16
Table 2: Activation of c-YES-1 [75]	31
Table 3: Medium and additional substances for production of a full medium	41
Table 4: List of Instruments	42
Table 5: List of Equipment	43
Table 6: List of kits, reagents and buffers	44
Table 7: Nuclear and cytoplasmic extraction reagents	44
Table 8: Components of lysis buffer/ wash buffer 1	45
Table 9: Components of wash buffer 2	45
Table 10: Components of wash buffer 3	45
Table 11: HEPEX lysis buffer	46
Table 12: Composition of TBS-T buffer	46
Table 13: Dilution of 20x XT MOPS	47
Table 14: Composition of blocking milk	47
Table 15: Composition of BSA blocking solution	47
Table 16: List of protein ladders	47
Table 17: List of primary antibodies	48
Table 18: List of secondary antibodies	48
Table 19: List of siRNAs	49
Table 20: PLK-1 shRNA	50
Table 21: List of shRNAs	50
Table 22: List of plasmids	51
Table 23: List of antibiotics	52
Table 24: List of Compounds	52
Table 25: AAV Particles	53
Table 26: Necessary reagent volumes according to cell packed volumes (Thermo Scientific)	60
Table 27: Lethal concentration [$\mu\text{g}/\text{ml}$] of Puromycin for 23 different HCC cell lines	78
Table 28: Summary of cell lines	105
Table 29: IC_{50} values for 23 HCC cell lines treated with Dasatinib or Verteporfin.	108

Table 30: Analysis of HCC cell lines according to mutations in Hippo pathway related-
or regulatory genes. 146

8.2 List of Figures

The Hallmarks of Cancer by Hanahan and Weinberg [1]:	1
Hippo pathway ON and OFF in mammals [31]	10
Regulation of the Hippo pathway in Drosophila compared to those in mammals	12
Protein domains of YAP and Interaction partners [18]	18
TEAD protein domains and interaction partners [19]	19
Biological functions of the Hippo pathway relevant to cancer [71]	20
Hippo-mutant phenotypes in Drosophila and mice [31]	26
Structure of the YAP-TEAD complex, interfaces and sequence conservation [82]	35
Poor overall survival of patients characterized as YAP positive based on YAP immunoreactivity by immune-histochemistry [80]	35
Hypotheses of contribution of YES-1 to YAP/TEAD dependent transcription activation	37
Hypothetical model of YES-1 location and contribution to YAP dependent transcription	38
Structural formula of Dasatinib	52
Structural formula Verteporfin	52
Formula for calculation of ml lentiviral particle needed for a certain MOI and cell number	54
Standard curve for determination of protein concentration	62
Western blot analysis of Hippo-relevant proteins in 21 HCC cell lines	65
Nuclear vs. cytoplasm YES-1, YAP and TAZ protein levels in hepatocellular carcinoma cell lines	69
SK-HEP-1 after 72 hours of siRNA treatment	72
HLF after 72 hours of siRNA treatment	73
HLE after 72 hours of siRNA treatment	74
huH-1 after 72 hours of siRNA treatment	75
JHH-4 after 72 hours of siRNA treatment	76
Puromycin titration from 4-0.06 µg/ ml in 23 HCC cell lines	77

Characterization of five different YAP shRNA lentiviruses in cell line JHH-7	78
Characterization of five different TAZ shRNA lentiviruses in cell line JHH-7	79
Characterization of five different YES-1 shRNA lentiviruses in JHH-7 cell line	80
Characterization of five different TEAD1 shRNA lentiviruses in cell line JHH-7	80
Characterization of five different TEAD2 shRNA lentiviruses in cell line JHH-7	81
Characterization of five different TEAD3 shRNA lentiviruses in cell line JHH-7	82
Characterization of five different TEAD4 shRNA lentiviruses in cell line JHH-7	82
Hep3B2.1-7 proliferation data	84
Hep3B2.1-7 Western blot data	85
HLE Proliferation data relative to non-targeting- including untreated control	86
HLE Western blot data (500 cells/ well)	87
HLE Proliferation data relative to non-targeting- without untreated control	87
HLE Western blot data (1000 cells/ well)	88
HLF Proliferation data	89
HLF Western blot data	89
HuCCT-1 proliferation data	91
HuCCT-1 Western blot data	91
JHH-6 proliferation data	92
JHH-6 Western blot data	92
JHH-7 proliferation data	93
JHH-7 Western blot data	94
SK-HEP-1 proliferation data	95
SK-HEP-1 Western blot data	95
SNU-398 proliferation data	97
SNU-398 Western blot data	97
SNU-423 proliferation data	99
SNU-423 Western blot data	99
SNU-475 proliferation data	100
SNU-475 Western blot data	101
Sensitivity towards YAP knockdown	102
Sensitivity towards TAZ knockdown	103
Sensitivity towards YES-1 knockdown	104
Rescue of YES-1 knockdown in JHH-7	106

Western blot analysis of JHH-7 cell lysates after 13 days of shRNA-mediated YES-1 knockdown.	107
Proliferation rates [relative fluorescence units; RFU] of differently treated SK-HEP-1 cells. Dasatinib:	110
Evaluation of transfection efficiency using AMAXA Electroporation and Fluorescence microscopy	111
pGL4.16 Vector map	112
pGL4.28 [<i>Luc2CP/minP/Hygro</i>] Vector map	112
Human promoter region of the connective tissue growth factor (<i>CTGF</i>) [93]	112
Promoter sequences of various <i>CTGF</i> promoter-driven luciferase reporter vectors	113
Characterization of TEAD-driven reporter gene plasmids in SK-HEP-1	114
Reporter gene activity in SK-HEP-1 Clone-wt3 and SK-HEP-1 Clone-del1	115
TEAD-driven reporter gene activity after 24 hours of kd or over-expression of YES-1	116
Cell density and Reporter gene assay in SK-HEP-1 harboring <i>CTGF</i> -promoter driven luciferase reporter gene plasmid pGL4_16 <i>CTGF</i> -wt	117
<i>CTGF</i> -promoter-driven luminescence after 24h Dasatinib treatment in SK-HEP-1 Clone wt3	118
SK-HEP-1 Clone-wt3 transduced with AAV particles expressing the YAP/TEAD interphase peptide	119
AA sequences of the inhibitory peptide of the YAP/ TEAD interaction as published by Li, 2010 [82]	119
Co-Immunoprecipitation of YAP, YAP/ TAZ, YES-1 and TEAD in JHH-7	121

8.3 Mutation Analysis

Table 30: Analysis of HCC cell lines according to mutations in Hippo pathway related- or regulatory genes.

Cell lines which have shown dependency on YES-1 are displayed in red.

Gene	Hep_G2	JHH-5	JHH-7	SK-HEP-1	HLE	HuCCCT1	JHH-4	JHH-6	C3A	HuH-1	HuH7	SNU-398	Hep_3B2 1-7	JHH-1	SNU-423	SNU-475	HUH-6 Clone 5	HLF	JHH-2	SNU-387	SNU-449	SNU-182	RH-41
AREG	0	0		0	0	0	0	0	0	0	0	0	0	0	0	0	0	0	0	0	0	0	0
BIRC5	0	0		0	0	0	0	0	0	0	0	0	0	0	0	0	0	0	0	0	0	0	0
CSNK1A1	0	0		0	0	0	0	0	0	0	0	0	0	0	0	0	0	0	0	0	0	0	0
CSNK1E	0	0		0	0	0	0	0	0	0	0	0	0	0	0	0	0	0	0	0	0	0	0
CSNK1G1	0	0		0	0	0	0	0	0	1	0	0	0	0	0	0	0	0	0	0	0	0	0
CSNK1G2	0	0		0	0	0	0	0	0	0	0	0	0	0	0	0	0	0	0	0	0	0	0
CSNK1G3	0	0		0	0	0	0	0	0	0	0	0	0	0	0	0	0	0	0	0	0	0	0
CTGF	0	0		0	0	0	0	0	0	0	0	0	0	0	0	0	0	0	0	0	0	0	0
CTNNB1	0	0		0	0	0	0	0	0	0	0	1	0	0	0	0	1	0	0	0	0	0	0
DCHS1	0	0		0	0	0	0	0	0	0	0	0	0	0	0	0	0	0	0	0	0	0	0
DCHS2	0	0		0	0	0	0	0	0	0	0	0	1	0	0	0	0	0	0	0	0	0	0
DVL1	1	0		0	0	1	0	0	1	0	0	0	0	0	0	0	0	0	0	0	0	0	0
DVL2	0	0		0	0	0	0	0	0	0	0	1	0	0	0	0	0	0	0	0	0	0	0
DVL3	0	0		0	0	0	0	0	0	0	0	0	0	0	0	0	0	0	0	0	0	0	0
FAT4	0	0		0	1	1	0	0	0	0	0	0	0	0	0	0	0	1	1	0	0	1	0
FRMD6	0	0		0	0	0	0	0	0	0	0	0	0	0	0	0	0	0	0	0	0	0	0
JUB	0	0		0	0	0	0	0	0	0	0	0	0	0	0	0	0	0	0	0	0	0	0
LATS1	0	0		1	0	0	0	0	0	0	0	0	0	0	0	0	0	0	0	0	0	0	0
LATS2	0	0		0	0	0	0	0	0	0	0	0	0	0	0	0	0	0	0	0	0	0	0
MEF2A	0	0		0	0	0	0	0	0	0	0	0	0	0	0	0	0	0	0	0	0	0	0
MEF2B	0	0		1	0	0	0	0	0	0	0	0	0	1	0	0	0	0	0	0	0	0	0
MEF2C	0	0		0	0	0	0	0	0	0	0	0	0	0	0	0	0	0	0	0	0	0	0
MERTK	0	0		0	0	0	0	0	0	0	0	0	0	0	0	0	0	0	0	0	0	0	0
MOB1A	0	0		0	0	0	0	0	0	0	0	0	0	0	0	0	0	0	0	0	0	0	0
MOB1B	0	0		0	0	0	0	0	0	0	0	0	0	0	0	0	0	0	0	0	0	0	0
MST1	0	0		0	0	0	0	0	1	0	1	0	0	0	0	0	1	0	0	1	0	0	0
MYC	0	0		0	0	0	0	0	0	0	0	0	0	0	0	0	0	0	0	0	0	0	0
NFE2	0	0		0	0	0	0	0	0	0	0	0	0	0	0	0	0	0	0	0	0	0	0
RAC3	0	0		0	0	0	0	0	0	0	0	0	0	0	0	0	0	0	0	0	0	0	0
RASSF1	0	0		0	0	0	0	0	0	0	0	0	0	0	0	0	0	0	0	0	0	0	0
RASSF2	0	0		0	0	0	0	0	0	0	0	0	0	0	0	0	0	0	0	0	0	0	0
RASSF3	0	0		0	0	0	0	0	0	0	0	0	0	0	0	0	0	0	0	0	0	0	0
SAV1	0	0		0	1	0	0	0	0	0	0	0	0	0	0	0	0	1	0	0	0	0	0
SRF	0	0		0	0	0	0	0	0	0	0	0	0	0	0	0	0	0	0	0	0	0	0
STK3	0	0		0	0	0	0	0	0	0	0	0	0	0	0	0	0	0	0	0	0	0	0
STK4	0	0		0	0	0	0	0	0	0	0	0	0	0	0	0	0	0	0	0	0	0	0
TAZ	0	0		0	0	0	0	0	0	0	0	0	0	0	0	0	0	0	0	0	0	0	0
TEAD1	0	0		0	0	0	0	0	0	0	0	0	0	0	0	0	0	0	0	0	0	0	0
TEAD2	0	0		0	0	0	0	0	0	0	0	0	0	0	0	0	0	0	0	0	0	0	0
TEAD3	0	0		0	0	0	0	0	0	0	0	0	0	0	0	0	0	0	0	0	0	0	0
TEAD4	0	0		0	0	0	0	0	0	0	0	0	0	0	0	0	0	0	0	0	0	0	0
TEF	0	0		0	0	0	0	0	0	0	0	0	0	0	0	0	0	0	0	0	0	0	0
TP53BP2	0	0		0	0	0	0	0	0	1	0	0	0	0	0	0	0	0	0	0	0	0	0
TP73	0	0		0	0	0	0	0	0	0	0	0	0	0	0	0	0	0	0	0	0	0	0
WWC1	0	0		0	0	1	0	0	0	0	0	0	1	0	0	0	0	0	0	0	0	0	0
WWTR1	0	0		0	0	0	0	0	0	0	0	0	0	0	0	0	0	0	0	0	0	0	0
YAP1	0	0		0	0	0	0	0	0	0	0	0	0	0	0	0	0	0	0	0	0	0	0
YES1	0	0		0	0	0	0	0	0	0	0	0	0	0	0	0	0	0	0	0	0	0	0
YWHAZ	0	0		0	0	0	0	0	0	0	0	0	0	0	0	0	0	0	0	0	0	0	0

Curriculum Vitae

Persönliche Angaben

Name: **Katharina Ehrenhöfer, Bakk. techn.**

Staatsbürgerschaft: Österreich

Ausbildung

2011-2015 **Master Studium: Molekular Biologie, UNI Wien**

Schwerpunkt: Molekulare Medizin

Masterarbeit: „Molecular Cross-talk of the Src-family tyrosine kinase YES-1 with the Hippo Pathway contributes to survival and proliferation of Hepatocellular carcinoma cells“

2007-2011 **Bachelor Studium: Lebensmittel- und Biotechnologie, BOKU Wien**

Bachelorarbeit: „Transiente DNA Transformation in die Tabakpflanze“
Department für Angewandte Genetik und Zellbiologie

1999-2007 Evangelisches Realgymnasium, Oberschützen

Berufserfahrung & Praktika

- 03/2013-04/2014 Praktikum im Zuge der Masterarbeit, Boehringer Ingelheim, Wien
Betreuer: Doz. Dr. Wolfgang Sommergruber, Lead Discovery
- 10/2012- 12/2012 Praktikum im Zuge des Wahlbeispiels, Medizinische Universität
Wien
- 08/2011- 09/2011 Ferialpraktikum, JTI Austria GmbH, Wien
- 07/ 2011 Praktikum im Zuge des Wahlbeispiels, Pharmakologie,
Medizinische Universität Wien
- 09/2010 Praktikum im Zuge der Bachelorarbeit, Department für
Angewandte Genetik und Zellbiologie, BOKU Wien
Betreuer: Univ.Prof. Dipl.-Ing. Dr.rer.nat. Eva Stöger
- 08/2010 Praktikum Schutzengel - Apotheke, Großpetersdorf
- 09/2009 Praktikum Laborgemeinschaft Südburgenland, Güttenbach